MAGNETIC FIELD-INDUCED MARTENSITIC TRANSFORMATIONS IN A FEW FERROUS ALLOYS

BY

TOMOYUKI KAKESHITA

DISSERTATION IN PHYSICS

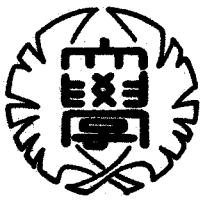

THE OSAKA UNIVERSITY

GRADUATE SCHOOL OF SCIENCE

TOYONAKA, OSAKA

MAGNETIC FIELD-INDUCED MARTENSITIC TRANSFORMATIONS IN A FEW FERROUS ALLOYS

BY

TOMOYUKI KAKESHITA

Contents

Abstract

The magnetic field-induced martensitic transformation has been systematically studied for poly- and single-crystalline Fe-Ni alloys, Invar and non-Invar Fe-Ni-C alloys, ordered and disordered Fe-Pt alloys, a paramagnetic Fe-Mn-C alloy and an ausaged Fe-Ni-Co-Ti alloy showing a thermoelastic martensitic transformation. As a result, following characteristic features are clarified:

(i) Considerably large change in the martensitic transformation temperature, M_S, has been found, and the change is quantitatively explained by cumulative three effects of the magnetostatic energy, high field susceptibility and forced volume magnetostriction.

(ii) The amount of magnetic field-induced martensites is independent of the strength of an applied magnetic field for some Fe-Ni alloys but is dependent for other alloys.

(iii) The morphology of magnetic field-induced martensites is the same as that of thermally-induced ones.

(iv) Directional growth of magnetic field-induced martensite plates is observed parallel to the magnetic field.

(v) Magnetoelastic martensitic transformation is firstly verified to be realized in an ausaged Fe-Ni-Co-Ti alloy, in which the martensitic transformation occurs only while a magnetic field is applied.

Chapter 1

General Introduction and Purpose of the Study.

1. General aspects of martensitic transformations.

1-1 Definition and characteristic features of martensitic transformation.

Mechanical properties and structures of iron based alloys and steels have long been studied because of their technological importance. Through these studies, a number of characteristic phenomena have been discovered. One of such phenomena was that a steel quenched to room temperature from its high temperature phase (fcc structure) has a very fine microstructure in the retained parent phase, which is different from the equilibrium phase (consisting of two phases, α phase with a bcc structure and cementite, Fe_3C) obtained by slow cooling. Moreover, it was found that the appearance of such a fine structure results in an increase in hardness of the steel. This fine structure in quenched steel was first named as "martensite" by F. Osmond[1] of France in 1894, in honor of Professor A. Martens, the famous pioneer German metallurgist. Thereafter, the fine structure was clarified to be formed by a transformation from the fcc austenite lattice to a bcc or bct lattice without long distance diffusion of atoms. This type of transformation was ambiguously adopted as "martensitic transformation", and the bcc or bct product phase was renamed "martensite". Since then, many studies on the martensitic transformation and martensite have been carried out in order to know their characteristics from the physical, metallographi-

cal, crystallographical and technological points of views.

Up to now, the martensitic transformation has widely been found in a large number of metals (Co[2] and Li[3]), ferrous alloys and steels (Fe-Ni[4], Fe-Pt[5], Fe-Mn[6], Fe-Ni-C[7], Fe-Cr-C[8], Fe-Mn-C[9] etc.), non-ferrous alloys (Au-Cd[10], Cu-Al-Ni[11], Cu-Zn-Al[12], Ti-Ni[13] etc.) and metallic compounds (Nb_3Sn[14], Vi_3Si[15] etc.). It has been defined as a typical first order structural phase transition from solid to solid phases which is performed by a cooperative movement of atoms without long distance diffusion.

Phases before and after the transformation are almost quasi equilibrium ones, and they are called the parent phase (austenitic phase denoted γ for ferrous alloys and β-phase for non-ferrous alloys) and martensite phase (denoted α' for ferrous alloys and β', γ' and α' for non-ferrous alloys depending on its crystal structure), respectively. The physical and crystallographical characteristics associated with the martensitic transformation are summarized below in more detail:

Physical characteristics

(1) The martensitic transformation is accompanied by some change in many physical quantities such as volume, latent heat, electrical resistance and so on. It is clear to be the first order phase transition referring to the change in the former two quantities. Therefore, transformation temperatures can be known by detecting the change. A typical electrical resistivity vs. temperature relation is shown in Fig. 1, which has been obtained from an Fe-29.9at%Ni alloy polycrystal examined in the present study. When the alloy of the austenitic phase is cool-

ed down, an abrupt change in electrical resistivity is observed at a certain temperature, M_s, indicated with an arrow. This change corresponds to the occurence of martensitic transformation, and M_s means the start temperature of martensitic transformation. Further cooling down from M_s, the transformation continues down to the M_f temperature, indicated with another arrow, M_f meaning the finish temperature of martensitic transformation. On the other hand, when temperature is raised from a temperature below M_f, the reverse transformation to the austenitic phase starts at A_s temperature and finishes at A_f temperature, as indicated with arrows, respectively. In this way, the transformation temperatures can be determined by measuring the change of electrical resistivity as a function of temperature. Another characteristic feature in this figure is that a hysterisis is always observed between forward and reverse transformation temperatures for any martensitic transformation. The amount of the hysterisis depends on the alloy system, as will be described later.

(2) The martensitic transformation is diffusion-less (diffusion in this case means long-distance one), and therefore it differs from other diffusional solid-solid phase transformations, such as phase decomposition, spinodal decomposition and order-disorder transition. The diffusionless nature leads to the fact that no difference in composition exists between the parent and martensite phases.

Crystallographical characteristics

(3) The transformation is from a single phase to another single phase, and the change of their crystal structures depends

on alloy systems, for example, it is fcc → bcc (bct) or fcc → hcp in many ferrous alloys and DO_3 or B2 → 18R(9R) or 2H in many non-ferrous alloys (the notations of 18R, 9R and 2H are the Ramsdell's).

(4) Definite surface relief effect is observed, being associated with the martensitic transformation.

(5) Macroscopically straight interface is observed between the parent and martensite phases. The plane corresponding to the interface is called "habit plane", which is almost unrotated and undistorted one during the transformation. Indices of the habit planes are represented with respect to the parent crystal axes, and are generally irrational ones, for example, they are nearly {225}, {259} or {3 10 15} in many ferrous alloys and {551} or {331} in non-ferrous alloys. Characteristics described in the items 3 and 4 means that the martensitic transformation is accompanied by a definite shape change, as will be mentioned in 1-2.

(6) Crystallographic axes of a martensite crystal have a definate relation to those of the retained parent crystal, such as $(111)_\gamma // (011)_{\alpha'}$, $[\bar{1}01]_\gamma // [\bar{1}\bar{1}1]_{\alpha'}$ (Kurdjmov-Sachs (K-S) relation[16]), and $(111)_\gamma // (011)_{\alpha'}$, $[11\bar{2}]_\gamma // [0\bar{1}1]_{\alpha'}$ (Nishiyama (N) relation[17]) in many ferrous alloys.

(7) Martensite crystals contain many lattice imperfections, such as dislocations, twins and stacking faults. These are considered to be caused by complementary deformation neccessary for the martensitic transformation, which are called "lattice invariant strain".

1-2 Phenomenological crystallographic theory

The characteristics described in the preceding 2, 4 and 5 items mean that the martensitic transformation is performed by a cooperative movement of atoms without long distance diffusion, namely by a shear-like mechanism. By this standpoint, the phenomenological crystallographic theory[18)~(22)] was introduced to predict crystallographical characteristics, such as the shape change, habit plane and orientation relationship, which will be described below. A cental idea of this theory is that the shape deformation consists of three kinds of deformation, that is, P_1=RPB in the matrix form, where P_1 represents the matrix of total deformation associated with a transformation, P the matrix of lattice invariant shear mentioned before, B and R the matrices of Bain distortion and lattice rotation, respectively, and these deformation occur to satisfy the condition that there must be an unrotated and undistorted plane, which correspond to the habit plane. If these matrices are known, the crystallographical geometry between the parent and martensite crystals are uniquely determined, and crystallographical characteristics are known. Among these deformations, Bain distortion is the most principal one, which is neccessary to transform from the parent to martensite lattices. The Bain distortion for a fcc→bcc transformation is shown in Fig. 2. That is, the Bain distortion is introduced to generate a bcc lattice from a fcc lattice, which consists of a compression along one principle axis, for example [001]P, and a simultaneous uniform expansion along other two axes perpendicular to it. This deformation is most reasonable because it involves the smallest relative atomic displacement. According to the

Bain distortion, a correspondence uniquely exists between lattice points in the initial and final lattices, and this is called "Bain correspondence", shown with the heavy-lined portion in the fcc lattice. The process for determing P_1 is as follows: B is known from lattice constants of both the parent and martensite crystals, and the shear plane of P is known by observing internal imperfections of the martensite although its shear magnitude is set as a parameter. Using these values, R and P are determined so that an unrotated and undistorted plane exists even if P_1 is operated. Therefore, this comes to be the problem to solve the characteristic equation and to determine the eigen value. Thus, the habit plane, shape change and orientation relationship can be predicted by using the determined R and P, and their predicted values are good agreement with the experimentally observed ones in many materials undergoing a martensitic transformation[23)~25)]. Inversely speaking, this indicates that martensitic transformation occurs by a shear like mechanism. Incidentally, according to the theory, shape deformation can be macroscopically described by a shear parallel to the habit plane and a uniform expansion or contraction normal to it, the latter corresponding to the volume change, as shown in Fig. 3. In the matrix form, the shape deformation can be written as $P_1=I+m\vec{d}\cdot\vec{p}_1'=I+(\varepsilon\vec{d}_1+\varepsilon_0\vec{p}_1)\vec{p}_1'$, where P_1 represents the matrix of shape deformation, I the identity matrix, $\vec{d}$ the unit vector in the direction of the shape deformation, m the magnitude of the shape deformation, $\vec{d}_1$ and $\vec{p}_1$ the unit vectors of shear and normal expansion to the habit plane, respectively. $\vec{p}_1'$ is the same as $\vec{p}_1$ but the prime means a row vector. ε and ε_0 are the shear and dilatational components, res-

pectively, and ε_0 corresponds to the volume change ratio.

1-3 Kinetics of martensitic transformation.

The martensitic transformations may be classified into two groups, that is, isothermal and athermal ones by a difference in time and temperature dependences of the amount of martensites. That is, the amount of martensites is a function of both temperature and time in the former, but of only temperature in the latter. Materials undergoing such an isothermal martensitic transformation are very few in number, and an Fe-Ni-Mn alloy[26] is the typical one.

However, it seems to be more logical to treat the isothermal transformation as general one, and the athermal one as a special one, because it can be considered that the time dependence of the amount of athermal martensites may exist but is undetectably short. Unfortunately, this problem has not been clarified yet in the present. The athermal martensitic transformations may also be roughly classified into two groups, which are thermoelastic one observed in many non-ferrous alloys and intermetallic compounds (Cu-Al-Ni, Au-Cd, Ti-Ni and Nb_3Sn alloys etc.) and non-thermoelastic one observed in many ferrous alloys and steels (Fe-Ni and Fe-C alloys etc.). This classification is phenomenologically due to the fact whether the interface between parent and martensite phases is mobile or not. That is, the thermoelastic martensite can gradually grow or shrink by forward or backward movement of its interface as temperature is lowered below M_S or raised above A_S, respectively, being under a balance between the thermal and elastic energies

due to the strain by the shape change (shape strain) etc. On the other hand, the non-thermoelastic martensite can not grow or shrink in such a manner, that is, it nucleates and grows instanteneously to its final size below M_s and never grow even if temperature is lowered, while on the reverse transformation, many parent crystals with different orientations nucleate and grow in the martensite instantaneously.

Therefore, the amount of thermoelastic martensites increases or decreases by the growth or shrink of martensite themselves nucleated in the parent phase, respectively, and it is 100% at M_f temperature. On the other hand, the amount of non-thermoelastic martensites increases by producing new martensites with infinite size in the retained parent phase below M_s and its value at M_f depends on the alloy system, generally about 60~80%, and it decreases on the reverse transformation by the process described above. Such a difference in interface features results in some difference in other physical and crystallographical features between the thermoelastic and non-thermoelastic martensites, which is shown below, although these differences are not always the neccessary and sufficient conditions.

(i) Volume change ratio associated with the transformation is small (-10^{-3} ~-5×10^{-3}) in the thermoelastic one[27] but large (10^2 ~ 4×10^2) in the non-thermoelastic one[28].

(ii) Hysterisis between M_f and A_f is small (<50K) in the thermoelastic one[28], but large (300~500K) in the non-thermoelastic one[28].

(iii) The latent heat of transformation is small (<~100 cal/mol) in the thermoelastic one[29], but large (300~500 cal/mol) in the non-thermoelastic one[28].

(iv) As described above, forward and reverse transformations are quitely different between the thermoelastic and non-thermoelastic martensitic transformations. This is due to the fact that the thermoelastic martensitic transformation is crystallographically reversible but the non-thermoelastic one is not. It was proposed by Otsuka and Shimizu[30] that this crystallographic reversibility is characteristic of ordered alloys because non-reversible paths create the wrong ordered structure which raise the free energy of the alloys. Thus, except for alloys undergoing a thermoelastic fcc $\rightleftarrows$ fct martensitic transformation, many thermoelastic alloys have an ordered structure.

On the other hand, many alloys undergoing a non-thermoelastic martensitic transformation have disordered structure, and therefore there is no need of crystallographic reversibility. In this way, the thermoelastic martensitic transformation has very interesting properties. Moreover, it is now well known that most of the alloys undergoing this type of transformation have shape memory and pseudoelasticity effects, and they are applied as new functional materials in the field of technology. These effects will be discussed later.

1-4 Thermodynamics of martensitic transformation.

The Gibbs chemical free energies of parent and martensite phases are schematically shown in Fig. 4, as a function of temperature. In this figure, To represents the equilibrium temperature where the Gibbs chemical free energies of both the phases are equal, that is, $G^P = G^M$. Martensitic trnasformation, however, does not occur at To but M_S temperature below To.

This is because interfaces and strain are introduced within both the phases by forming martensites, and therefore an additional energies are needed to start the transformation. Therefore, the martensitic transformation does not occur until the additional energy is supplied by cooling down below To[31]. This energy mainly consists of three parts, interfacial energy between the parent and martensite phases (W_1), and energies for elastic deformation (W_2) and plastic one (W_3) associated with the transformation, they being named non-chemical free energy. According to the above consideration, M_S may be said to be the temperature where the chemical free energy balances with the non-chemical free energy, and the following equation holds at M_S,

$$G^P(M_S) - G^M(M_S) = W_1 + W_2 + W_3$$

where the term $G^P(M_S) - G^M(M_S) = \Delta G^{M-P}(M_S)$ is called chemical driving force. If the quantities of G^P, G^M, W_1, W_2 and W_3 are known as a function of temperature, M_S temperature may be predicted. The same situation may fold for A_S temperature.

1-5 Origin of martensitic transformation.

It is very important to know the origin of martensitic transformations. Many studies have been done on the origin of transformations, but any conclusion has not been obtained yet. Because the martensitic transformation is the first order transition which has not been well understood physically except for its thermodynamics. Recently, precusor phenomena have been reported to occur prior to the martensitic transformations, and they are considered to be related to the origin of the trans-

formation. One of such phenomena is an abnormal decrease in the shear modulus, as observed in Au-Cu-Zn[32] and In-Tl[33] alloys etc. That is, the shear modulus, $C'(C_{11}-C_{12}/2)$, abnormally decreases with lowering temperature towards M_S temperature. This abnormal decrease has been explained by a soft phonon mode of $\vec{q}//[110]^*$, $\vec{e}//[1\bar{1}0]$. Recently, this effect of the lattice softening is reported to relate to the appearance of tweed contrasts and diffuse streaks, which are observed by electron microscopy in In-Tl[33], Fe-Pd[34] and other alloys exhibiting a thermoelastic martensitic transformation in a wide temperature range above M_S. Moreover, Yamada[35] et al. recently proposed a modulated lattice softening in order to explaine the appearance of extra spots in X-ray and electron diffraction patterns taken from the parent phase of a Ti-Ni shape memory alloy. The extra spots are observed in a wide temperature range before the R phase transformation. However, the soft phonon energy in those alloys described above does not fall into zero at M_S temperature, being different from the case of Nb_3Sn[36]. Therefore, those explanations by the lattice softening are not sufficient as the origin of martensitic transformation.

1-6 Effect of external forces on martensitic transformation and its thermodynamics.

1-6-1 Uniaxial stress and hydrostatic pressure.

The effect of stresses and hydrostatic pressures on martessitic transformations has been studied by many workers[31),(37)~(41)].

As a result, following characteristic features have been

found:

(1) Transformation temperatures are extensively shifted by these external forces, that is, they always increase in Fe-Ni-C[31] and Cu-Al-Ni[37)~(40)] alloys under a uniaxial stress. On the other hand, they decrease in an Fe-Ni alloy[31], but increase in a Au-Cd alloy[41] under a hydrostatic pressure.

(2) In addition to the shift of transformation temperatures, Otsuka et al[37)~(40)] have shown by using Cu-Al-Ni alloy single crystals that the stress-induced martensite is different from the thermally-induced one in crystal structure and morphology, depending upon test temperature. After their detailed investigations on the stress-induced martensitic transformations, they have proposed a phase diagram in stress-temperature coordinates [38], as schematically shown in Fig.5. According to this figure, β_1'(18R) martensite is stress-induced from the parent phase (β_1, DO_3) at temperatures above a critical one ($\sim A_f$), and on further loading new martensite α_1'(6R) is successively stress-induced from the β_1'. On unloading, reverse transformation $\alpha_1' \rightarrow \beta_1' \rightarrow \beta_1$ successively occurs. At temperatures below M_S, β_1'' ($18R_2$) martensite is stress-induced from γ_1'(2H) martensite and by further loading α_1' is successively induced from the β_1'', and upon unloading successive reverse transformation, $\alpha_1' \rightarrow \beta_1' \rightarrow \gamma_1'$ occurs. Otsuka et al. have also shown that each of the stress-induced martensites is a kind of long-period stacking order structures with a common basal plane. Those martensites are different only in their stacking order. Otsuka et al. have moreover shown[37)~(40)] that the interfaces between parent and martensite and between martensites are mobile, and crystal-

lographic correspondence between those two phases is reversible. Incidentally, shape memory and transformation pseudoelastisity effects are related to the characteristics of the crystallographic reversibility of martensites. That is, shape memory effect in a material is such that the shape change introduced by deformation of the martensites, excluding slip, reverts to the original shape of the parent state by heating the material above A_f, because of the unique correspondence between the parent phase and each martensite variant. In this sense, the material comes to memorize its original shape.

On the other hand, transformation pseudoelasticity effect is such that the strain due to the stress-induced transformation occurs or reverts under loading or unloading, respectively, because of the unique correspondence between the parent and stress-induced martensite phases.

In this way, stresses and hydrostatic pressures influence on martensitic transformations in not only the transformation temperature but also the inducement of a new martensite whose structure and morphology are different from those of thermally-induced one.

The effect of stresses and hydrostatic pressures on the shift of transformation temperatures was first explored theoretically by Scheil[42], and discussed more quantitatively by Patel and Cohen[31] and by Wollants[43] et al. According to the study by Wollants et al., the Gibbs chemical free energy G^* and entalpy H^* under the stress F and the hydrostatic pressure P are represented as follows,

$$H^* = U + PV - F\ell,$$

$$G^* = U + PV - TS - F\ell,$$

where U represents an internal energy, V a volume, T a temperature, S a entropy and ℓ the length of a specimen. They have shown that the thermodynamic equilibrium is attained by the condition of $G^{*M-P} = G^{*P} - G^{*M} = 0$, and they derived the Clausius-Clapeyron equation for the equilibrium between two phases under a stress or hydrostatic pressure,

$$\frac{dF}{dT} = -\frac{\Delta H^{*M-P}}{T\Delta\ell^{M-P}},$$

$$\frac{dP}{dT} = \frac{\Delta H^{*M-P}}{T\Delta V^{M-P}},$$

where $\Delta\ell^{M-P}$ represents the difference in elongation between two phases, that is, $\Delta\ell^{M-P} = \ell^P - \ell^M$, ΔV^{M-P} the volume change associated with the martensitic transformation, that is, $\Delta V^{M-P} = V^P - V^M$.

By the way, $\Delta\ell^{M-P}$ and ΔV^{M-P} in the above equation can be expressed with the shear (ε) and dilatational (ε_0) components of the habit plane since martensitic trnasformation occures by the shear-like mechanism, as mentioned before. That is,

$$\Delta\ell^{M-P} \simeq -(\varepsilon\cos\chi\cos\lambda + \varepsilon_0\cos^2\chi)\ell^P,$$

$$\Delta V^{M-P} = -\varepsilon_0 \cdot V^P,$$

where χ is the angle between the habit plane normal and tensile axis and λ the angle between the shear direction and tensile axis. As known from the Clausius-Clapeyron equation described above, the quantities of ΔH^{*M-P} and T are all positive, and therefore the shift of equilibrium temperature under a uniaxial stress or hydrostatic pressure depends on the value of $\Delta\ell^{M-P}$ or ΔV^{M-P}, respectively. However, martensitic transformation

does not occur at the equilibrium temperature but M_s, and therefore the above formula can not be applied to transformation temperatures. Then, Patel and Cohen[31] have proposed an equation to determine the shift of M_s temperature under a uniaxial stress or hydrostatic pressure. Outline of their work is as follows. The effect of an external force on the Gibbs chemical free energy curve is shown in Fig. 6, where $\Delta G^{M-P} = G^P - G^M$ represents the difference in Gibbs chemical free energy between the parent and martensite phases without external force. Under an external force, both of the Gibbs chemical free energies are changed, and the difference, ΔG^{*M-P}, is raised or lowered than ΔG^{M-P} by the quantity ΔW, that is

$$\Delta G^{*M-P} = \Delta G^{M-P} + \Delta W.$$

They derived the quantity of ΔW for stress and hydrostatic pressure as follows;

$$\Delta W = \sigma(\varepsilon \cos\chi\cos\lambda + \varepsilon_0 \cos^2\chi) = \varepsilon\tau + \varepsilon_0\,\sigma',$$

(for a uniaxial stress, per unit length of the parent phase),

$$\Delta W = -P\frac{\Delta V^{P-M}}{V^P} = -P\varepsilon_0,$$

(for a hydrostatic pressure, per unit volume of the parent phase) where σ represents the applied stress, τ and σ' are the stresses resolved parallel and perpendicular to the habit plane, respectively. Here, they made a very important hypothesis that as mentioned before the chemical driving force, $\Delta G^{M-P}(M_s)$, is independent of external forces but is dependent on only the composition of materials. By this hypothesis, the following equation has been derived to determine the transformation temperature, M_s', under an external force as follows;

$\Delta G^{*M-P}(M_s') = \Delta G^{M-P}(M_s)$, that is,

$$\Delta G^{M-P}(M_S') + \Delta W = \Delta G(M_S)^{M-P}.$$

According to the above equation, the shift of M_S temperature can be calculated if ΔG and ΔW are known. In order to confirm the propriety of the above equation, Patel and Cohen[31] have measured the relation between the shift of M_S temperature and critical stress or hydrostatic pressure to induce martensite, and compared these experimental relations with the calculated ones from the proposed equation. As a result, the experiment and calculation were in good agreement, and thus the propriety of the equation has been confirmed. After that, such propriety has been also confirmed by many workers[44],[45].

1-6-2 Magnetic field

A magnetic field is also one of external forces, and may influence on martensitic transformations in ferrous alloys and steels, because a large difference in magnetism exists between the austenitic and martensitic states. A study on the effect of a magnetic field on martensitic transformations was traced back to 1929, when Herbert[46] found that a quenched steel under a magnetic field increases in hardness, being compaired with the steel without a magnetic field. However, this finding was not understood as an interaction between magnetic field and martensitic transformation until 1961. In that year, Sadovsky et al. in the U. S. S. R.[47] firstly found that the martensitic transformation was induced by applying the pulsed magnetic field of 27.78 MA/m to an Fe-23Ni-1.5Cr-0.5C alloy. Since that time, many studies on the effect of a magnetic field on martensitic transformations have been carried out by using

a pulsed magnetic field, especially by Sadovsky's group[48)~(50)]. As a result, many characteristics have been found, as follows;

(1) Magnetic field-induced martensitic transformations are observed in many ferrous alloys and steels, such as Fe-Ni-Cr-C[48)], Fe-Ni-C[49)], Fe-Mn-C[50)] alloys, and so on.

(2) M_S temperature is raised by about 60K at the pulsed magnetic field of 27.78 MA/m.

(3) The amount of magnetic field-induced martensites depends on the strength of a pulsed magnetic field.

Moreover, Sadovsky's group investigated the effect of a steady magnetic field (~1.2 MA/m) on martensitic transformations in Fe-Ni-C alloys[51)], and showed that the amount of the steady magnetic field-induced martensites was the same as that of pulsed magnetic field-induced ones. From this fact, they concluded that there was no difference between the effects of steady and pulsed magnetic fields on martensitic transformations. The effect of a steady magnetic field on the martensitic transformation in an Fe-Ni alloy was examined in more detail by Saito and Suzuki[52)]. Sadovsky's group also investigated the effect of a pulsed magnetic field on the isothermal martensitic transformation in an Fe-Ni-Mn alloy[53)], and showed a magnetic field dependence on the amount of martensites. A similar work was done in more detail by Korenko and Cohen[54)], and they reported that a magnetic field influences on the nucleation rate of martensitic transformation.

Taking account of the above characteristics on the magnetic field-induced martensitic transformations, Sadovsky's group

proposed that the magnetic effect on martensitic transformation is due to the Zeeman energy effect alone, and they derived an equation to estimate the shift of M_S temperature due to this effect[55]. Outline of their work is as below. Under a magnetic field, each of the Gibbs chemical free energies of the austenitic and martensitic states is changed by the Zeeman energy which is the bilinear product of the magnetization and magnetic field, as follows:

$$G^{\gamma}(T,H) = G^{\gamma}(T) - M^{\gamma}(T)\cdot H, \quad \text{(1)}$$

$$G^{\alpha'}(T,H) = G^{\alpha'}(T) - M^{\alpha'}(T)\cdot H, \quad \text{(2)}$$

where G(T,H) and G(T) represent the Gibbs chemical free energies with and without a magnetic field, respectively, M(T) the spontaneous magnetization at a temperature, T, and γ and α' the austenitic and martensitic states, respectively. From the equations (1) and (2), the difference in Gibbs chemical free energy under a magnetic field is expressed as

$$\Delta G^{\alpha'-\gamma}(T,H)=\Delta G^{\alpha'-\gamma}(T)-\Delta M^{\alpha'-\gamma}(T)\cdot H=\Delta G^{\alpha'-\gamma}(T)+\Delta M(T)\cdot H, \quad \text{(3)}$$

where $\Delta M(T) = M^{\alpha'}(T) - M^{\gamma}(T)$. Using the equation (3), they derived an equation to determine the shift of M_S temperature under a magnetic field by referring to the idea previously described by Patel and Cohen[31]. That is,

$$\Delta G^{\alpha'-\gamma}(M_S) - \Delta G^{\alpha'-\gamma}(M_S') = \Delta M\cdot H, \quad \text{(4)}$$

where M_S' represents the transformation temperature under a critical magnetic field, H. In this equation they approximated that Gibbs chemical free energies of the austenitic and martensitic phases without a magnetic field are simply linear with temperature, and thus that $\Delta G^{\alpha'-\gamma}$ may be expressed by

using the quantities of the latent heat of transformation, q, and the equilibrium temperature of the two phases, To, as follows,

$$\Delta G^{\alpha'-\gamma}(M_S) = \frac{q}{To}(To - M_S), \quad \text{——— (5)}$$

$$\Delta G^{\alpha'-\gamma}(M_S') = \frac{q}{To}(To - M_S'). \quad \text{——— (6)}$$

From the equations (4), (5) and (6), the shift of M_S temperature, $\Delta M_S = M_S' - M_S$, under a magnetic field, is determined by the following equation,

$$\Delta M_S = \Delta M(M_S') \cdot H\ To/q. \quad \text{——— (7)}$$

In the above equation, ΔM is positive because the spontaneous magnetization in the austenite phase is well known to be generally lower than that in the martensite phase in many ferrous alloys undergoing a martensitic transformation, and therefore M_S temperatures for many ferrous alloys are raised under a magnetic field. They confirmed the propriety of the proposed equation by using an Fe-Ni alloy[55]. The same treatment was done by Satyanaryan et al.[56]. It is, thus, sure that magnetic fields influence on martensitic transformation like other external forces.

2. Purpose of the Study.

As mentioned above, martensitic transformations are influenced by a magnetic field in transformation temperature and the amount of martensite. Therefore, it is important to clarify the effect of a magnetic field on martensitic transformations to understand the kinetics, thermodynamics and mechanism. In carrying out such a clarification, not only systematic detailed measurements but also precise analyses are needed.

However, the previous studies made on magnetic field-induced martensitic transformations were not sufficient as to such systematic measurements and precise analyses. That is, relation between transformation temperature and critical magnetic field to induce martensitic transformation was not examined over so wide ranges of temperature and magnetic field, even though such an examination may bring in very important information for the effect of a magnetic field on martensitic transformations. Moreover, data on magnetic field dependences of the amount and morphology of magnetic field-induced martensites have not been obtained so much. Furthermore, the materials examined so far were mainly commercial ones containing many elements, whose magnetic properties of both the austenitic and martensitic states and thermodynamics and crystallography of thermally-induced martensitic transformations have not been well investigated. Therefore, their thermodynamical analysis for the effects of a magnetic field on martensitic transformations were made ambiguously. In addition to the problems described above, there remain many problems on magnetic field-induced martensitic transformations. Those problems are also very important to know magnetic effects on martensitic transformations, and they are summerized as follows;

(1) All of previous studies were concerned with polycrystalline specimens and therefore the obtained information might be affected by the existence of grain boundaries. Moreover, no information has been obtained about the influence of crystal orientations on magnetic field-induced martensitic transformations.

(2) Some of ferrous alloys and steels undergoing a martensitic transformation have an invar effect, and there may be an influence of the invar effect on magnetic field-induced martensitic transformations. However, there is no information on this problem.

(3) All of previous studies were concerned with disordered alloys, and there is no information about the effect of the degree of order on magnetic field-induced martensitic transformations.

(4) Ferrous alloys and steels undergoing a martensitic transformation are ferromagnetic or paramagnetic in the austenite states, but they are all ferromagnetic in the martensitic state. Therefore, there may be some influence of the difference in the austenitic magnetism on magnetic field-induced martensitic transformation, but there is no work about it.

(5) All of previous studies were concerned with materials undergoing a non-thermoelstic martensitic transformation, and there is no information on the effect of a magnetic field on thermoelastic martensitic transformations. Incidentally, thermoelstic martensitic transformation with a small temperature hysterisis is known to be accompanied by a pseudoelastic effect, as mentioned before. That is, if strain is caused by stress-induced martensitic transformation on loading, it disappears by the reverse transformation on unloading. It can therefore be expected that the magnetic field-induced martensite behaves to be similarly reversible under a magnetic field.

(6) As mentioned before, Sadovsky's group have proposed an equation to estimate the shift of M_S temperature under a mag-

netic effect[65]. However, its propriety has been shown only for the case of H=27.78 MA/m and $\Delta M_S \simeq 50K$ for a few materials. Moreover, the proposed equation has been derived by assuming that Gibbs chemical free energy of the austenite and martensite phases is simply a linear relation with temperature. However, the situation is not so simple in real alloy systems, and therefore the equation may be said to be an approximation. Thus, the equation is needed to reexamine its propriety.

In the present study, therefore, magnetic field-induced martensitic transformations in ferrous alloys (Fe-Ni poly and single crystals, invar and non-invar Fe-Ni-C polycrystals, disordered and ordered Fe-Pt polycrystals, paramagnetic Fe-Mn-C polycrystals and ausaged Fe-Ni-Co-Ti polycrystals) are examined in detail to make the above problems clearer, by carrying out magnetization measurements and optical microscopy, a pulsed magnetic field being applied at the High Magnetic Field Laboratory of Osaka University. The present paper consists of the following seven chapters, and the content and the materials used in each Chapter are shown below;

Chapter 2 Influence of the alloy composition on magnetic field-induced martensitic transformation:
Fe-29.9, -31.7 and -32.5at%Ni polycrystal alloys.

Chapter 3 Influence of crystal orientation and contribution of grain boundary:
Fe-31.6at% single crystal alloy.

Chapter 4 Influence of the invar effect:
Fe-28.7Ni-1.8C, Fe-29.0Ni-1.4C invar alloys and
Fe-24.7Ni-1.8C (at%) non-invar alloy.

Chapter 5 Influence of the degree of order:
Fe-24.0at%Pt polycrystal alloy
($S<0.5$, $S\sim0.7$, $S\sim0.8$)

Chapter 6 Influence of the difference in austenitic magnetism:
Fe-3.9at%Mn-5.0at%C alloy

Chapter 7 Influence of the thermoelastic nature on martensitic transformations and verification of magnetoelastic martensitic transformation:
Fe-31.9Ni-9.8Co-4.1Ti alloy (at%)

Chapter 8 Derivation of new formula to determine the shift of M_S temperature due to a magnetic field and quantitative verification of the formula:
Fe-29.9, -31.7 and 32.5at%Ni, Fe-24.0at%Pt ($S\sim0.8$) and Fe-24.7at%Ni-1.8C alloys

In Chapter 8, it will be quantitatively verified that the influence of a magnetic field on martensitic transformations in invar alloys consists of three effects, that is, the magnetostatic energy, high field susceptibility and forced volume magnetostriction effects.

References

(1) F. Osmond: Compt. rend., 118 (1894), 532.

(2) H. Shoji: Zeits Krist., 77 (1931), 381.

(3) J. S. Bowles: Trans. AIME, 189 (1951), 44.

(4) Z. Nishiyama: Sci. Rep. Tohoku Univ., 23 (1934), 637.

(5) E. J. Efsic and C. M. Wayman: Trans. AIME., 239 (1967),873.

(6) W. Schmidt: Arch. Eisenhütt., 3 (1929/30), 293.

(7) V. V. Nemirovsky: Fiz metal. metalloved., 25 (1968), 900.

(8) H. M. Otte: Acta Met., 8 (1960), 892.

(9) P. M. Kelly: Acta Met., 13 (1965), 635.

(10) R. S. Toth and H. Sato: Acta Met., 16 (1968), 413.

(11) D. Hull and R. D. Garwood: J. Inst. Metals., 86 (1957/58) 485.

(12) L. Delaey: Z. f. Metallk., 58 (1967), 388.

(13) W. J. Buehler, J. V. Gilfrich and R. C. Wiley: J. appl. Phys., 34 (1963), 1475.

(14) H. M. King: Inst. Metals Monograph, 33 (1969), 196.

(15) B. M. Batterman and C. S. Barrett: Phys. Rev. Letters, 13 (1964), 390.

(16) G. V. Kurdjumov and G. Sachs: Z. Phys., 64 (1930), 325.

(17) Z. Nishiyama: Sci. Rep. Tohoku Univ., 23 (1934), 637.

(18) M. S. Wechsler, D. S. Lieberman and T. A. Read: Trans. AIME, 197 (1953), 1503.

(19) D. S. Lieberman, M. S. Wechsler and T. A. Read: J. Appl. Phys. 26 (1955), 473,

(20) J. S. Bowles and J. K. Mackenzie: Acta Met., 2 (1954), 129.

(21) J. K. Mackenzie and J. S. Bowles: Acta Met., 2 (1954), 138.

(22) J. S. Bowles and J. K. Makenzie: Acta Met., 2 (1954), 224.

(23) J. F. Breedis and C. M. Wayman: AIME, 224 (1962), 1128.

(24) E. J. Efsic and C. M. Wayman: AIME, 239 (1967) 873.

(25) K. Otsuka and K. Shimizu: Trans. Jpn Inst. Met., 15 (1974), 103.

(26) G. V. Kurdjumov and O. P. Maximova: Dokl. Akad. Nauk S. S. S. R., 61 (1948), 83.

(27) T. Tadaki and K. Shimizu: Scripta Metall, 9 (1975), 771.

(28) L. Kaufman and M. Cohen: Thermodynamics and Kinetics of Martensitic Transformation, Progress in Metal Physics Vol. 7 NO. 3 (1958) p. 165.

(29) K. Otsuka and K. Shimizu: Proc Int. Conf. Solid-Solid Phase Transformations. Pittsburgh(1981) p. 1261.

(30) K. Otsuka and K. Shimizu: Scripta Met., 11 (1977), 757.

(31) J. R. Patel and M. Cohen: Acta Met., 1 (1953), 531.

(32) N. Nakanishi, Y. Murakami and S. Kachi: Scripta Met., 2 (1968), 673.

(33) A. Lasalmonie and P. Costa: Proc of Int. Conf. on Martensitic Transformations, ICOMAT-79, Cambridge, (1979), 538.

(34) M. Sugiyama, R. Oshima and F. E. Fijita: Trans. JIM., 10 (1986), 719.

(35) Y. Yamada, Y. Noda, M. Takimoto and K. Furukawa: J. Phys. Soc. Japan. 55 (1985), 2940.

(36) J. D. Axe and G. Shirane: Phys. Rev., B8 (1973), 1965.

(37) K. Otsuka, T. Nakamura and K. Shimizu: Trans. JIM, 15 (1974), 200.

(38) K. Otsuka, H. Sakamoto and K. Shimizu: Scripta Met., 10 (1976), 983.

(39) K. Otsuka, C. M. Wayman, N. Nakai, H. Sakamoto and K. Shimizu: Acta Met., 24 (1976), 207.

(40) K. Otsuka, H. Sakamoto and K. Shimizu: Acta Met., 27 (1979), 585.

(41) Y. Gefen, A. Halwany and M. Rosen: Phil. Mag., 28 (1974),1.

(42) E. Scheil: Z. Anorg. Allg. Chem., 207 (1932), 21.

(43) P. Wallants, M. DeBonte and J. R. Roos: Z. Metallkd., 70 (1979), 113.

(44) H. POPS: Metall. Trans., 1 (1970), 251.

(45) R. W. Rohde: Acta Met., 18 (1970), 903.

(46) E. G. Herbert: iron and Steel Inst., 120 (1929), 239.

(47) V. D. Sadovsky, N. M. Rodigin, L. V. Smirnov, G. M. Filonchik and I. G. Fakidov: Fiz. metal. metalloved., 12 (1961), 302.

(48) YE. A. Fokina and E. A. Zavadsky: Fiz. metal metalloved., 16 (1963), 313.

(49) YE. A. Fokina, L. V. Smirnov and V. D. Sadovsky: Fiz. metal. metalloved., 27 (1969), 756.

(50) P. A. Malinen and V. D. Sadovsky: Fiz. metal. metalloved., 28 (1969), 1012.

(51) YE. A. Fokina, L. V. Smirnov, V. D. Sadovsky and A. F. Prekul: Fiz. metal. metalloved., 19 (1965), 932.

(52) H. Saito and Y. Suzuki: Collected Abstracts of the Autumn Meeting of Japan Inst. Metals. (1972), P. 27 (in Japanese)

(53) YE. A. Fokina, L. V. Smirnov and V. D. Sadovsky: Fiz. metal. metalloved., 19 (1965), 722.

(54) M. K. Korenko and M. Cohen: Proc of Int. Conf. on Martensitic Transformations, ICOMAT-79, Cambridge, MA, 1979, p. 388.

(55) M. A. Krivoglaz and V. D. Sadovsky: Fiz. metal. metalloved., 18 (1964), 502.

(56) K. R. Satyanaryan, W. Eliasz and A. P. Miodownik: Acta Met., 16 (1968), 877.

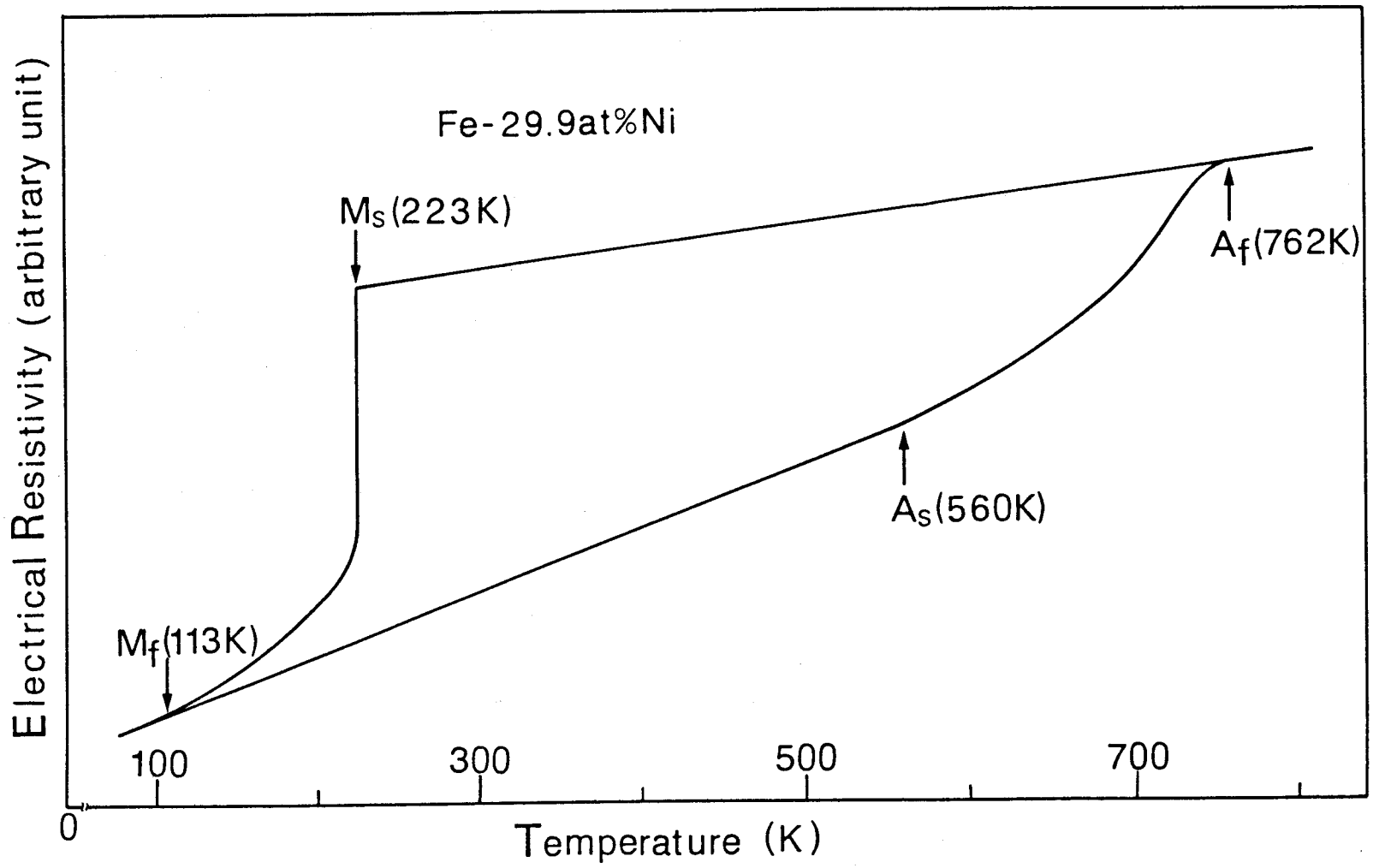

Fig. 1 Electrical resistivity vs. temperature relation in an Fe-29.9at%Ni polycrystal.

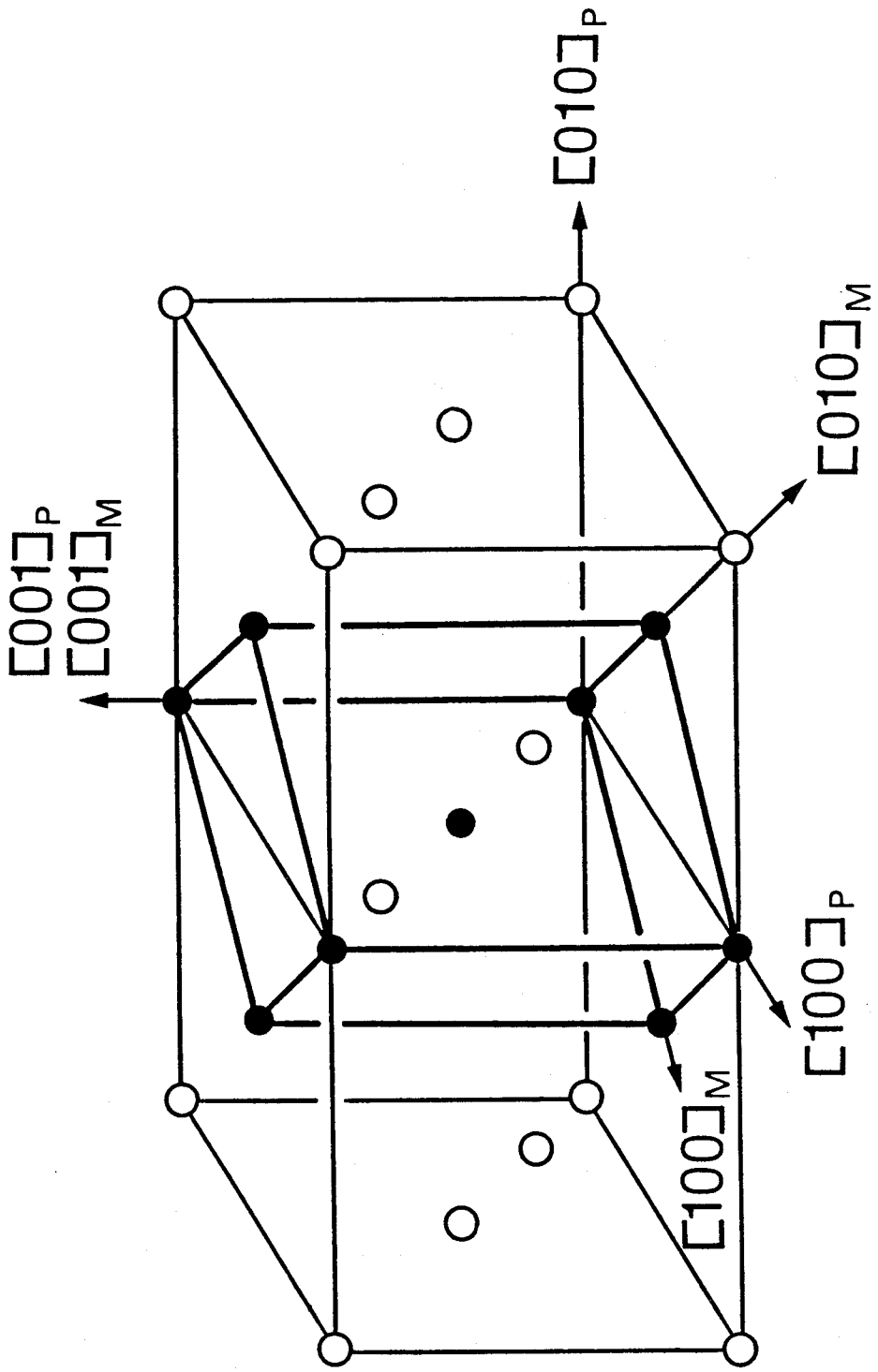

Fig. 2 Bain correspondence in the transformation from fcc to bcc.

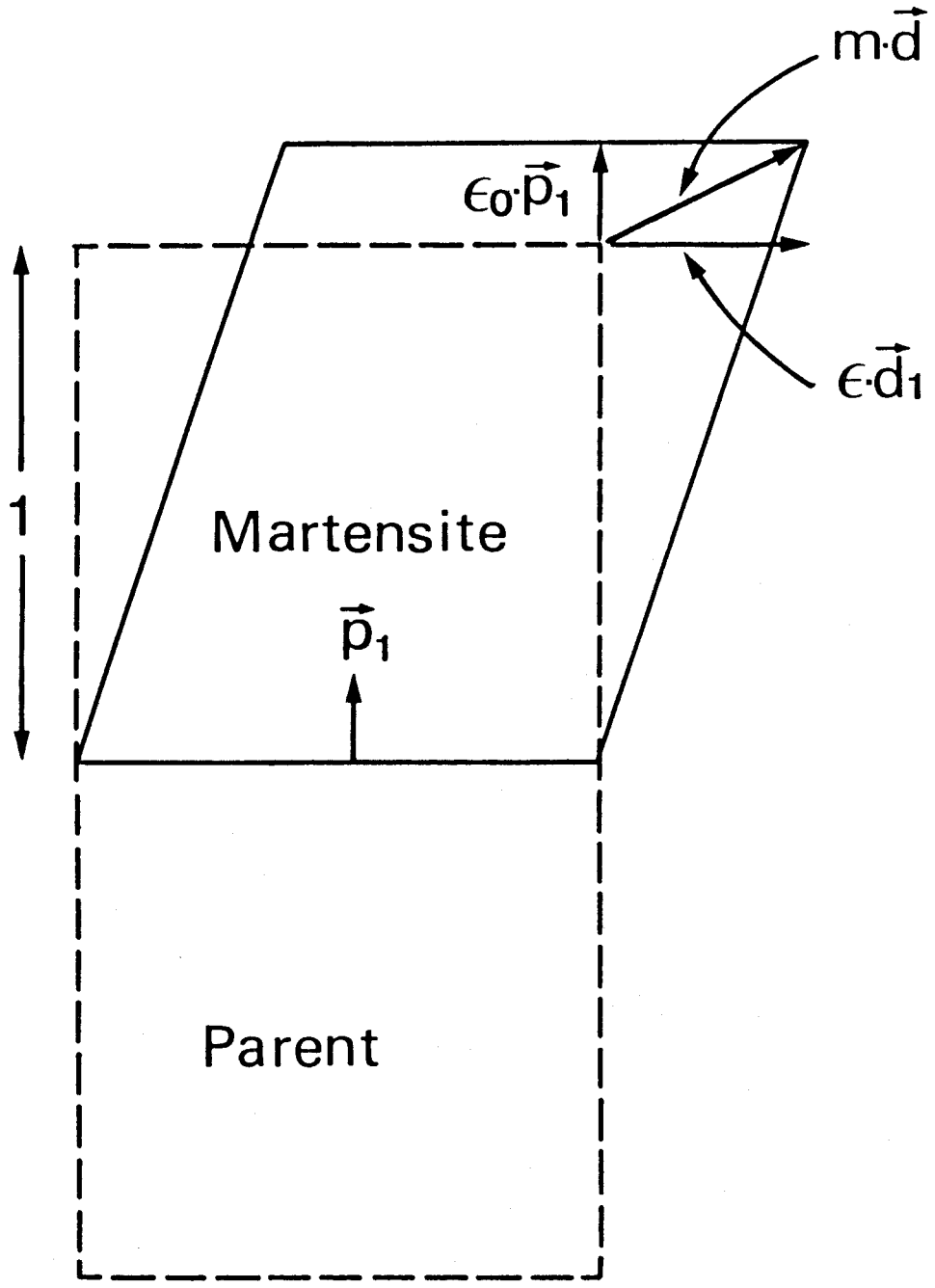

Fig. 3 Schematic illustraction of the shape change associated with a martensitic transformation.

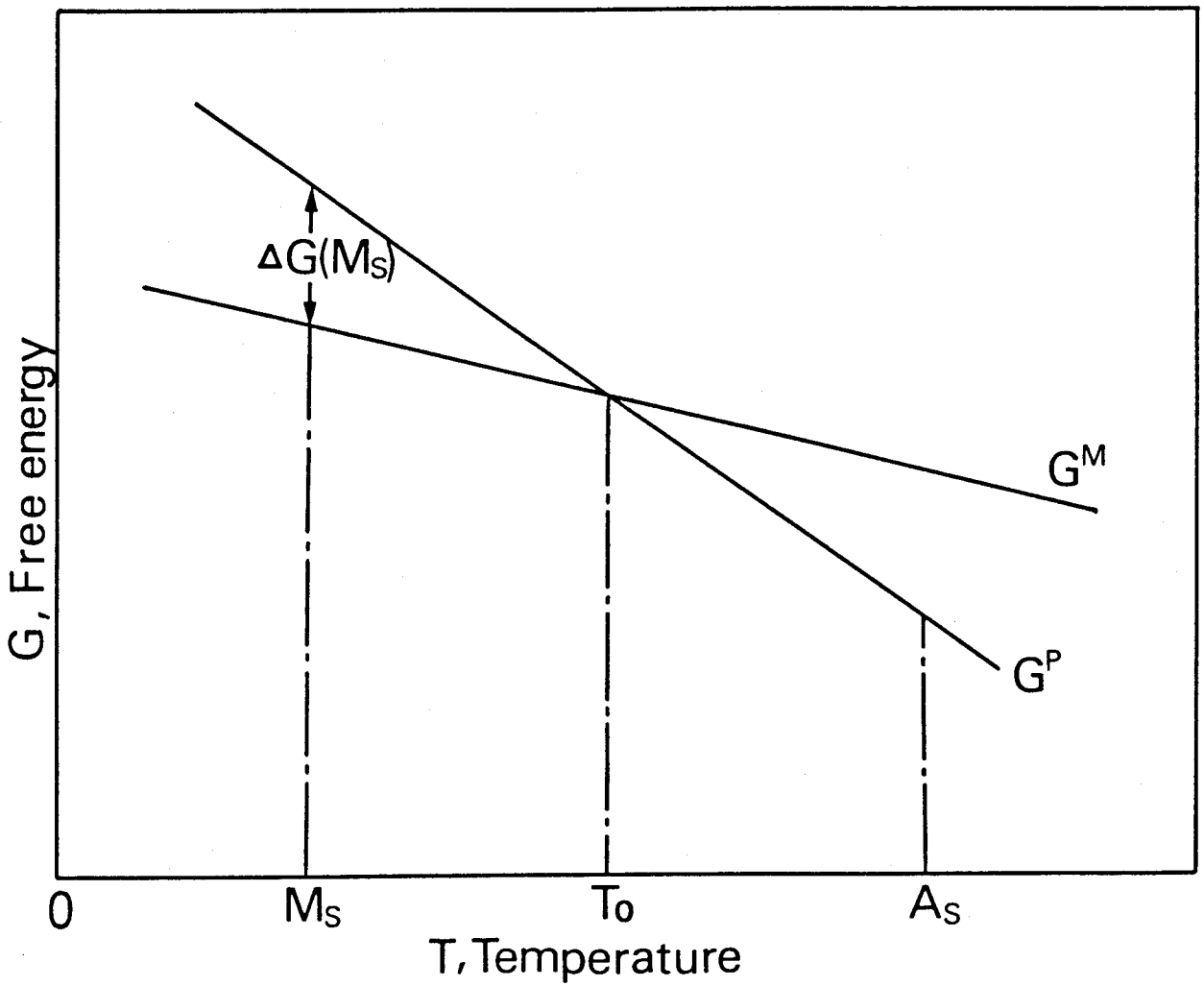

Fig. 4 Schematic Gibbs chemical free energies of the parent and martensite phases as a function of temperature.

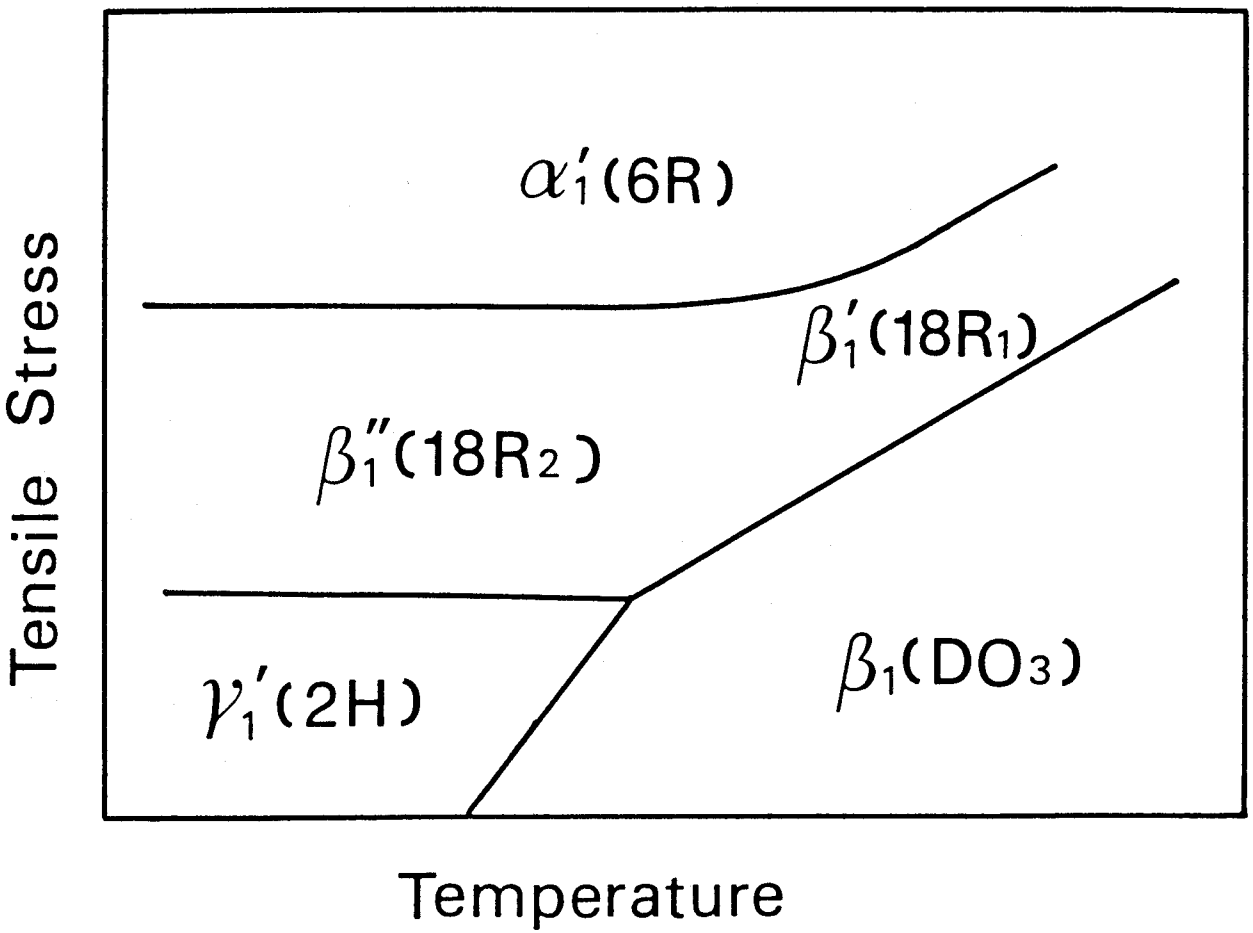

Fig. 5 Schematic phase diagram in temperature-stress coordinates of an Cu-Al-Ni alloy. (after Otsuka et al.).

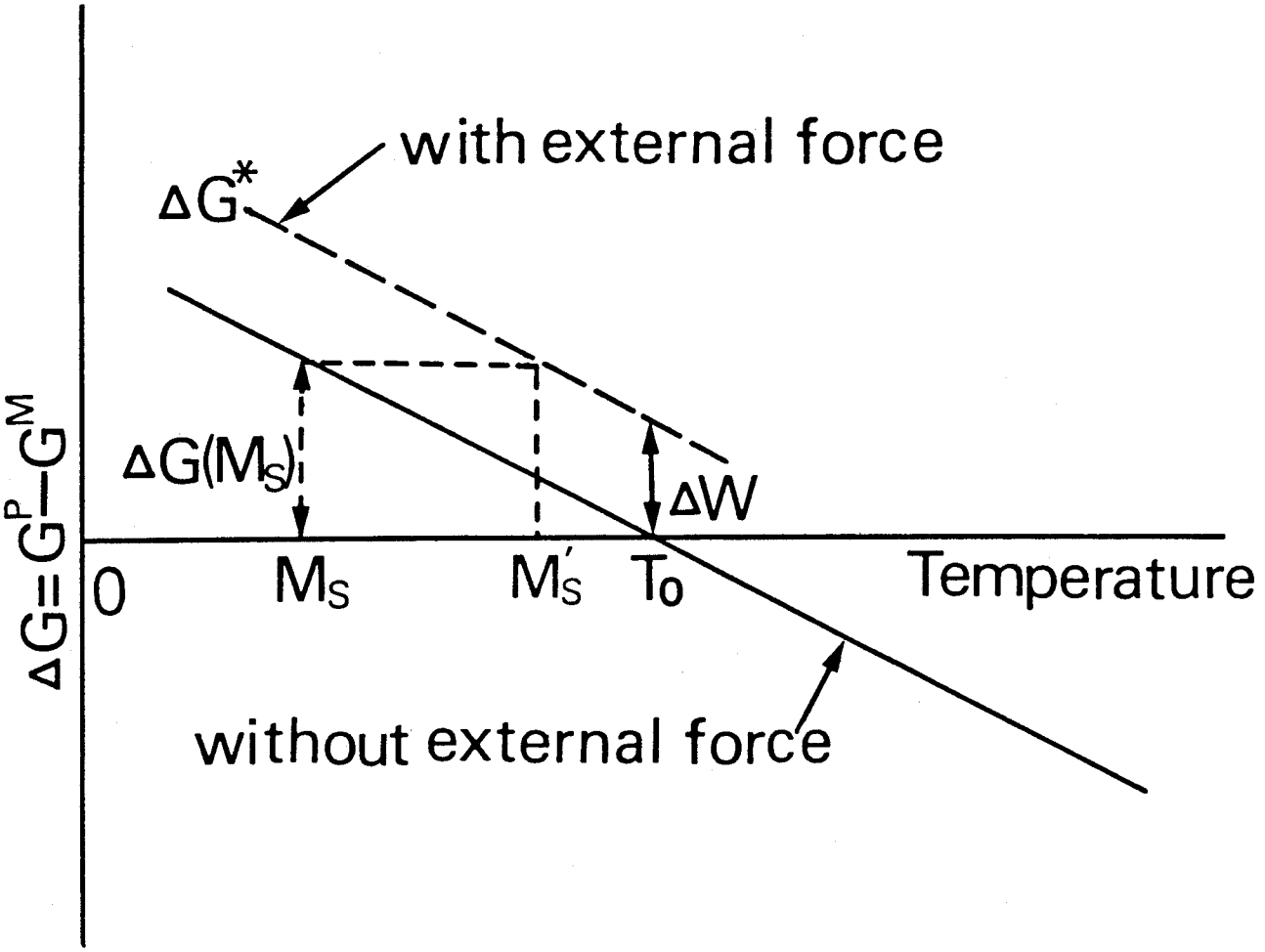

Fig. 6 Schematic diagram of the shift of M_s temperature due to an external force (after Patel and Cohen.).

Chapter 2

Magnetic Field-Induced Martensitic Transformations in Fe-Ni Alloys and Their Composition Dependence.

Synopsis

The magnetic field-induced martensitic transformations in Fe-Ni alloys and their composition dependence have been examined by carrying out magnetization measurements and optical microscopy of Fe-29.9, -31.7 and -32.5 at%Ni alloys. Critical magnetic field dependence of the shift of M_S temperatures of martensitic transformations in the alloys exhibits a little curved line. The slope of the little curved lines becomes larger in the order of 31.7, 29.9 and 32.5 at%Ni compositions. That is, the influence of magnetic field on the shift of M_S temperature is most effective in the Fe-31.7 at%Ni alloy.

The amount of magnetic field-induced martensites in the Fe-29.9, -31.7 at%Ni alloys is almost constant without regard to the strength of magnetic field, if $\Delta T(=T-M_S)$ is kept constant, but that in the 32.5 at%Ni alloy increases with the strength of applied magnetic field for any ΔT.

The morphology of magnetic field-induced martensites (including internal structures) is the same as that of thermally-induced ones in each alloy irrespective of ΔT and the strength of magnetic field, and therefore the morphology is independent of the formation temperature. It is suggested from a thermodynamical analysis that the effect of a magnetic field on the martensitic transformations in Fe-Ni alloys is due to not only the Zeeman and high field susceptibility effects but also other unknown effects.

I. Introduction

Martensitic transformations from fcc to bcc in Fe-Ni alloys with the Ni content of 0~33 at% have been extensively investigated by many researchers[1]~[4], and their thermodynamics and crystallography of the thermally-induced martensitic transformations have been well known until now. Fe-Ni alloys with the Ni content of 30~50 at% are known to have an invar effect, and a lot of physical quantities of the alloys have been investigated as a function of composition, such as the spontaneous magnetization in the austenitic state etc.[5]~[8]. Therefore, the Fe-Ni alloys are most suitable for investigating the effect of a magnetic field on the martensitic transformations and their composition dependence. However, such an investigation has not been systematically done, and moreover the amount and morphology of magnetic field-induced martensites have not been examined by varying the formation temperature. In the present investigation, therefore, the Fe-Ni alloys with different Ni contents have been examined to make the above problems clearer, by carrying out magnetization measurements under a pulsed ultra high magnetic field and optical and transmission electron microscopy.

II. Experimental Procedures

Fe-Ni alloys with the compositions of 29.9, 31.7 and 32.5 at%Ni were prepared by melting in an induction furnace under argon atomosphere and by casting into a water-cooled iron mold, the ingot size being 18mmϕ × 50mm. Chemical analysis was done for both the top and bottom sides of the ingots. The composi-

tions of both the sides were in good agreement within error, and the above compositions are averaged ones. Each ingot was hot-forged at 1373K, homogenized at 1473K for 8.64×10^4s in an evacuated silica capsule, and then cut into 40mm length pieces. Each of the pieces was hot-rolled into a 0.5mm thick sheet and then cold-rolled into a 0.3mm thick sheet. Specimens of 3mm × 20mm × 0.3mm size were cut from the sheet, and they were austenitized at 1473K for 1.08×10^4s in evacuated silica capsules, followed by furnace-cooling in order to avoid quenching strain. All the austenitized specimens were cut into a half length (3mm × 10mm × 0.3mm) by a spark-cutting machine, and one was used for electrical resistivity measurements to determine M_S temperature, and the other for magnetization measurements. Specimens exhibiting the same M_S temperature for each alloy were used for the present experiments. The size of the specimens was optimized to avoid the Joule heating and skin effect.

High field magnetization measurements were performed at the High Magnetic Field Laboratory, Osaka University. Reproducible fields up to 31.75 MA/m are generated in a 60mm bore single layer magnet with a 1.25 MJ capacitor bank. The typical pulse durations were 0.3~0.4m sec. Pulsed magnetic fields H(t) were measured by electrically integrating the out put of a single-turn pick-up coil set in the magnet. The value of H (t) was calibrated by the submillimeter ESR within the accuracy of ±0.3%. Magnetizations of the specimens were measured using balanced pick-up coils.

A block diagram for magnetization measurements is shown

in Fig. 1. Pick-up coils consist of three parts, A-C and they are coaxially wound to each other. Coil A is wound with 100 turns, the inner diameter being 4mm, and picks up the magnetic flux change in the specimen, Coil B is wound on the coil A with 50 turns in opposite direction to compensate the background flux change due to the transient field, Cross section of the coil B is twice as large as that coil A so as to make the net flux in coil A equal that in coil B. The out put signal of the pick-up coils was also electrically integrated to give the Magnetization, M(t). Both H(t) and M(t) were recorded in a dual-channel 8 bit digital transient recorder with the time resolution of 0.5μsec. The residual back ground noise in M(t) was elimenated by a microcomputer, substracting data without the specimen in the pick up coils from M(t). The magnetization measurements were carried out in the temperature range of 77K~300K.

The pick-up coils, specimens and a heater were set in a glass dewar of 2.5 cm i. d.. The temperature regulation was done by adjusting current of the heater and the evaporation of liq. N_2 contained below the specimen.

The accuracy of the temperature was within ±0.5K. More details of the pulsed magnetic field instrument were described in (9). Incidentally, the out put corresponding to the magnetization from pick-up coil is proportional to $\frac{dM}{dt}$, the cross section of specimen and $1-N(\equiv\alpha)$, where N is the demagnetizing factor.

The value of α depends on the length of the specimen, and the dependence must be measured in order to know the absolute

value of magnetization.

In the present study, therefore, the dependence of α on specimen length of the pure iron has been obtained by magnetization measurements because the spontaneous magnetization of a pure iron has been well investigated.

After a magnetic field was applied, each of the specimens was chemically etched by 5% nital solution and supplied for an optical microscopy observation. Then, thin foils for electron microscopy observation were made by electro-polishing the specimens. The electron microscope used was a Hitachi HU-650, operated at 500kV.

III. Results

3-1. Transformation temperature and austenitic magnetic moment

Electrical resistivity vs. temperature measurements were made in order to determine M_S temperatures of the present Fe-Ni alloys in the temperature range from 293 to 77K. The M_S temperatures determined are listed in Table 1. They clearly decrease with increasing Ni composition, as have been reported by many workers. Spontaneous magnetization in the austenitic state has been measured as a function of temperature, and the magnetic moment for the alloys at 273K are listed in Table 1. It is known from the table that the austenitic magnetic moment changes greatly in spite of the small change of Ni composition. Such a large change is well known as a characteristic feature of Fe-Ni alloys in the invar region, and thus the present Fe-Ni alloys are known to surely be in the invar region. The austenitic magnetic moments as a function of temperature

difference, $\Delta T(=T-M_S)$, from M_S temperature for the alloys are shown in Fig. 2. These values indicate that the austenitic magnetic moment decreases with decreasing Ni composition and with increasing ΔT. On the other hand, according to an earlier paper[5], the magnetic moment of the martensitic state of Fe-Ni alloys changes little with Ni composition even if the alloys are in the invar region, and its value at 0K is known to be about $2\mu B$. This value may be considered to be valid in the temperature range examined in the present study, because the Curie point of the martensitic state is so high. Accordingly, the difference in the magnetic moment between the austenitic and martensitic states becomes smaller with increasing Ni composition and decreasing ΔT. The difference at $\Delta T=70K$ is shown for the three Fe-Ni alloys in Table 1. Therefore, the change in Ni composition is expected to have a significant influence on the magnetic field-induced martensitic transformations at temperatures above respective M_S.

3-2. Critical magnetic field to induce martensite

The critical magnetic field to induce martensitic transformation has been determined by performing magnetization measurements as follows: The length-wise direction of each specimen was setted parallel to the applied direction of magnetic field, and the specimen was kept at a temperature (T) higher than M_S. A low magnetic field (1.59 MA/m) was first applied to the specimen in order to know the magnetic properties in the austenitic state. This magnetic field was lower than the critical one to induce the martensitic transformation. After

that, M(t)-H(t) curves have been recorded every maximum strength which is increased by about 0.8 MA/m, and an increase of magnetization due to the occurence of martensitic transformation becomes to be recognized when the maximum strength of magnetic field has reached a certain value. This maximum strength of magnetic field is defined as a critical magnetic field at the temperature, T, which corresponds to the transformation temperature, M_S'.

On the other hand, M-H curve was recorded using another specimen, a magnetic field higher than the critical one being applied from the beginning. In this curve, an increase of magnetization due to the martensitic transformation is recognized at a certain strength of the magnetic field, and this strength is found to be the same as that of the critical field obtained as above. Such typical M(t)-H(t) curves thus obtained are shown in Fig. 3 (a), (b) and (c), which have been obtained for the Fe-29.9, -31.7 and -32.5 at%Ni alloys, respectively. It is noted in Fig. 3 that a change of magnetization due to the martensitic transformation occurs at the critical field, as indicated with an arrow on each curve. The relation between the critical fields thus obtained and the shift of M_S temperature, $\Delta M_S (=M_S'-M_S)$, is shown in Fig. 4. This figure indicates that the critical fields increase with increasing ΔM_S for all the alloys, forming a curved line. Another characteristic feature noted in Fig. 4 is that the critical fields for the Fe-31.7 at%Ni alloy are lower than those of the other two alloys without regard to ΔM_S. This means that the influence of a magnetic field on the increase of M_S temperature is mostly effective in the Fe-31.7 at%Ni alloy. This result can not be explained by the

previous formula, $\Delta M_S = \Delta M(M_S') \cdot H \cdot To/q$, proposed by Krivoglaz and Sadovsky[10], which was derived by considering that the effect of a magnetic field on martensitic transformations results in the Zeeman effect alone, as mentioned Chapter 1. The formula suggests that critical magnetic field at a given ΔM_S becomes smaller with decreasing Ni composition, because the difference in spontaneous magnetization between the austenitic and martensitic states becomes larger with decreasing Ni composition if To/q is constant irrespective of the Ni comtent. To/q has been calculated following Kaufman and Cohen's equation[2] for the present alloys. As a result, it has been confirmed to be almost the same for all the alloys, being about 0.16K mol/J. Therefore, the critical field at a given ΔM_S is expected to becomes smaller in that order of the magnitude of $\Delta M(M_S')$, namely in the order of Fe-29.9, -31.7 and -32.5 at%Ni alloys.

However, the experimentally determined critical fields are not in that order. This means that Krivoglaz and Sadovsky's formula does not hold in the case of Fe-Ni alloys. Moreover, ΔM_S calculated from the formula is not agreement with that experimentally measured, especially for large values of applied magnetic fields. For example, ΔM_S of the Fe-31.7 at%Ni alloy has been calculated by inserting 0.8 μB, 26.98 MA/m and 0.16K mol/K for $\Delta M(M_S')$, H and To/q, respectively, into the formula. The calculated ΔM_S was about 24K, but it differs from the experimental one, 70K. These results indicate that the effect of magnetic field on martensitic transformations results in not only the Zeeman effect but also other magnetic effects. The other effects will be discussed later.

3-3. Amount of magnetic field-induced martensite

The amount of magnetic field-induced martensites can be obtained by calculating from the result of magnetization measurements, because the fraction of the martensites, C (%), is related to the magnetization and is given by the following equation,

$$C = \frac{M^{\alpha'+\gamma}(T) - M^{\gamma}(T)}{M^{\alpha'}(T) - M^{\gamma}(T)} \times 100 ,$$

where $M^{\gamma}(T)$ and $M^{\alpha'}(T)$ represent the spontaneous magnetization in the austenitic and martensitic phases at a temperature, T, and $M^{\alpha'+\gamma}(T)$ the spontaneous magnetization of the mixture of martensitic and austenitic phases at T. The calculated amounts by this method for the three Fe-Ni alloys are shown in Fig. 5, which are plotted as a function of the maximum strength of the pulsed magnetic fields. In order to check the propriety of the above method, the amount of thermally-formed martensites in the Fe-31.7at%Ni alloy was also calculated in the same way as to the specimens cooled to various temperatures below M_S, as shown in Fig. 6. It was consistent with that obtained by another metallographic method[11], meaning that the amounts in Fig. 5 are appropriate ones.

It is noted in Fig. 5 that the amount of martensites in the Fe-32.5at%Ni alloy increases with the maximum strength of the magnetic field, but that in the Fe-29.9 and -31.7 at%Ni alloys does not change, provided that ΔT is kept constant. Such a difference in martensite amounts of two groups of alloys can also be seen on the magnetization curves in Fig. 3, (c) for the former alloy exhibiting a gradual increase of magnetization, and (a) and (b) for the latter two alloys exhibiting

an abrupt increase of magnetization after the strength of magnetic field has reached the respective critical one. The gradual increase of martensite amounts in the former alloy can be observed by optical microscopy. According to the observation, the increase of martensite amounts is due to not only the formation of new martensite plates but also the growth of existing plates, as seen in Fig. 7 which is a series of optical micrographs. (a) shows a martensite structure after the critical magnetic field has been applied at $\Delta T=25K$, which was taken at room temperature after polishing and etching with 5% nital. (b) shows an unetched martensite structure after a magnetic field higher than the critical field has been successively applied to the same alloy at the same temperature, which was taken from the same place as in (a). Surface relief in (b) newly forms at the interface of the existed martensite, as indicated with an arrow in (a). This indicates that the existed martensite grows by applying a higher magnetic field. In order to make it more clear, the specimen was etched, and the etched structure is shown in (c). Comparison of (b) with (c) clearly indicates that the martensite exhibiting the surface relief in (b) has the same orientation as that indicated with an arrow in (a). That is, the surface relief in (b) arises as a result of the growth of arrowed martensite in (a). This indicates that martensite plates in the Fe-32.5at%Ni alloy can successively grow by applying a higher magnetic field, that is, they are partly thermoelastic. On the other hand, martensite plates in the Fe-29.9 and -31.7 at%Ni alloys are spontaneously formed when magnetic field has reached the critical one, provided that ΔT is kept constant, and they do not grow fur-

ther even if a higher magnetic field has been applied; that is, they are non-thermoelastic. However, all the alloys exhibit a similar tendency in that the amount of magnetic field-induced martensites increases with decreasing ΔT.

3-4. Morphology of magnetic field-induced martensite

Fig. 8 shows optical micrographs of thermally-induced lenticular martensites formed by cooling a little below the respective M_S temperatures, (a) (d) and (g), and those of magnetic field-induced ones, (b), (c), (e), (f), (h) and (i), which were taken from the present three alloys. ΔT, formation temperature and H for the magnetic field-induced martensites are inscribed in each photograph of the figure. It is noted in the figure that the morphology (including internal structures) of the magnetic field-induced martensites is almost the same as that of the thermally-formed ones without regard to ΔT and H, provided that the Ni cmoposition is the same. That is, the magnetic field-induced martensites are lenticular, interfaces between austenite and martensite crystals become more smooth, and the internally twinned regions corresponding to the mid-rib become wider with increasing Ni content. These features are the same as those of thermally-induced martensites, as is easily seen from a comparison among (a), (d) and (g). Such a morphological change with Ni content of martensites in Fe-Ni alloys is the same as that reported by Patterson and Wayman[4]. Fig. 9 shows typical electron micrographs of magnetic field-induced martensites, (a) and (b) being a bright and dark field images, respectively. There are seen a mid-rib with twin

faults, as have been observed in thermally-induced martensites. Therefore, no difference between magnetic field-induced and thermally-induced martensites can be conceived even in the electron microscopic observation.

By the way, it is well known in the Fe-Ni alloys that lath and lenticular martensites are thermally-induced at temperatures above and below 273K, respectively. However, the magnetic field-induced martensites in Fig. 8 (c) exhibit a lenticular shape even though they are produced at 295K. This suggests that the formation temperature itself is not an essential factor to determine the morphology of martensites in Fe-Ni alloys. This is different from the observation that martensite morphology in Fe-Ni-C alloys is determined mainly by the formation temperature[12]. The reason for such a differences in morphological variation between Fe-Ni and Fe-Ni-C alloys is not yet clear.

IV. Discussion

As pointed out already, effects of a magnetic field on martensitic transformations in Fe-Ni alloys can not be explained by the Krivoglaz-Sadovsky's formula, $\Delta M_S = \Delta M(M_S') \cdot H \cdot To/q$. To begin with, it should be pointed out that two important things were not taken into consideration in deriving the formula. One is that the Gibbs chemical free energies of the austenite and martensite phases are simply assumed to be a linear relation with temperature. However, the situation is not so simple in real alloy systems, and therefore the formula is an approximation. The other point is that an increase of magneti-

zation, which is accompanied by increasing the strength of the magnetic field, is neglected, even though it is fairly large as seen from the M(t)-H(t) curves of Fig. 3. That is, in Fig. 3, the magnetization in the austenitic state increases considerably with increasing strength of magnetic field before martensites have been induced, especially in the case of Fe-29.9 at%Ni alloy, while the magnetization in the almost martensitic state does not so increase. This suggests that the high field susceptibility in the austenitic state, $\overset{\gamma}{\chi}hf$, is substantially large but that in the martensitic state is neglegibly small, χhf being an increasing ratio of magnetization per unit strength of magnetic field at a given temperature, T. However, the effect of the high field susceptibility on martensitic transformations has not been taken into consideration in the previous formula. Consequently, a more exact expression must be used for the Gibbs chemical free energy, as proposed by Kaufman and Cohen[2]. Fig. 10 shows the calculated $\overset{\alpha'-\gamma}{\Delta G}(M_S) - \overset{\alpha'-\gamma}{\Delta G}(T)$ as a function of temperature, where $\overset{\alpha'-\gamma}{\Delta G}(T)$ is the same as that mentioned in Chapter 1, and the values are shown in Table 2 for the present three alloys. Next, magnetic energy due to the high field susceptibility will be introduced in addition to that due to the Zeeman effect. It may be expressed approximately as $-1/2\chi hf \cdot H^2$, because the magnetization increases linearly with increasing magnetic field, as seen in Fig. 3. Incidentally, magnetic energy due to the Zeeman effect has been called the Zeeman energy, and is defined as a bilinear product of the magnetization and the magnetic field. Therefore, the magnetic energy term $\Delta M(M_S') \cdot H$ in the Krivoglaz-Sadovsky formula corresponds to the Zeeman energy. In such a sense, the magne-

tic energy term due to the high field susceptibility, $-1/2\overset{\gamma}{\chi}_{hf}\cdot H^2$, may be also a kind of the Zeeman energy, because it is equivalent to a bilinear product of magnetization and magnetic field, $1/2\cdot\{M^{\gamma}(T, H) - M^{\gamma}(T, 0)\}\cdot H$, where M(H, T) represents an austenite magnetization under a magnetic field H at temperature T. However, in the present paper, the terms $\Delta M(T)\cdot H$ and $-1/2\chi_{hf}\cdot H^2$ will be distinguished as Zeeman energy and high field susceptibility energy, respectively.

Patel and Cohen[13] have developed a theory to explain a change in M_S temperature when a uniaxial stress or hydrostatic pressure is applied to an alloy system, as described in Chapter 1. By analogy with the theory, the shift of M_S temperature under a magnetic field may be obtained from the following more generalized form;

$$\overset{\alpha'-\gamma}{\Delta G(M_S)} - \overset{\alpha'-\gamma}{\Delta G(M_S')} = -\overset{\alpha'-\gamma}{\Delta M(M_S')}\cdot H - 1/2\overset{\gamma}{\chi}_{hf}\cdot H^2.$$

The above equation is a quodratic equation of H, and the critical field can be obtained by solving the equation for a given temperature, M_S', if ΔG, ΔM and $\overset{\gamma}{\chi}_{hf}$ is obtained as a function of temperature. In the present calculation, $\Delta M(T)$ is obtained from the measured austenitic and referred martensitic spontaneous magnetizations (Fig. 2), and $\overset{\gamma}{\chi}_{hf}$ is obtained from M(t)-H(t) curves (Fig. 3), whose values for the present alloys are shown in Fig. 11 as a function of temperature. The quantity of $\Delta G(M_S) - G(T)$ is obtained following the equation proposed by Kaufman and Cohen[2] described before (Fig. 10, Table 2). By using these values, the critical field vs. shift of M_S relations thus calculated for the three Fe-Ni alloys are shown in Fig. 12, together with the experimental ones. It is noted in this

figure that the calculated relation is not agreement with the experimental one for all the alloys, the calculated critical fields at larger ΔM_S being higher than the experimental ones. This means that other magnetic effects on the martensitic transformation may exist besides the Zeeman and high field susceptibility effects, and their effects on the shift of M_S temperature becomes larger with increasing strength of a magnetic field and/or temperature. However, the origine of the effects is not known yet now, and a further fundamental investigation is needed to clarify it.

References

(1) Z. Nishiyama: see Chapter 1, (4).

(2) L. Kaufman and M. Cohen: see Chapter 1, (28).

(3) Z. Nishiyama and K. Shimizu: Acta Met., 6 (1958), 125.

(4) R. P. Patterson and C. M. Wayman: Acta Met., 14 (1966), 347.

(5) J. Grangle and G. C. Hallame: Proc. R. Soc. A272 (1963), 119.

(6) M. Matsumoto, T. Kaneko and H. Fujimori: J. Phys. Soc. Japan 26 (1969), 1083.

(7) W. F. Schlosser, G. M. Graham and P. P. M. Meincke: J. Phys. Chem. Solids 32 (1971), 927.

(8) H. Hasegawa and J. Kanamori: J. Phys. Soc. Japan 31 (1972) 382, 33 (1972), 1599, 1607.

(9) M. Date, M.Motokawa, K. Okuda, H. Hori and T. Sakakibara: Physics in High Magnetic Fields (edited by S. Chikazumi and N. Miura), p. 44. Springer, Berlin (1981).

(10) M. A. Krivoglaz and V. D. Sadovsky: see Chapter 1, (55).

(11) I. Tamura, T. Maki, M. Nakanishi and Y. Oka: Syiyokwai-shi (Kyoto University, Japan), 17.

(12) T. Maki, M. Shimooka, M. Umemoto and I. Tamura: J. Jap. Inst. Metals 35 (1971), 1073, In Japanese.

(13) J. R. Patel and M. Cohen: see Chapter 1, (31).

Table 1. Transformation temperatures, austenitic magnetic moments (at 273K), and differences in magnetic moment between austenitic and martensitic states (at M_S + 70K) of Fe-29.9, -31.7 and -32.5at% Ni alloys.

Composition	Fe-29.9at%Ni	Fe-31.7at%Ni	Fe-32.5at%Ni
M_S (K)	223	164	113
M_f (K)	113	<77	<77
M_γ(273K)(μ_B)	0.75	1.00	1.24
$\Delta M_{(M_S+70K)}$(μ_B)	1.32	0.91	0.58

Table 2. Numerical values of $\Delta G(M_s)-\Delta G(T)$ as a function of ΔT for the three Fe-Ni alloys.

Fe-29.9at%Ni (Ms=223K)

ΔT (K)	ΔG(Ms)-G(T) (cal/mol)	ΔG(Ms)-ΔG(T) (J/mol)
-80	-88.5906	-370.84
-75	-83.5696	-349.822
-70	-78.4728	-328.487
-65	-73.3021	-306.842
-60	-68.0589	-284.895
-55	-62.7448	-262.65
-50	-57.3611	-240.114
-45	-51.9092	-217.292
-40	-46.3908	-194.192
-35	-40.8069	-170.818
-30	-35.1592	-147.176
-25	-29.4485	-123.272
-20	-23.6768	-99.1109
-15	-17.8444	-74.6968
-10	-11.9537	-50.0381
-5	-6.00501	-25.137
0	0	0
5	6.06006	25.3674
10	12.1743	50.9614
15	18.3412	76.7765
20	24.5598	102.807
25	30.8289	129.05
30	37.1472	155.498
35	43.5139	182.149
40	49.9275	208.996
45	56.3871	236.036
50	62.8917	263.265
55	69.4398	290.675
60	76.0305	318.264
65	82.6628	346.026
70	89.3355	373.958
75	96.0477	402.056
80	102.798	430.312
85	109.586	458.726
90	116.41	487.291

Fe-31.7at%Ni (Ms=164K)

ΔT (K)	ΔG(Ms)-G(T) (cal/mol)	ΔG(Ms)-ΔG(T) (J/mol)
-80	-74.935	-313.678
-75	-70.9074	-296.818
-70	-66.7814	-279.547
-65	-62.5601	-261.877
-60	-58.246	-243.818
-55	-53.8414	-225.38
-50	-49.3486	-206.573
-45	-44.7697	-187.406
-40	-40.107	-167.888
-35	-35.3622	-148.026
-30	-30.5372	-127.829
-25	-25.6339	-107.304
-20	-20.654	-86.4576
-15	-15.5991	-65.2977
-10	-10.4707	-43.8304
-5	-5.27057	-22.0626
0	0	0
5	5.33923	22.35
10	10.7459	44.9821
15	16.2182	67.8894
20	21.7554	91.0682
25	27.3556	114.511
30	33.0178	138.213
35	38.7405	162.168
40	44.5223	186.37
45	50.3622	210.816
50	56.2589	235.5
55	62.2111	260.416
60	68.2175	285.559
65	74.277	310.923
70	80.3886	336.507
75	86.5507	362.301
80	92.7624	388.303
85	99.0224	414.508
90	105.33	440.911

Fe-32.5at%Ni (Ms=113K)

ΔT (K)	ΔG(Ms)-G(T) (cal/mol)	ΔG(Ms)-ΔG(T) (J/mol)
-80	-59.5117	-249.116
-75	-56.7148	-237.408
-70	-53.7636	-225.054
-65	-50.6686	-212.099
-60	-47.4382	-198.576
-55	-44.0798	-184.518
-50	-40.5994	-169.949
-45	-37.0023	-154.892
-40	-33.293	-139.365
-35	-29.4756	-123.385
-30	-25.5538	-106.968
-25	-21.5308	-90.1278
-20	-17.4102	-72.8789
-15	-13.1939	-55.2297
-10	-8.88532	-37.1939
-5	-4.48657	-18.7808
0	0	0
5	4.5722	19.1393
10	9.22791	38.628
15	13.9652	58.4584
20	18.7823	78.6227
25	23.6772	99.1127
30	28.6482	119.921
35	33.6938	141.042
40	38.8122	162.468
45	44.0018	184.191
50	49.2612	206.207
55	54.5887	228.508
60	59.983	251.089
65	65.4429	273.944
70	70.9666	297.066
75	76.5529	320.45
80	82.2002	344.09
85	87.908	367.983
90	93.674	392.119

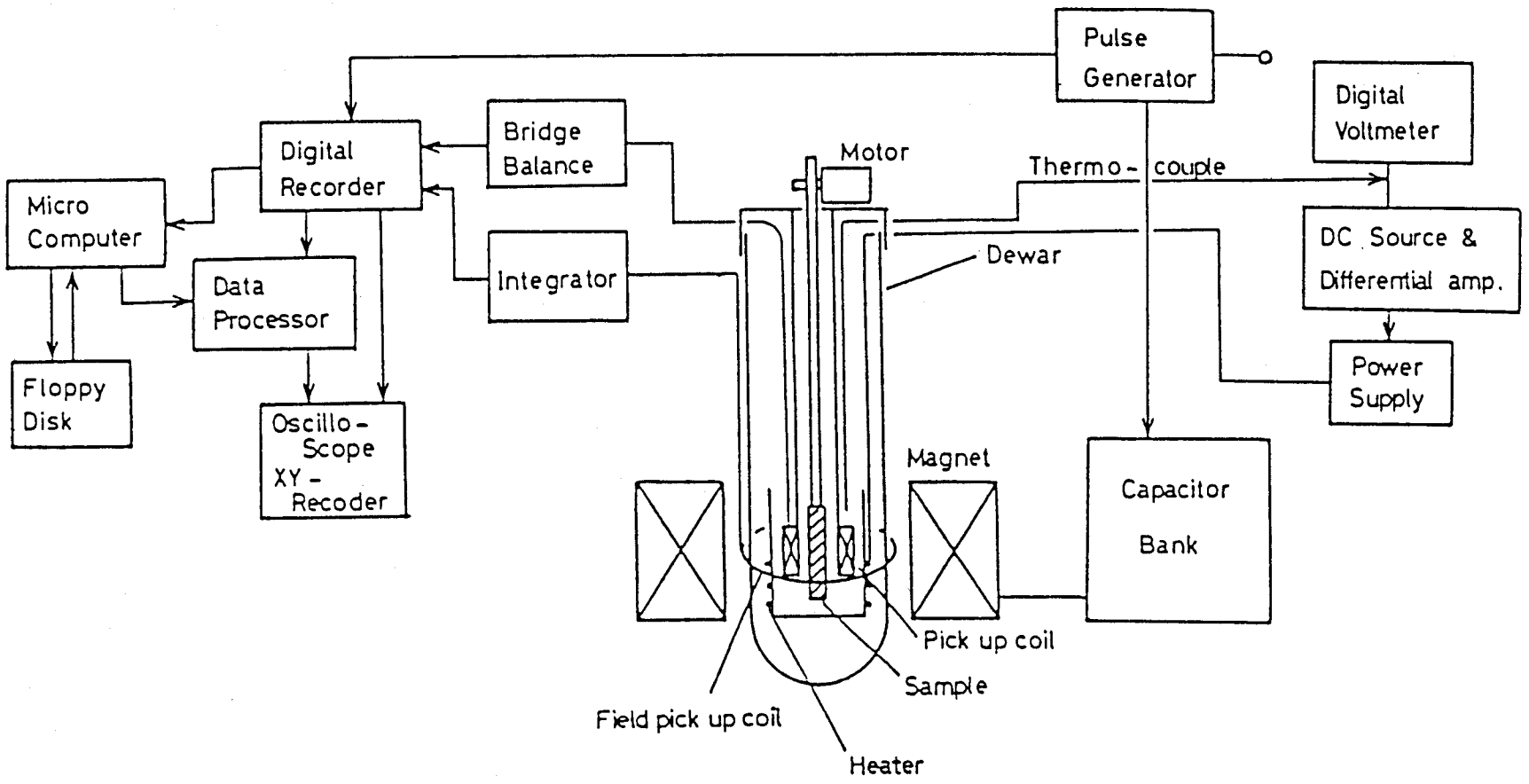

Fig. 1 Block diagram of the magnetization measurement under a pulsed magnetic field.

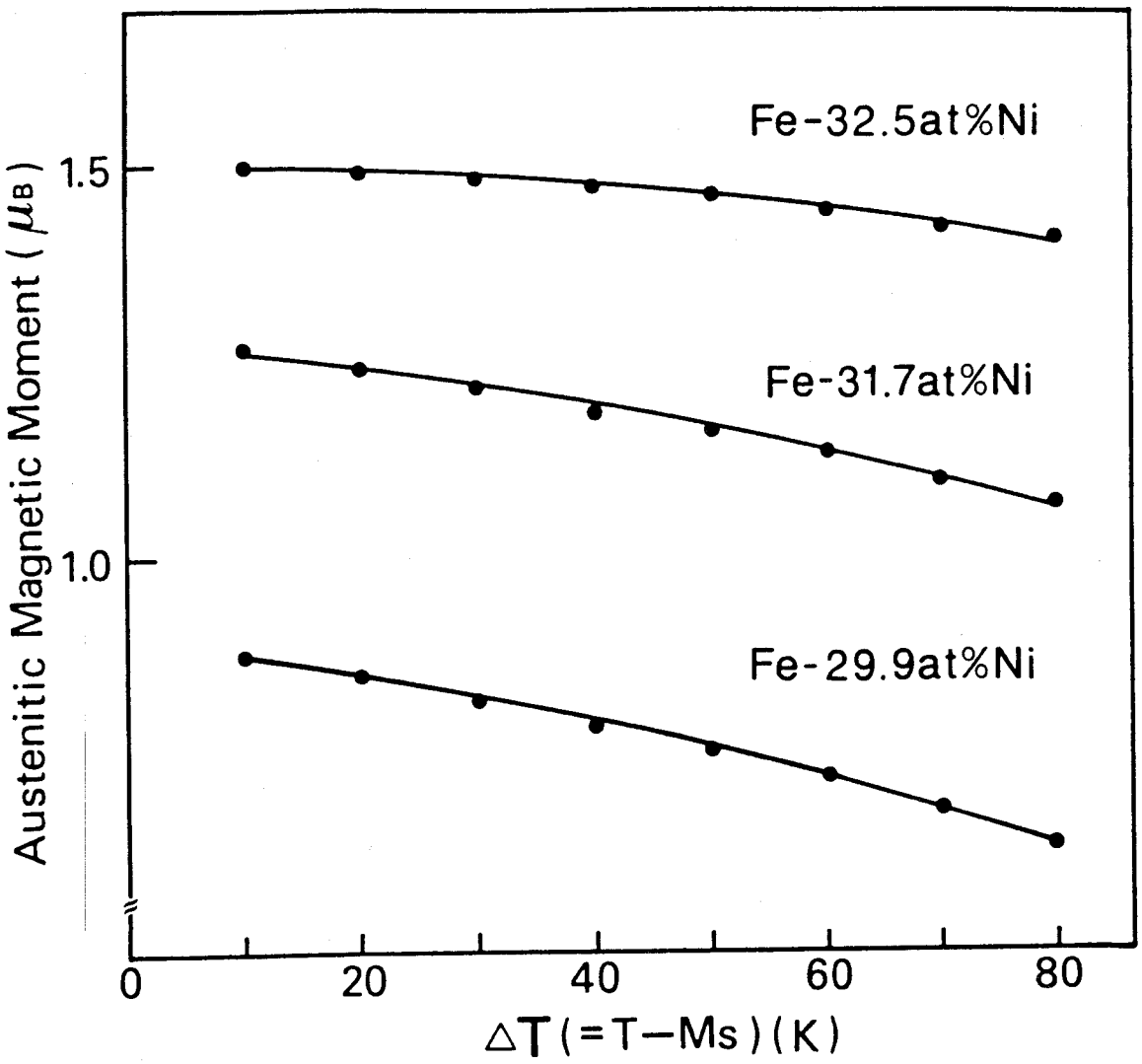

Fig. 2 Austenitic magnetic moments as a function of temperature difference, ΔT, from M_S temperature for Fe-29.9, -31.7 and -32.5 at% Ni alloys.

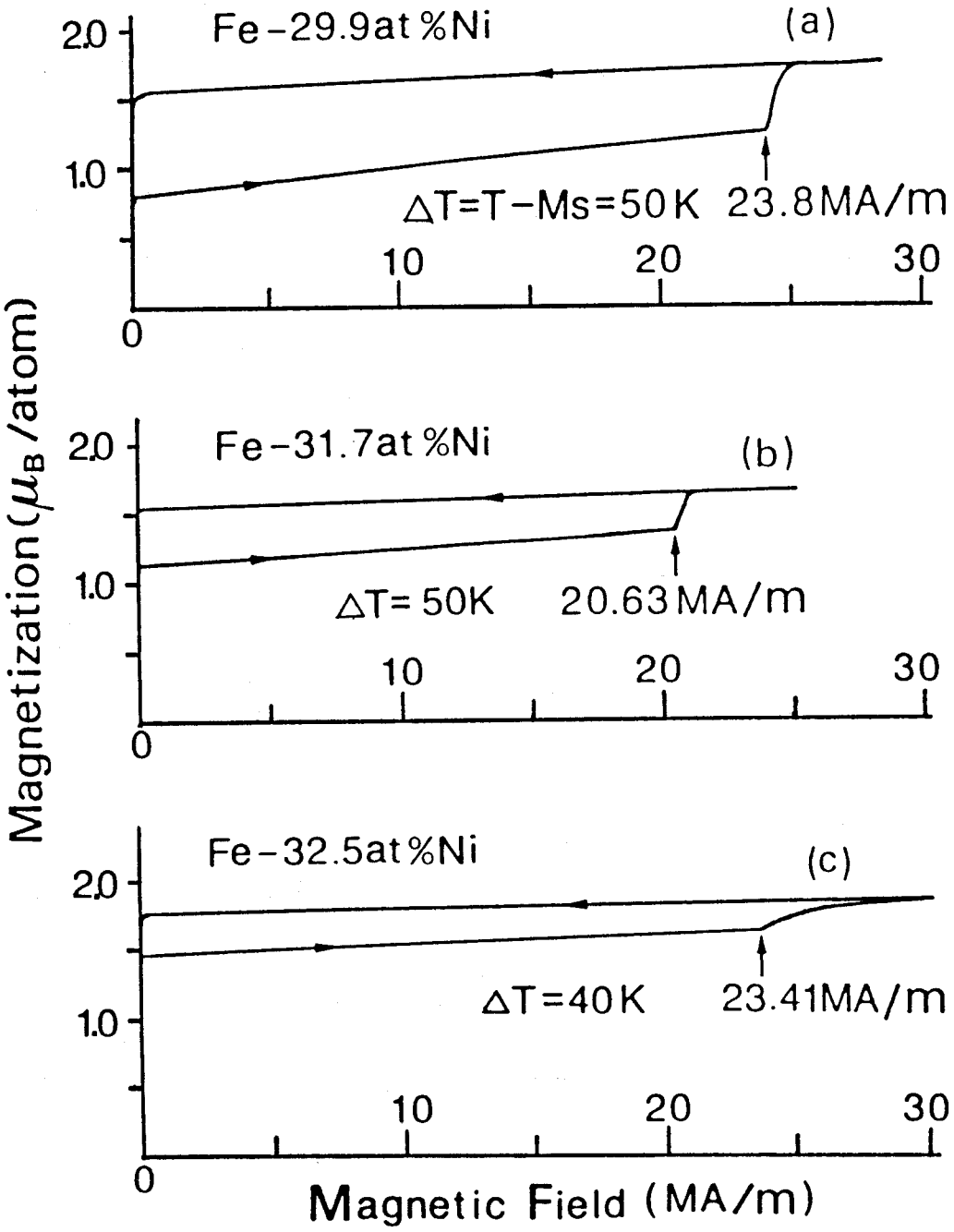

Fig. 3 Magnetization vs. magnetic field (M(t)-H(t)) curves for Fe-29.9, (a), -31.7, (b), and -32.5, (c), at% Ni alloys.

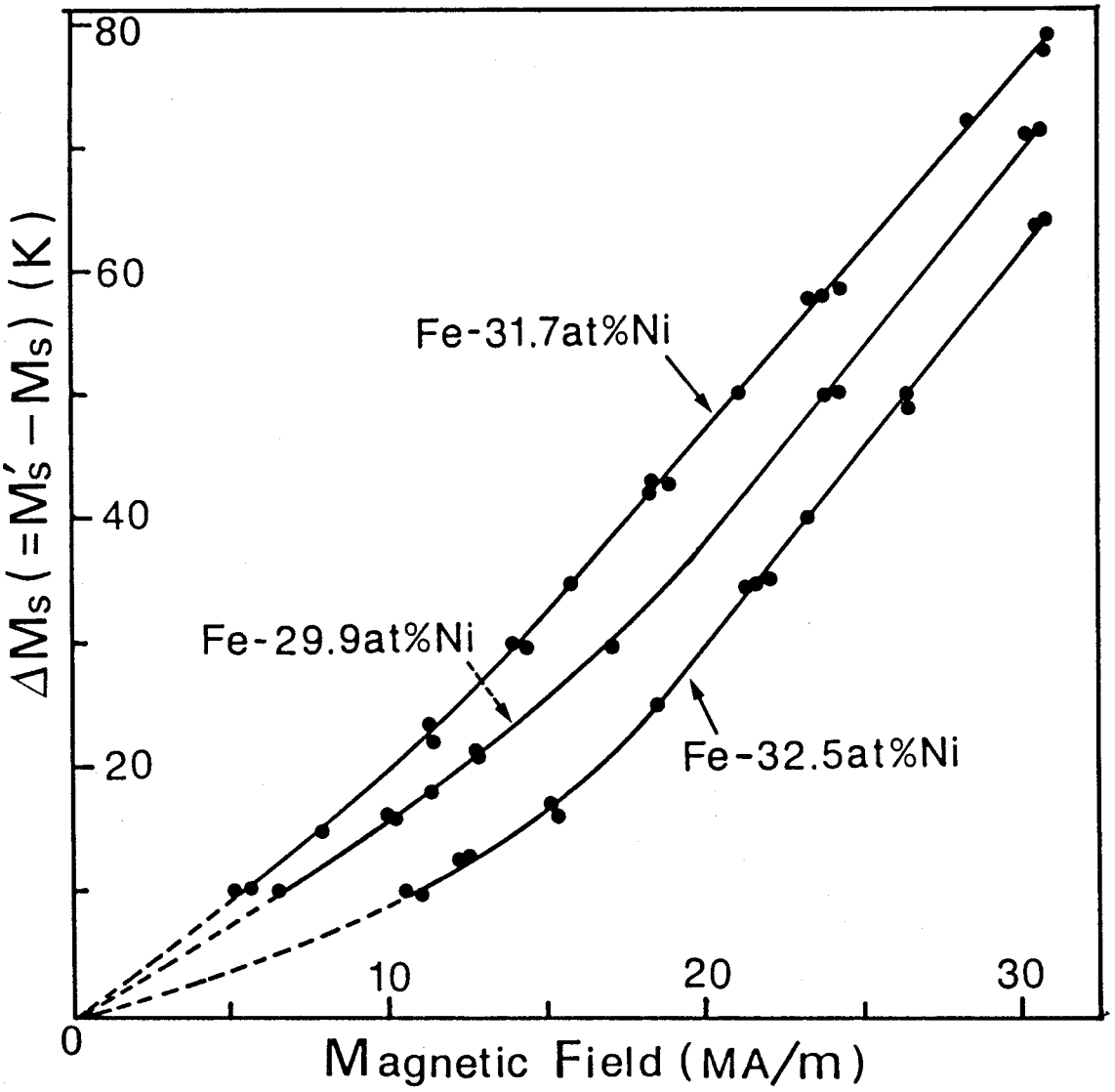

Fig. 4 Critical field dependence of the shift of M_S temperature, $\Delta M_S (M_S'-M_S)$, for Fe-29.9, -31.7 and -32.5 at% Ni alloys.

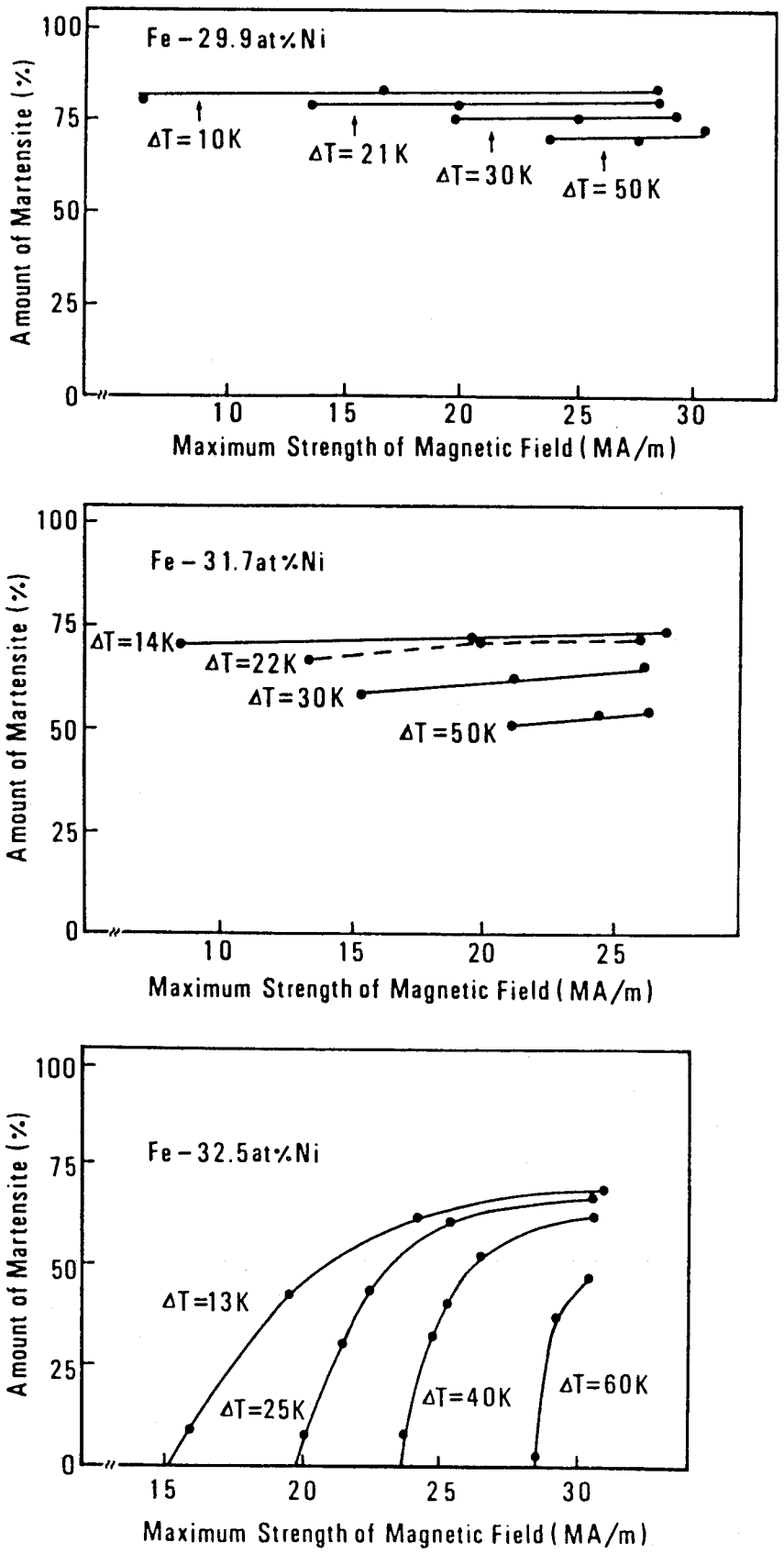

Fig. 5 Calculated amount of magnetic field-induced martensites, plotted as a function of maximum strength of pulsed magnetic field, of Fe-29.9, -31.7 and -32.5 at% Ni alloys.

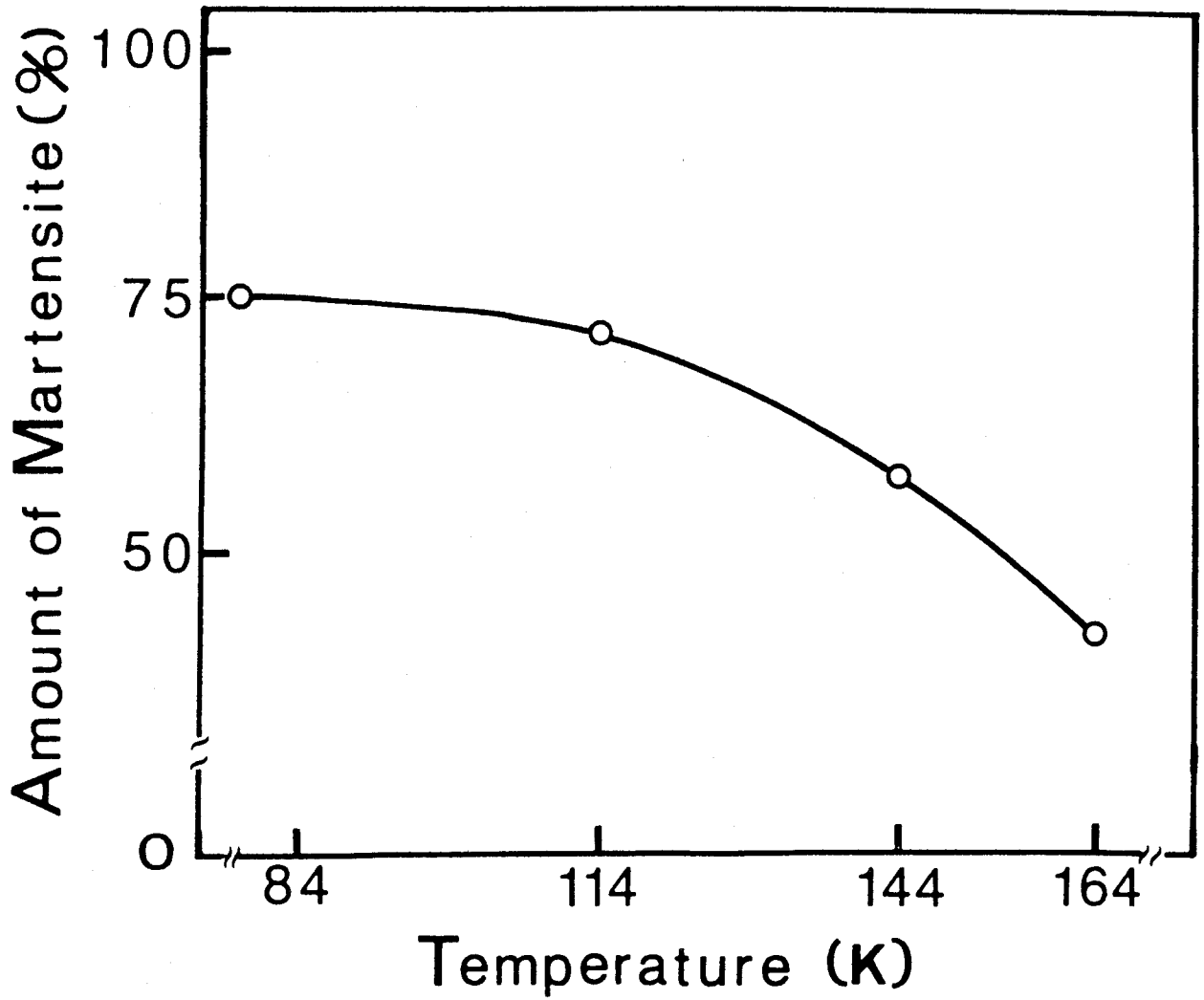

Fig. 6 Amount of thermally-induced martensites in the Fe-31.7 at% Ni alloy, which were plotted as a function of temperature.

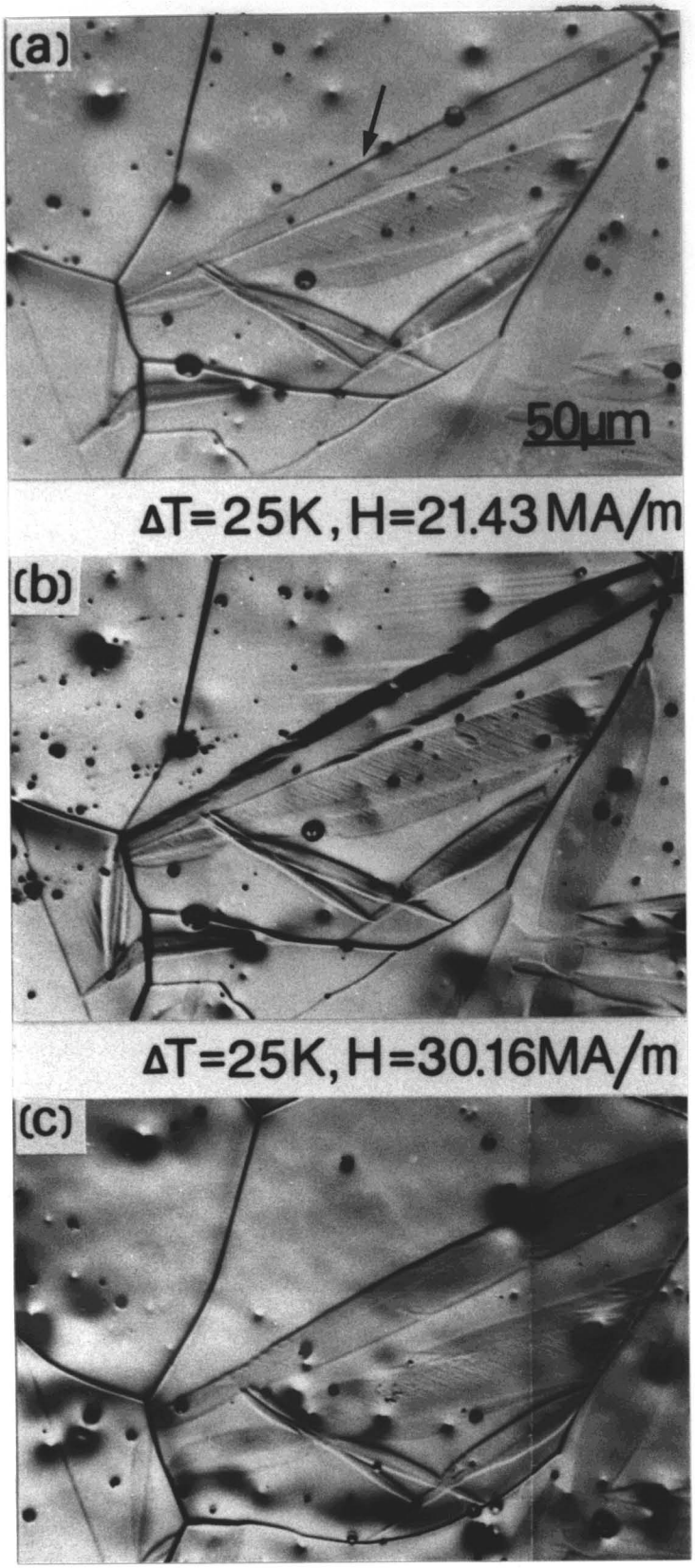

Fig. 7 Optical micrographs showing the growth of existing martensite plates in Fe-32.5at% Ni alloy, by applying a higher magnetic field, (c) is the etched structure of (b).

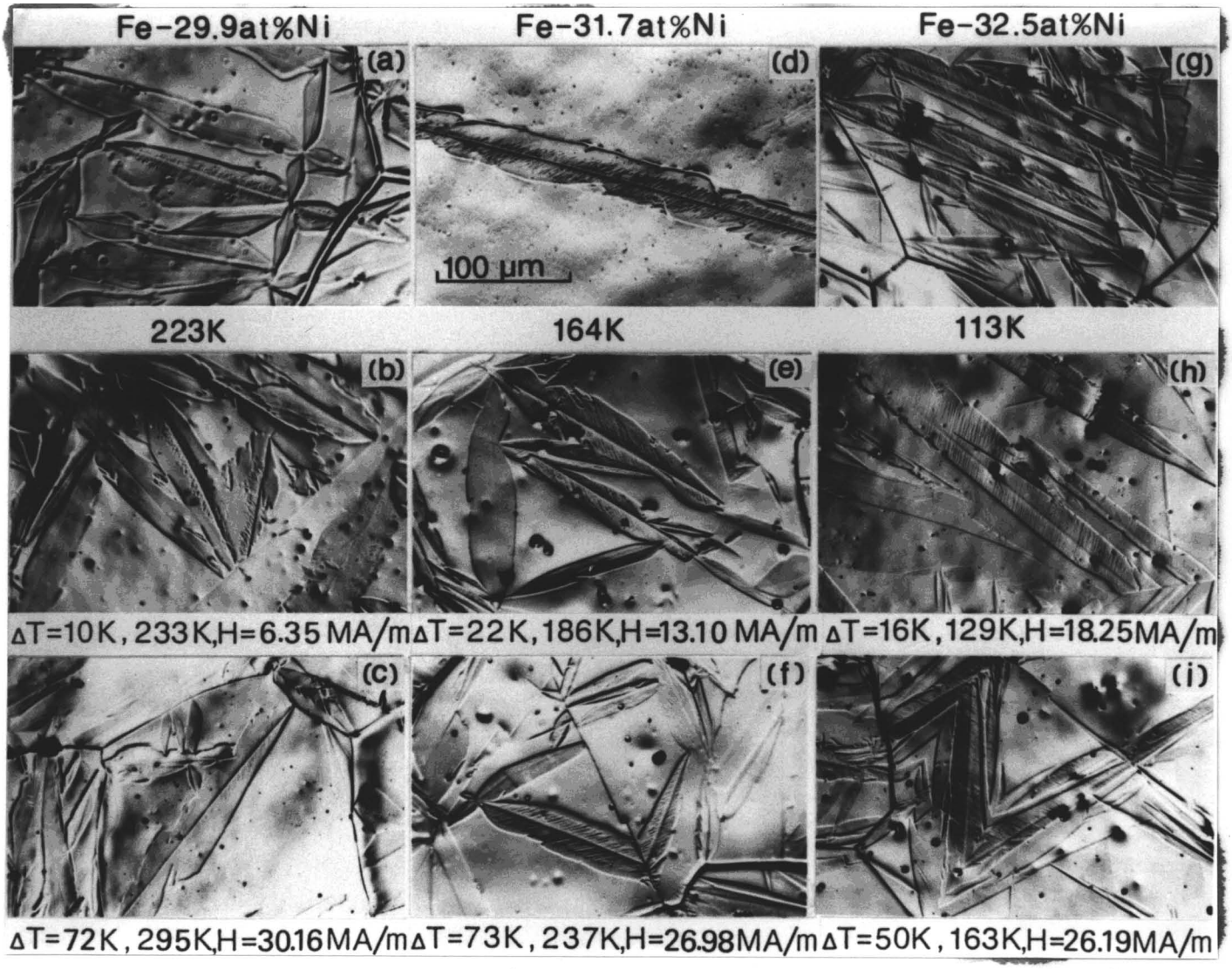

Fig. 8 Optical micrographs of thermally-induced martensites,(a), (d) and (g), formed by cooling a little below the respective M_s temperatures, and of magnetic field-induced ones, (b), (c), (e) (f), (h) and (i). ΔT and H for the magnetic field-induced martensites are inscribed in each photograph.

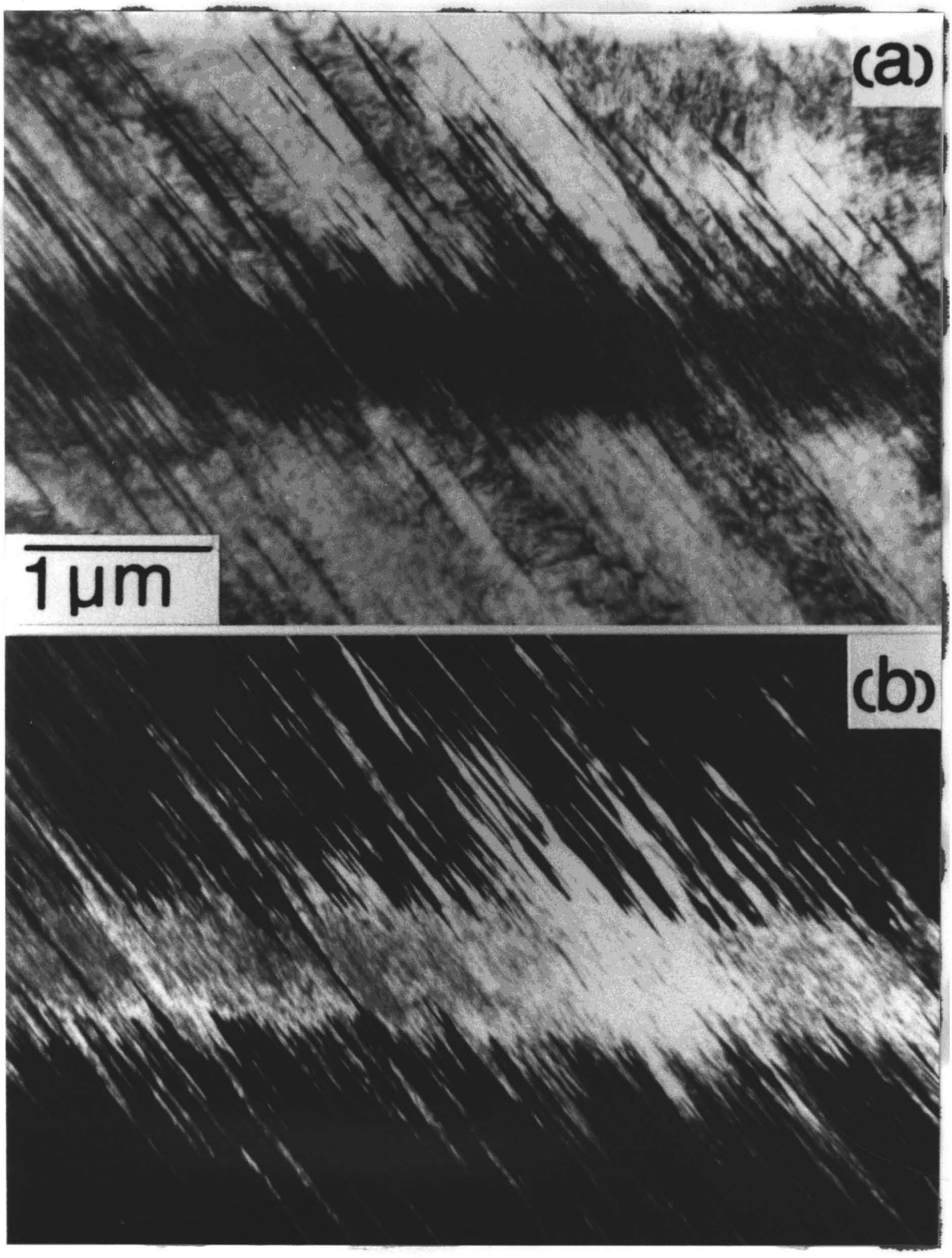

Fig. 9 Electron micrographs of a magnetic field-induced martensite in the Fe-31.7 at% Ni alloy at $\Delta T=14K$. (a) and (b) are bright and dark field images, respectively.

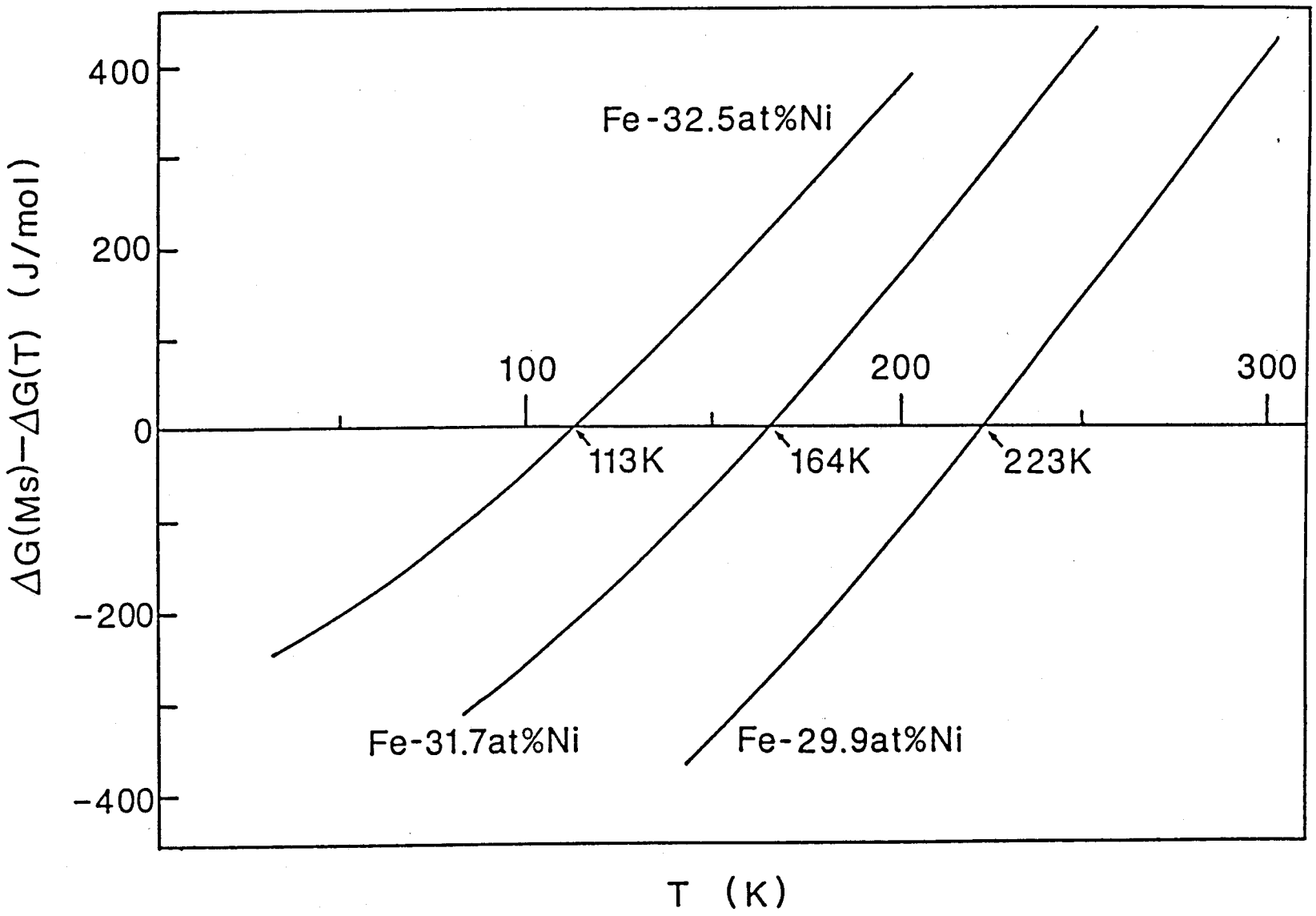

Fig. 10 Calculated $\{\Delta G(M_S)-\Delta G(T)\}$ as a function of temperature for the three Fe-Ni alloys.

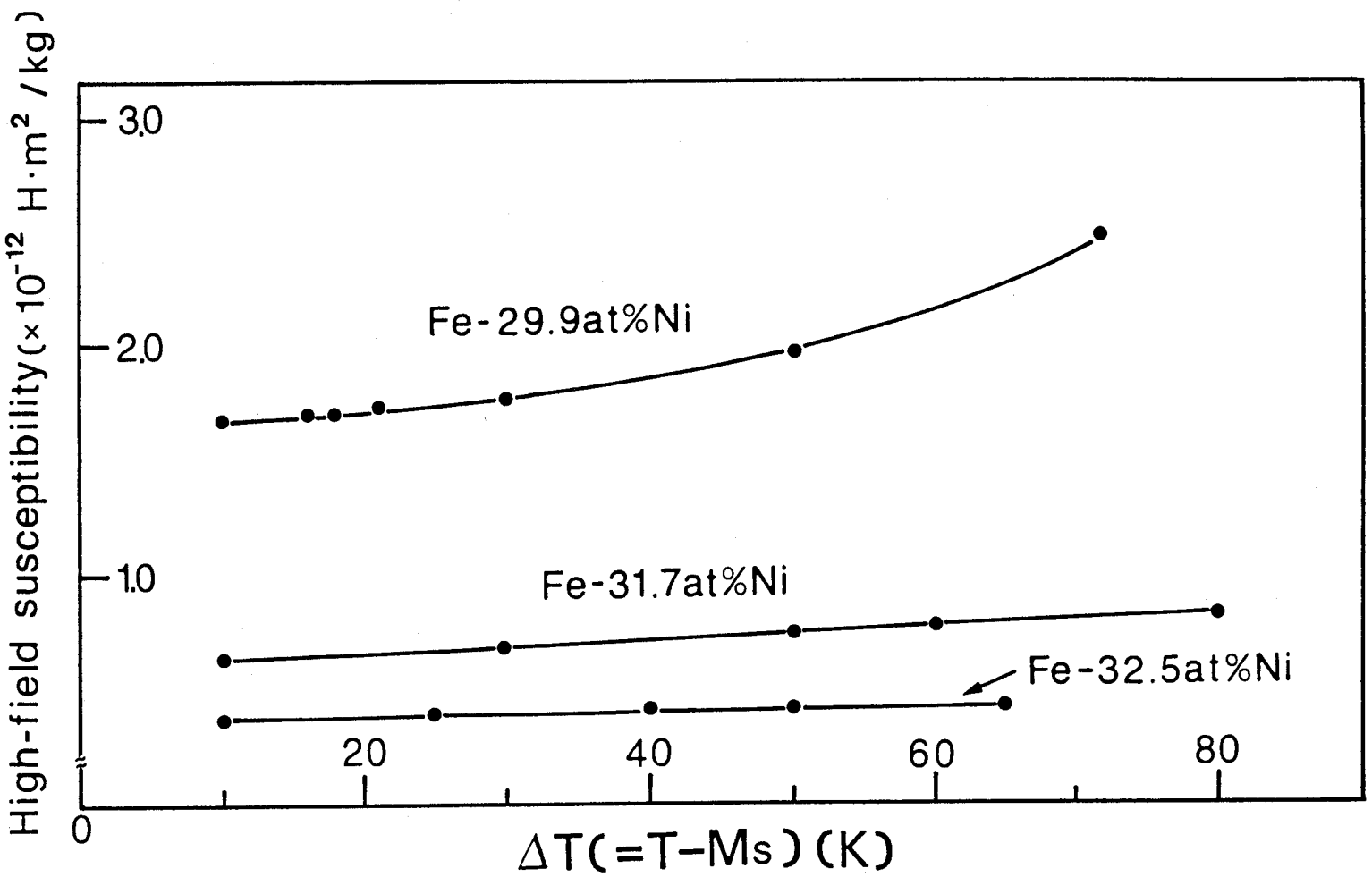

Fig. 11 High field susceptibility plotted as a function of ΔT for the three Fe-Ni alloys.

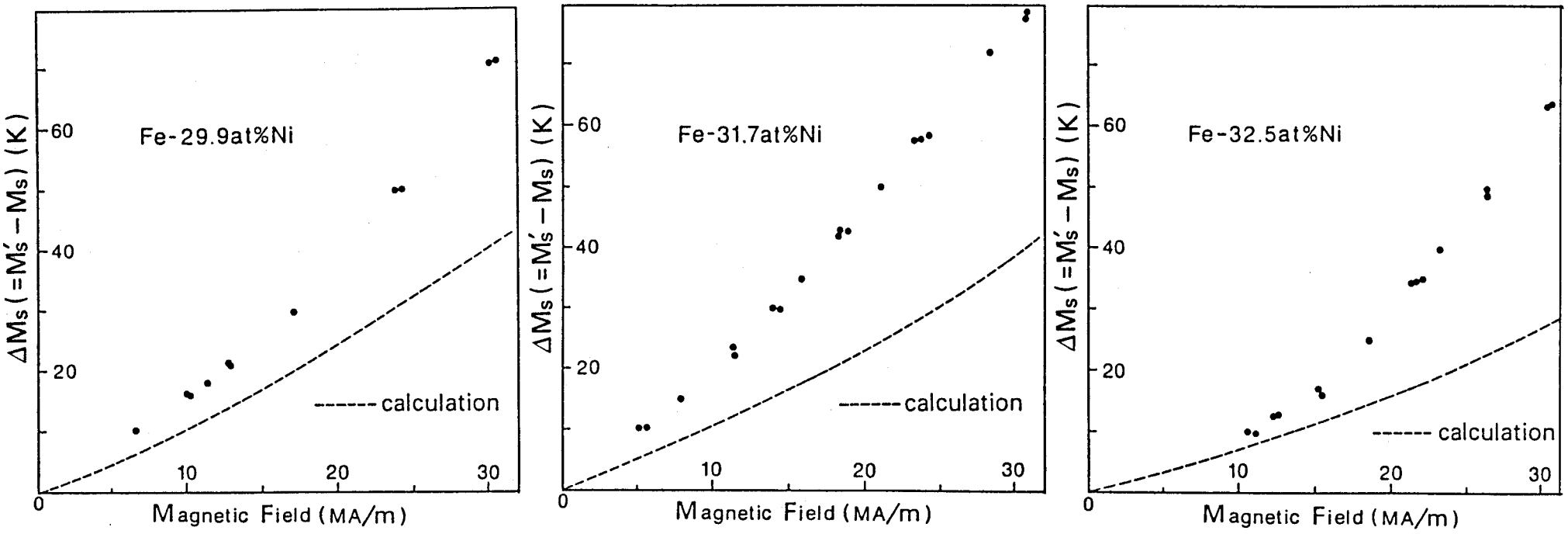

Fig. 12 Calculated and measured critical field dependences of the shift of M_s temperature for the three Fe-Ni alloys.

Chapter 3

Magnetic Field-Induced Martensitic Transformations in Single Crystals of an Fe-31.6at%Ni Alloy and Their orientation dependence.

Synopsis

The magnetic field-induced martensitic transformations in Fe-31.6at%Ni alloy single crystals, whose length-wise directions are nearly parallel to <100>, <110> and <111>, have been studied to clarify the influence of grain boundaries and crystal orientations on the transformation behavior by measuring magnetization and by observing microstructure, applying a pulsed ultra high magnetic field parallel to the length-wise directions.

As a result, the followings were found: (i) The critical magnetic field dependence of the shift of M_S temperature was consistent with that for a previously examined polycrystalline specimen with nearly the same composition irrespective of crystal orientations. That is, the magnetic effect on M_S temperature is not influenced by the existence of grain boundaries as well as the difference in crystal orientations. (ii) The amount of magnetic field-induced martensites was almost constant (about 80%) without regard to maximum strength of applied magnetic field, formation temperature and crystal orientation. (iii) Morphology of magnetic field-induced martensites (including internal substructures) was the same as that of thermally-induced ones irrespective of formation temperature and strength of magnetic field, as in polycrystalline specimens. (iv) Several plates of magnetic field-induced martensites were lengthily grown nearly parallel to the direction of an applied magne-

tic field irrespective of crystal orientation (sometimes they grow from one end to the other of 7mm length specimens).

I. Introduction

All of the previous studies on magnetic field-induced martensitic transformations were concerned with polycrystalline specimens, and therefore the information, such as critical magnetic field and amount of martensites etc., might be affected by the existence of grain boundaries. Moreover, no information has been obtained about the influence of crystal orientations on magnetic field-induced martensitic transformations. It is thus important to clarify the influences of grain boundaries and crystal orientations on the magnetic field-induced martensitic transformations. Furthermore, in Chapter 2, it has been pointed out that the martensitic transformation under a magnetic field is due to not only Zeeman and high field susceptibility effects but also the other unknown effects. However, the existence of grain boundaries and the difference in crystal orientation have not been taken into consideration in discussing those effects. In the present study, therefore, the magnetic field-induced martensitic transformations in Fe-Ni alloy single crystals with different crystal orientations have been examined to make the above problems clearer by magnetization measurement and optical microscopy, by applying a pulsed ultra high magnetic field pararell to the length-wise direction of the crystals. The results obtained have been compared with the previous ones for polycrystalline specimens with nearly the same composition.

II. Experimental Procedures

An Fe-31.6at%Ni alloy was prepared by melting the component metals in a high frequency induction furnace under argon atmosphere and casting into a water-cooled iron mold. Perfect single crystals were tried to get by the Bridgmen method. Unfortunately, they were not obtained, although a crystal with a large grain size was obtained. The large crystal (14ϕ × 30mm) was cut, and homogenized at 1473K for 8.64×10^4s in an evacuated silica capsule. Chemical analysis was done after the homogenization, the composition shown above being the analysed one. Orientation of the large crystal was determined by the back reflection Laue method, and ribbon-shaped specimens (4mm × 7mm × 0.3mm) were cut from the large crystal so that the length-wise direction might be parallel to the <100>, <110> and <111> of austenite crystal. They were austenitized at 1473K for 1.08×10^4 s in evacuated silica capsules and subjected to furnace cooling. All the austenitized single crystal specimens were cut into half width (2mm × 7mm × 0.3mm) by a spark cutting machine, and one half was used for electrical resistivity measurement to determine transformation temperatures and the other for magnetization measurements. Pulsed magnetic field whose maximum strength was about 31.75MA/m was applied along the length-wise direction of single crystals of three orientations. Details of the pulsed magnetic field instrument have been described in Chapter 2.

III. Results

3-1. Transformation temperature and austenitic magnetic moment

Electrical resistivity has been measured as a function of temperature in the range from 77K to 800K, in order to determine transformation temperatures M_s, M_f, A_s and A_f of each specimen. Fig. 1 shows the electrical resistivity vs. temperature relation together with that of the previous Fe-31.7at% polycrystal alloy. The determined transformation temperatures for three single crystal specimens are listed in Table 1, together with those for the previous polycrystalline specimen. It is noted in the table and figure that M_s and M_f temperatures are the same in each of single crystal specimens although they are different in the polycrystal. This means that all martensites in a single crystal are formed instantaneously at M_s temperature due to a burst phenomenon, and that those in a polycrystal are formed over some temperature range. Such a difference in transformation behavior may be attributed to whether grain boundaries exist or not. On the other hand, reverse transformation behavior is not so different between single crystal and polycrystalline specimens because a similar temperature difference exists between A_s and A_f temperatures of both the specimens. This may be due to the fact that the martensite state before the reverse transformation in both the specimens similarly consist of a large number of martensite plates. The spontaneous magnetization of austenite has been determined by measuring the magnetization in the austenitic state, as a function of temperature difference $\Delta T(=T-M_s)$, from M_s temperature as shown in Fig. 2. It is noted in this figure that

the magnetic moment is in good agreement with that of the previously examined Fe-31.7at%Ni alloy polycrystal in Chapter 2. The magnetic moment of the martensitic state can be assumed to be 2μB, as mentioned in Chapter 2.

3-2. Critical magnetic field to induce martensite.

Magnetization M(t) has been plotted as a function of magnetic field H(t) in one pulse whose maximum strength is higher than a critical field to induce martensitic transformation. Typical M(t)-H(t) curves are shown in Fig. 3, (a), (b) and (c) being for crystals with <100>, <110> and <111> orientations, respectively. On each of the curves, an abrupt increase in magnetization is recognized at a certain strength of the magnetic field, as indicated with an arrow, which corresponds to the occurrence of martensitic transformation. Such an abrupt increase in magnetization could not be observed if the maximum strength of a magnetic field below the one indicated with the arrow in Fig. 3 was applied to the another specimen at the same temperature. Therefore, the certain strength of the magnetic field corresponds to the critical one. The relation between the shift of M_S temperature, $\Delta M_S (=M_S'-M_S)$ and critical field has been measured and they are shown in Fig. 4. In this figure, symbols, ○ , ● and ■ represent the critical fields for the crystals with <100> <110> and <111> orientations, respectively, and the solid line represents the critical field vs. ΔM_S relation for the previously examined Fe-31.7at%Ni alloy polycrystalline specimen. The dotted line in this figure is the theoretical one described later. It is seen from the figure that the critical

field increases with increasing ΔM_S for all the single crystal specimens, and they lie nearly on the solid curve irrespective of crystal orientation. This result gives an important information with respect to the magnetic effect on M_S temperature, as will be discussed later.

3-3. Amount of magnetic field-induced martensite.

The amount of magnetic field-induced martensites has been calculated from the magnetization in the same manner as done in Chapter 2. The calculated amounts for three single crystal specimens at their critical fields are shown in Fig. 5 as a function of ΔT. This figure indicates that the amount is almost constant (about 80%) without regard to ΔT and crystal orientations. Moreover, it does not increase, even if any magnetic field higher than the critical field is applied from the beginning. This can be known from the magnetization curves in Fig. 3, that is, the abrupt increase of magnetization due to martensitic transformation is observed at the critical field, which is always the same even if any higher magnetic field is applied. Such a burst phenomenon of magnetic field-induced martensitic transformation at critical field is very similar to that of thermally-induced one at M_S temperature. Incidentally the amount (80%) of martensites in single crystals is larger than that (75%) in the Fe-Ni polycrystals previously studied in Chapter 2. This difference may be attributed to the existence of grain boundaries. Moreover, it should be noted from Fig. 3 that the magnetic field-induced martensites are all formed within 10^{-6} s, because the magnetization increases in this period. This forma-

tion period is consistent with that previously reported for thermally-formed martensites[2].

3-4. Morphology and arrangement of magnetic field-induced martensites.

Fig. 6 shows optical micrographs of thermally-induced lenticular martensites, (a), (d) and (g), and magnetic field-induced ones, (b), (c), (e), (f), (h) and (i). The micrographs of the first, second and third columns are taken from three single crystals with <100>, <110> and <111> orientations, respectively, and formation temperature, its difference from M_S, ΔT, and applied magnetic field H are inscribed in each of the micrographs. It is noted in the figure that the morphology (including internal substructures) of magnetic field-induced martensites is the same as that of thermally-induced ones irrespective of ΔT and H. This result is the same as that of the previously examined Fe-Ni alloy polycrystalline specimens. Fig. 7 shows more macroscopic photographs showing the whole view of thermally-induced martensites, (a), and magnetic field-induced ones, (b), (c) and (d). Crystal orientation, formation temperature, magnetic field H and its direction are inscribed in the figure. Photographs (b), (c) and (d) reveal that several martensite plates grow nearly parallel to the direction of applied magnetic field and some of them run through from one end to the other of crystals. However, such a characteristic array of martensite plates is not observed for thermally-induced martensite plates in (a). Therefore, the arrangement of martensite plates seems to be characteristic of magnetic field-induced martensites.

Fig. 7 (e) is an enlargement of the framed area of Fig. 7 (c), from which it is clearly known that one plate grows lengthily along the direction of magnetic field, and that the other plates terminate at the directionally grown martensite plate. This means that the directionally grown plate is first induced and then the other plates are induced. The reason for such a formation of lengthily grown martensite plates under a magnetic field is not clear now, but a shape magnetic anisotropy effect may be speculated to play an important role, as will be discussed later.

IV. Discussion

4-1. Calculation of critical magnetic field dependence of the shift of M_S temperature.

Critical magnetic field dependence of the shift of the M_S temperature, ΔM_S, has been calculated by taking account of the Zeeman and high field susceptibility effects mentioned in Chapter 2. In such a calculation, the high field susceptibility in the austenitic state and the difference in Gibbs chemical free energy between the austenite and martensite phases are needed beside the difference in spontaneous magnetization between both the phases. The high field susceptibility can be obtained form the M(t)-H(t) curves shown in Fig. 3, and is plotted as a function of temperature in Fig. 8. The difference in Gibbs chemical free energy is obtained by following the equation derived by Kaufman and Cohen[5]. The quantity $\Delta G(M_S)-\Delta G(T)$ is shown in Fig. 9 as a function of temperature and the values are shown in Table 2. The calculated critical magnetic field depend-

ence of ΔM_S is shown with dotted line in Fig. 4. It is noted from the figure that the calculated dependence is not agreement with the experimental one. This means that other magnetic effects on martensitic transformations may exist besides the Zeeman and high field susceptibility effects, as for the previous Fe-31.7at%Ni polycrystal alloy.

4-2. Influence of grain boundary and crystal orientation on the magnetic field-induced martensitic transformation.

It has been shown in the above that the critical field dependence of the shift of M_S temperature, ΔM_S, lies approximately on a little curved line, irrespective of crystal orientation. This is almost consistent with that for the previously examined Fe-31.7at%Ni alloy, and this result reveals two important facts. One is that the magnetic effect on M_S temperature is not influenced by the existence of grain boundaries, that is, the magnetic effect is the same in both single crystals and polycrystals. The other is that the magnetic energy contributing to the shift of M_S temperature must be an isotropic one because the magnetic effect is independent of crystal orientation. It is already pointed out that the magnetic energies contributing to the shift of M_S temperature consists of those due to the Zeeman, high field and other unknown effects. The magnetic energies due to the former two effects contain no anisotropic factor by crystal orientation when the strength of applied magnetic field is higher than several MA/m, which is the case in the present study. This means that the other unknown effects are also isotropic in that case. However, the nature of the unknown effects are not

known yet at present.

4-3. Reason for the formation of directionally grown martensite.

It has been found that several lengthily grown martensite plates are observed along the direction of an applied magnetic field irrespective of crystal orientation. Those plates appear to be first formed, judging from a characteristic arrangement of other plates around them. Such an arrangement of martensite plates can be supposed to correspond to the most favorable state for an unknown magnetic energy which depends on the direction of magnetic field. A shape magnetic anisotropic energy is possibly supposed as the unknown magnetic one, which has been adopted to explain the fact that the longitudinal direction of precipitates formed under a magnetic field orientates to the direction of an applied magnetic field. The shape magnetic anisotropic energy $E^{(3)(4)}$ is expressed by $-k\cdot\Delta M(T)\cdot\cos^2\theta$, where k is a constant containing a demagnetization factor, $\Delta M(T)$ the difference in magnetic moment between the matrix phase and the precipitate, and θ the angle between the longitudinal direction of precipitates and the direction of an applied magnetic field. When θ is zero, the energy becomes a minimum, and thus the longitudinal direction of precipitates has a tendency to orientate along the direction of applied magnetic field. The formation of lengthily grown magnetic field-induced martensite plates may be similarly explained by the shape magnetic anisotropic energy, because both the martensite plates and precipitates are lengthily grown along one direction. However, martensite plates are formed by a shear mechanism, as is well known, and so all the magne-

tic field-induced martensite plates can not orientate to the direction of magnetic field, being different from the case of a diffusion controlled precipitation. Only a few martensite plates induced in the beginning can orientate to the direction, and many other martensite plates form to relax the strain caused by the formation of initial lengthily grown martensite plates. In this way, the amount of lengthily grown martensite plates is not so large because of the beginning phenomenon of magnetic field-induced martensitic transformation. Incidentally, the shape magnetic anisotropic energy is very small compared with those due to the Zeeman, high field susceptibility and the other unknown effects, and therefore, it may be negligible for the shift of M_S temperature.

References

(1) J. Grangle and G. C. Hallame: see Chapter 2, (5).

(2) F. Förster and E. Scheil: Zeits. Metallk., 32 (1940), 165.

(3) L. Néel: Compt. rend., 225 (1947), 109.

(4) C. Kittle, E. A. Nesbitt and W. Shockley: Phys. Rev., 77 (1950), 839.

(5) L. Kaufman and M. Cohen: see Chapter 1, (28).

Table 1. Transformation temperatures of three Fe-Ni single crystals and an Fe-Ni polycrystal previously examined.

Composition		transformation temperature			
		M_s(K)	M_f(K)	A_s(K)	A_f(K)
Fe-31.6at%Ni single	<100>	165	165	504	670
	<110>	163	163	500	670
	<111>	160	160	498	667
Fe-31.7at%Ni poly		164	<77	584	723

Table 2. Numerical values of $\Delta G(M_S)-\Delta G(T)$ for various ΔT.

ΔT (K)	$\Delta G\ (Ms) - \Delta G\ (T)$ (cal/mol)	$\Delta G\ (Ms) - \Delta G\ (T)$ (J/mol)
-80	-74.7369	-312.4
-75	-70.7283	-295.644
-70	-66.6208	-278.475
-65	-62.4169	-260.903
-60	-58.1191	-242.938
-55	-53.73	-224.592
-50	-49.2518	-205.872
-45	-44.6867	-186.79
-40	-40.0369	-167.354
-35	-35.3039	-147.57
-30	-30.49	-127.448
-25	-25.5969	-106.995
-20	-20.626	-86.2168
-15	-15.5795	-65.1224
-10	-10.4585	-43.7165
-5	-5.26489	-22.0072
0	0	0
5	5.3346	22.2986
10	10.7375	44.883
15	16.2074	67.7469
20	21.7427	90.8844
25	27.3422	114.29
30	33.0045	137.959
35	38.7285	161.885
40	44.5128	186.063
45	50.356	210.488
50	56.257	235.154
55	62.2145	260.057
60	68.2275	285.191
65	74.2946	310.552
70	80.4149	336.134
75	86.5869	361.933
80	92.8096	387.944
85	99.0818	414.162
90	105.402	440.582
95	111.77	467.2
100	118.185	494.012

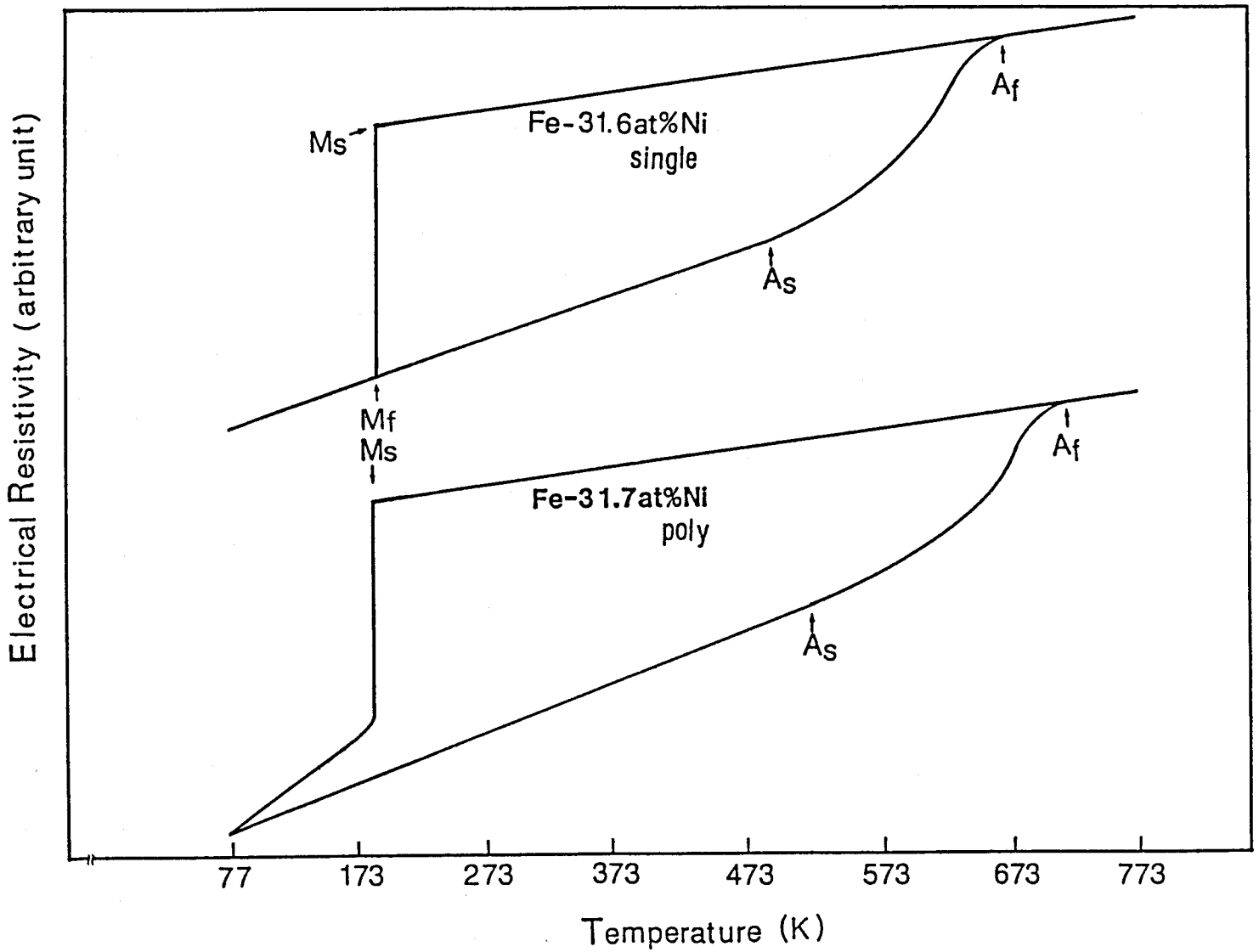

Fig. 1 Electrical resistivity vs. temperature curves of the Fe-31.6 at% Ni single crystal and previously examined Fe-31.7at% polycrystal.

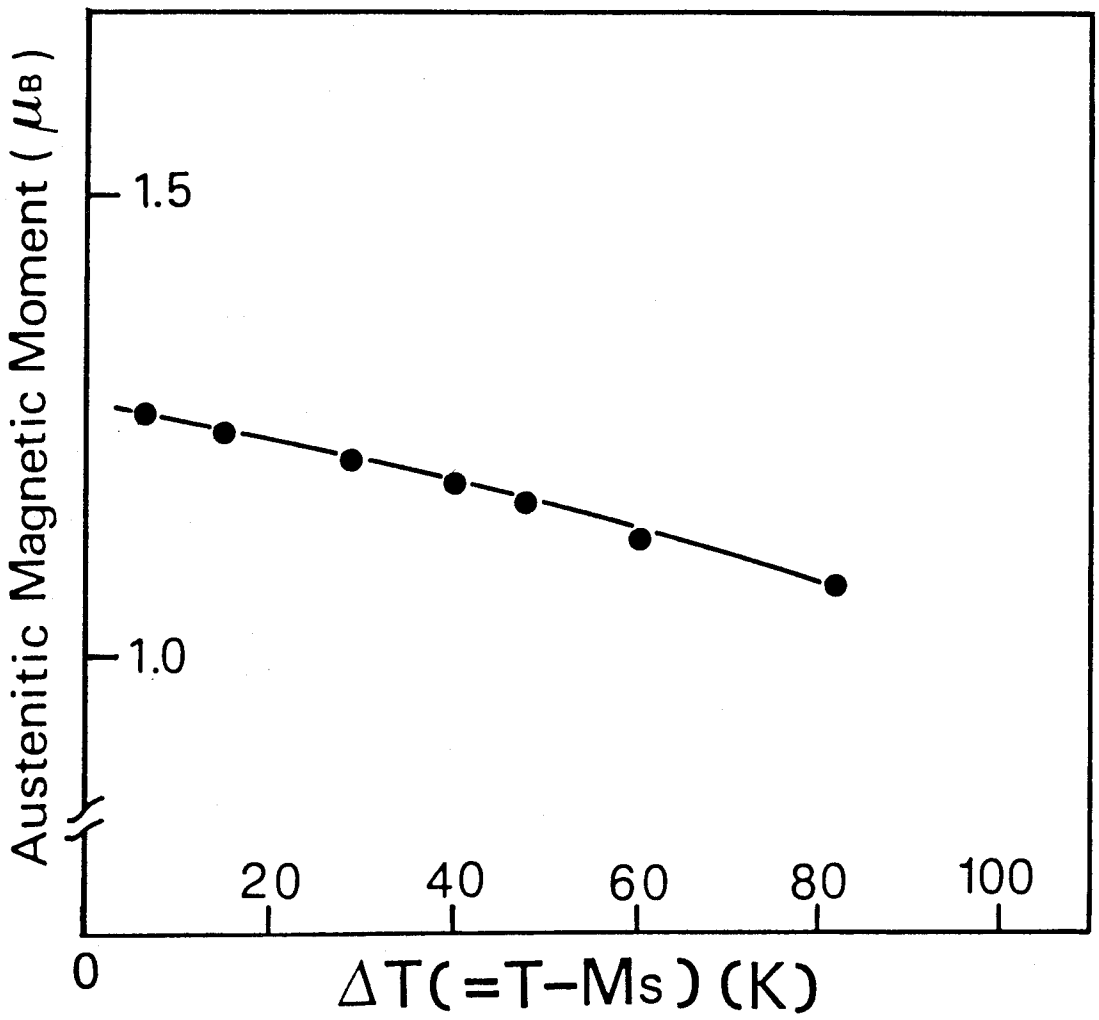

Fig. 2 Austenitic magnetic moment as a function of temperature in the Fe-31.6at% Ni alloy single crystal.

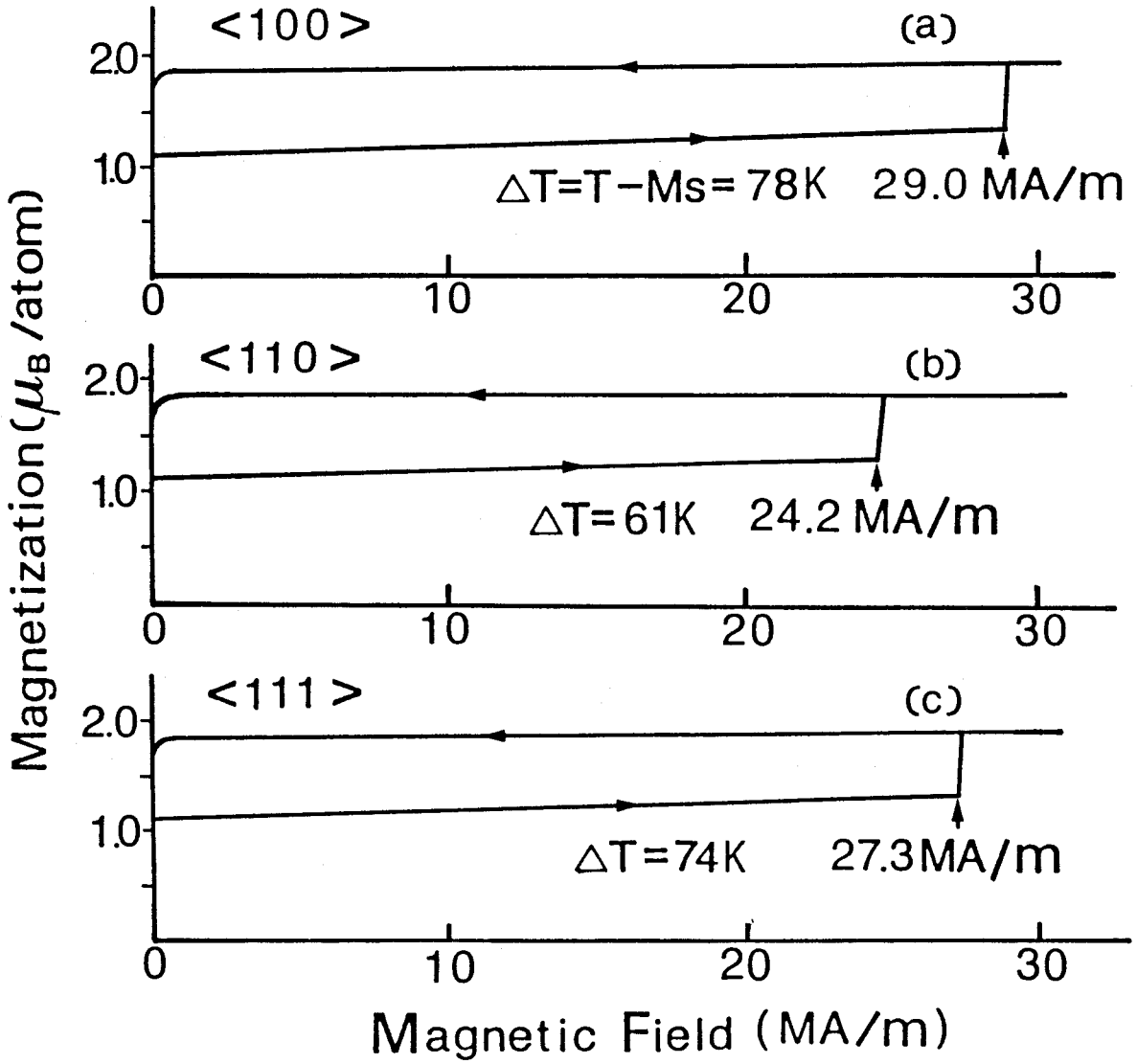

Fig. 3 Magnetization vs. magnetic field (M(t)-H(t)) curves for Fe-Ni single crystals of three kinds of orientations.

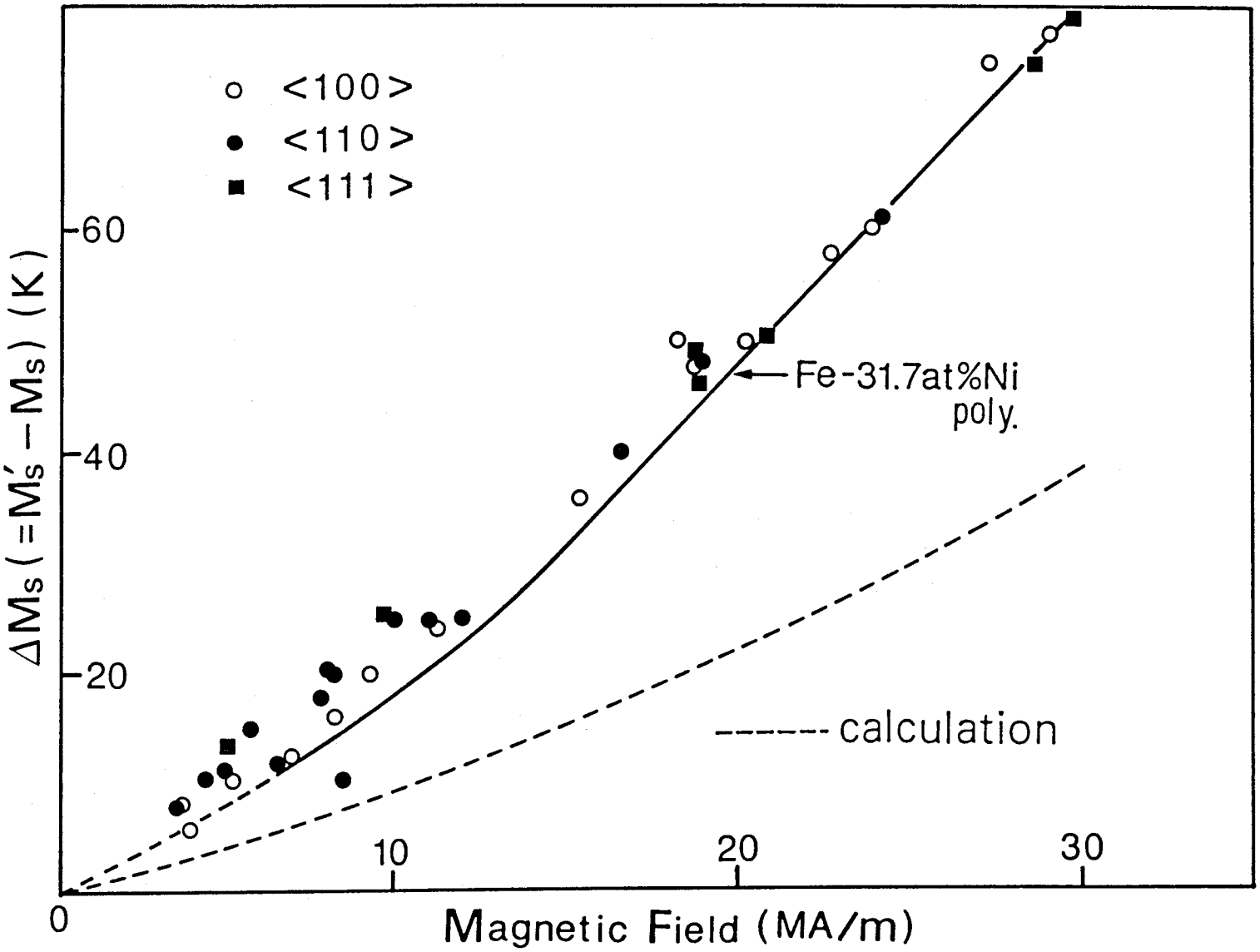

Fig. 4 Critical magnetic field dependence of $\Delta M_S (=M_S'-M_S)$, the dotted curve showing the calculated dependence.

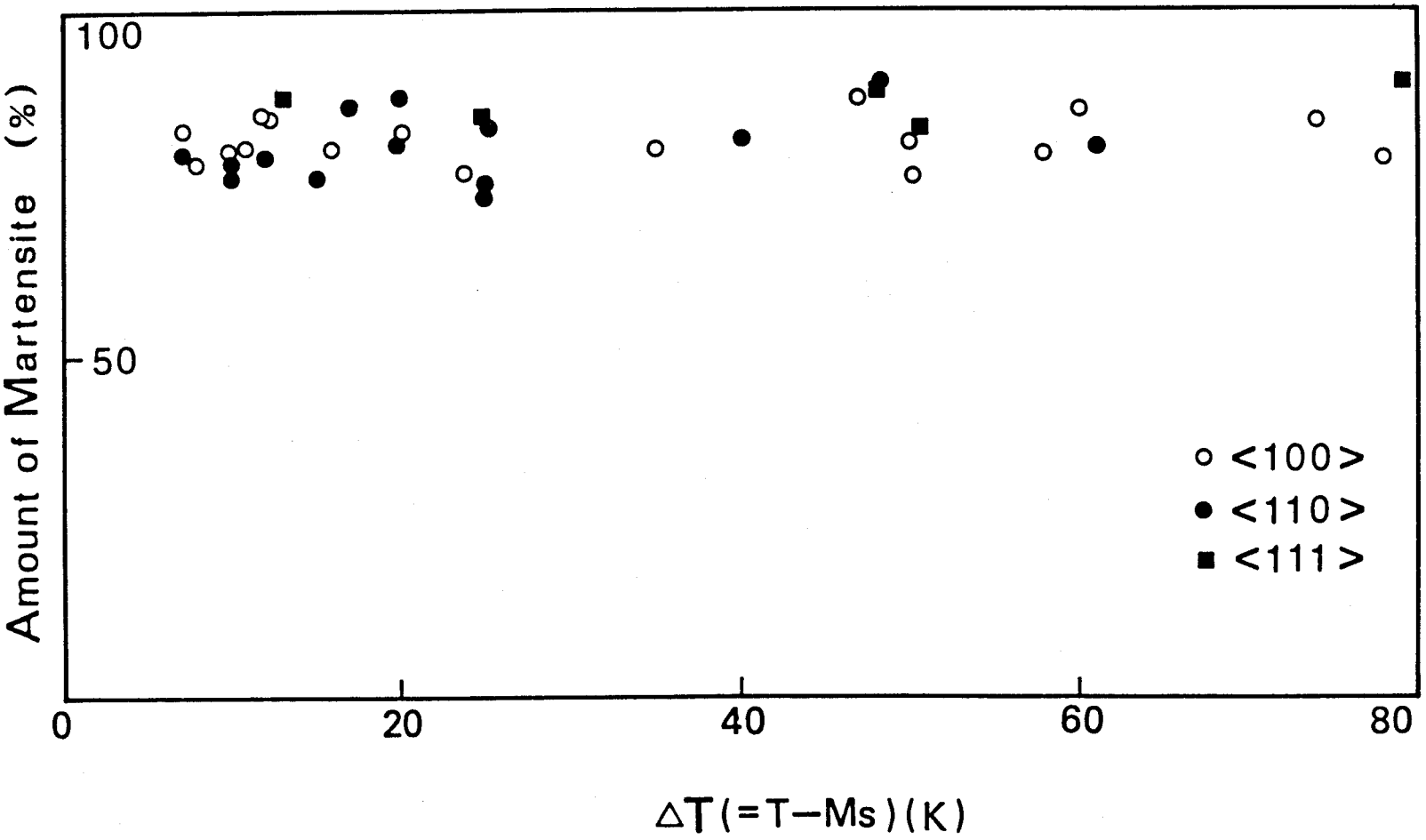

Fig. 5 Amount of magnetic field-induced martensites at the critical field, plotted as a function of ΔT.

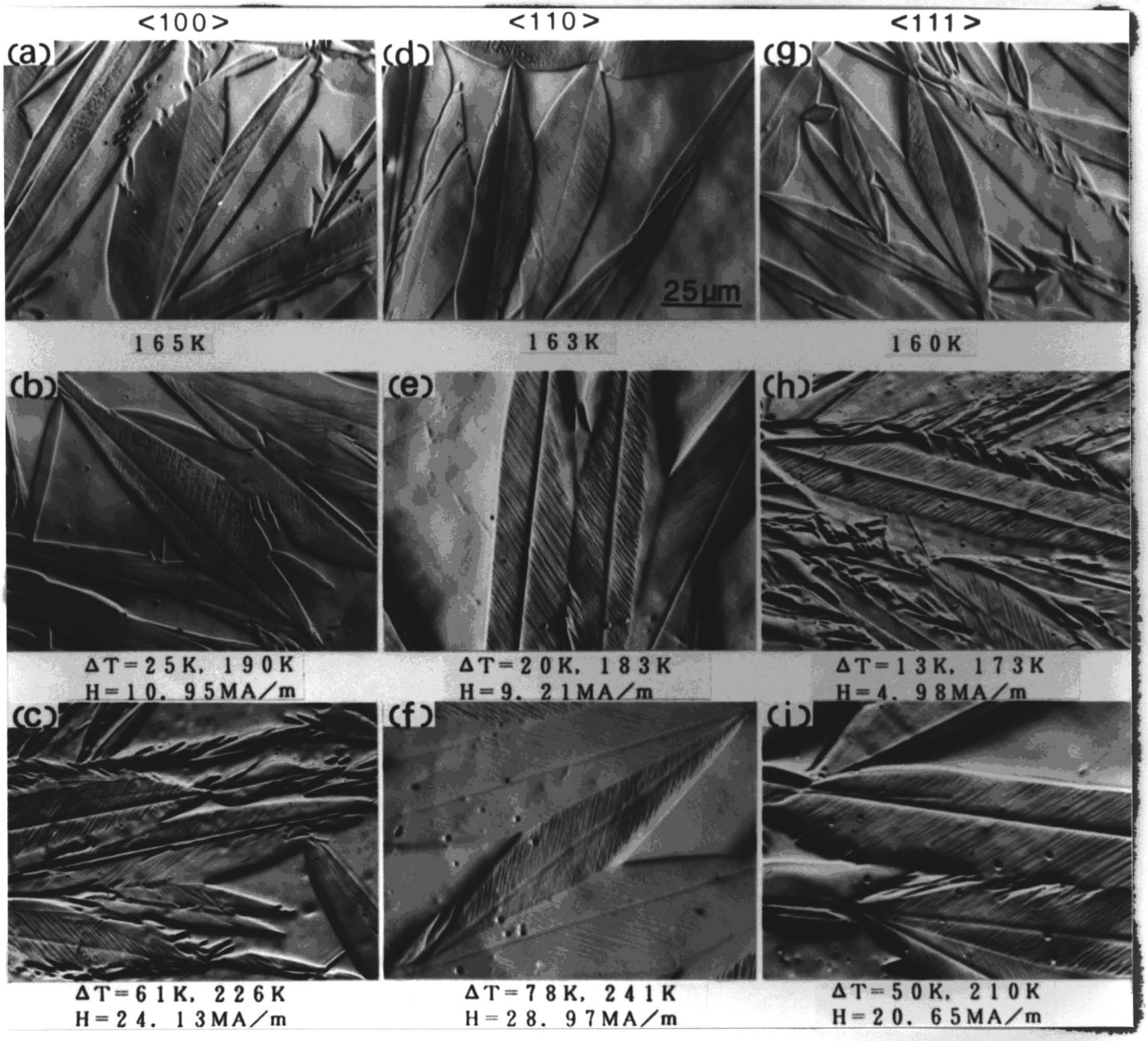

Fig. 6 Optical micrographs of thermally-induced martensites, (a), (d) and (g), and magnetic field-induced ones, (b), (c), (e), (f), (h) and (i). Transformation temperature, ΔT and H for the magnetic field-induced martensites are indicated in each photograph.

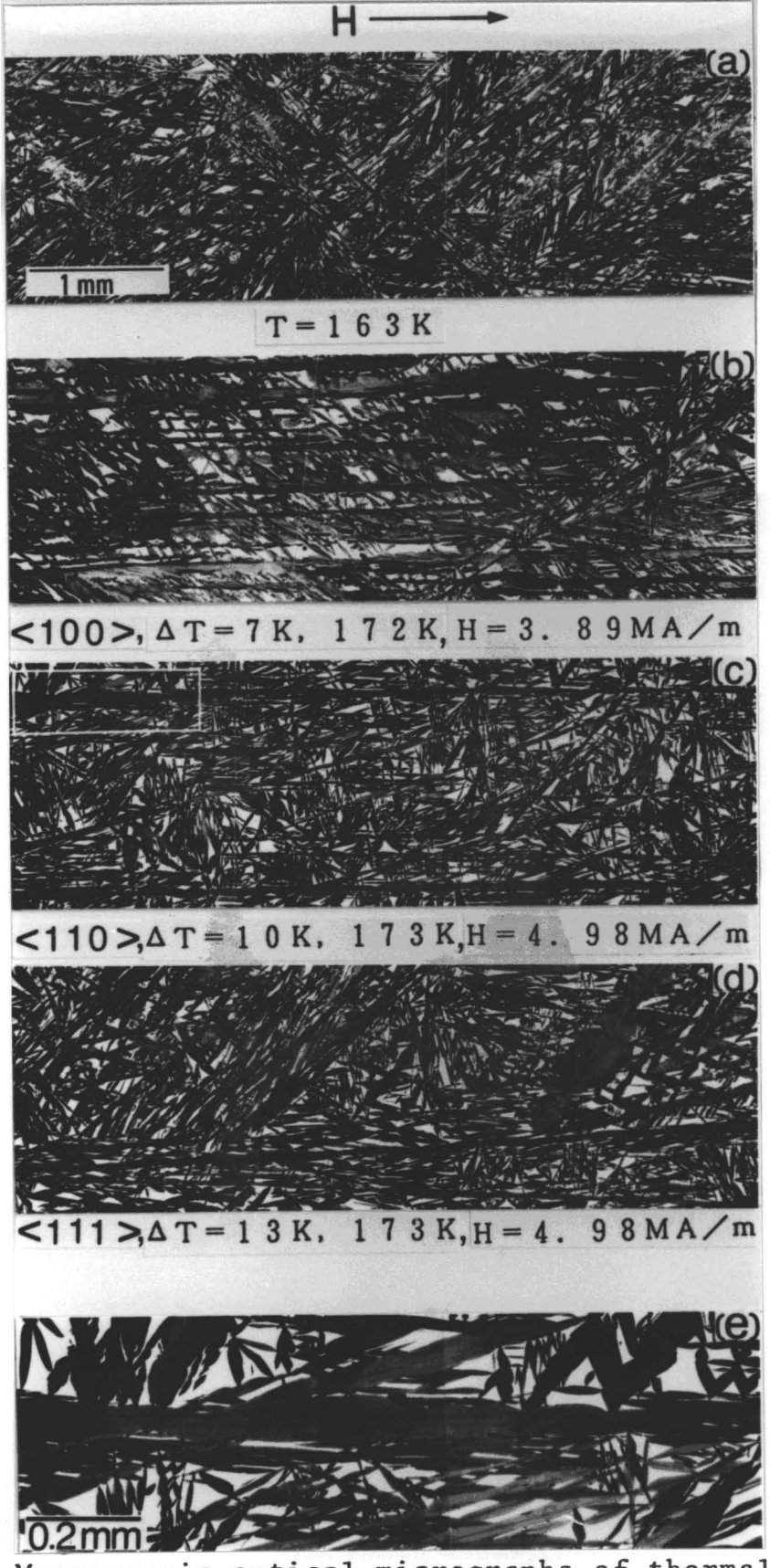

Fig.7 Macroscopic optical micrographs of thermally-induced, (a), and magnetic field-induced ones in three single crystal specimens with <100>, <110> and <111> orientations, (b), (c) and (d). (e) is an enlargement of the framed area of (c). The direction of an applied magnetic field, crystal orientation, transformation temperature, ΔT and H are indicated in each photograph.

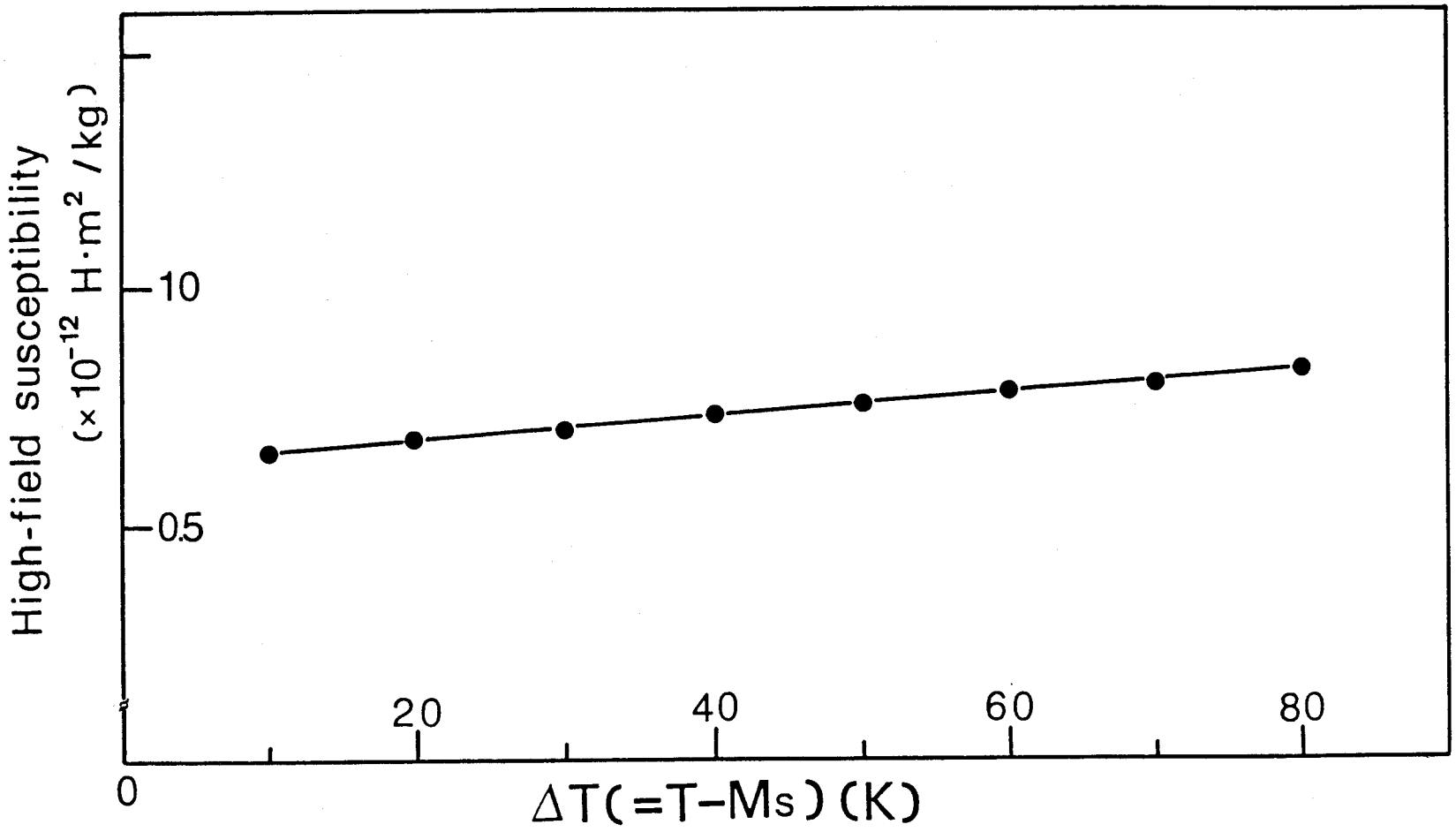

Fig. 8 High field susceptibility as a function of ΔT.

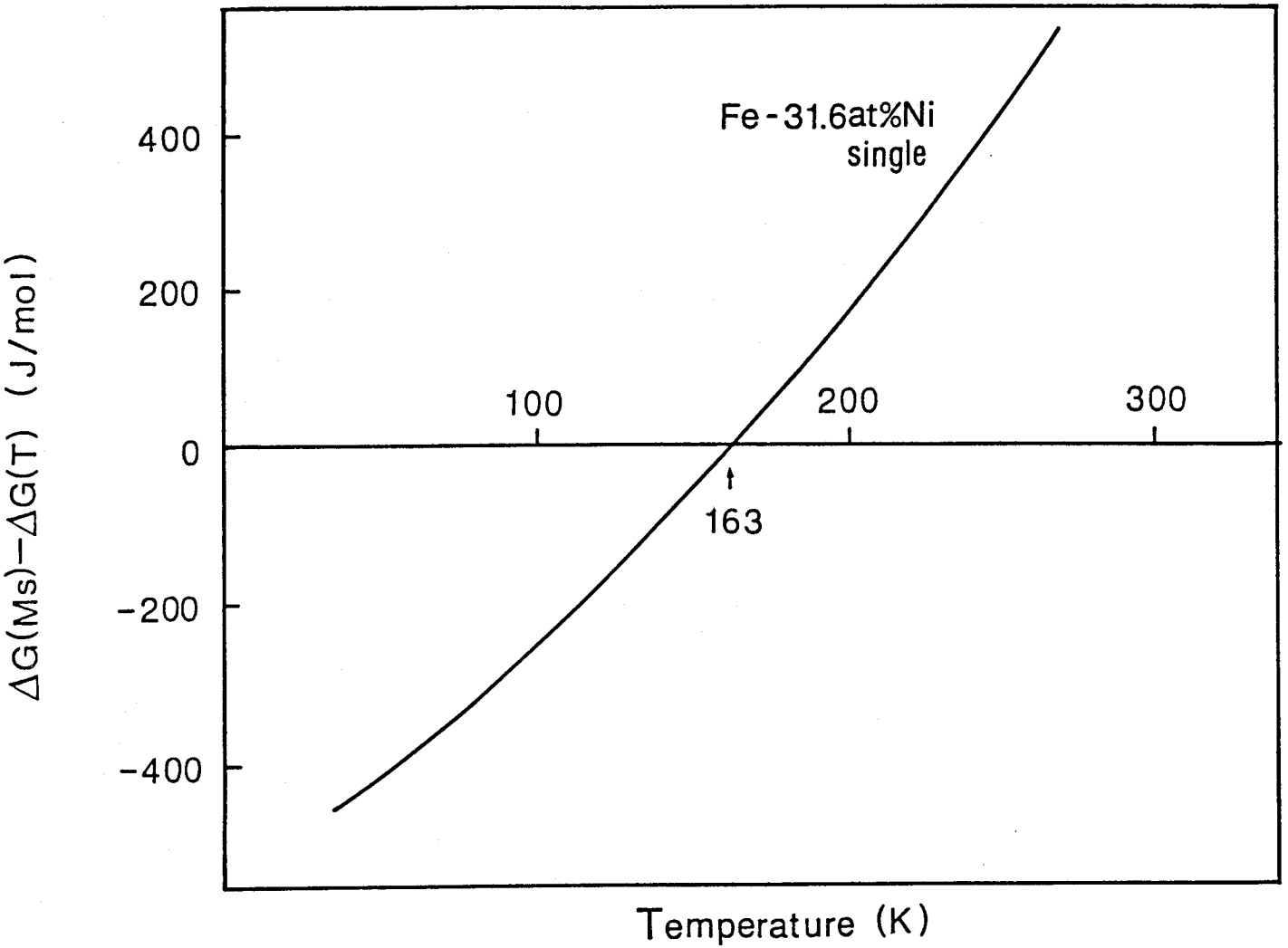

Fig. 9 Calculated $\{\Delta G(M_S)-\Delta G(T)\}$ as a function of temperature.

Chapter 4

Magnetic Field-Induced Martensitic Transformations in Fe-Ni-C alloys and the influence of the Invar effect on the transformations.

Synopsis

Magnetic field-induced martensitic trnasformations in Fe-Ni-C Invar (Fe-28.7Ni-1.8C and Fe-29.0Ni-1.4C (at%)) and non-Invar (Fe-24.7Ni-1.8C (at%)) alloys have been studies to clarify the Invar effect on the transformations by means of magnetization measurement and optical microscopy, applying a pulsed ultra high magnetic field. Morphology of the magnetic field-induced martensites was compared with that of deformation-induced martensites to examine the formation temperature effect on the martensite morphology. As a result, the followings were found. A magnetic field higher than a critical one was needed to induce the martensitic transformations above M_S irrespective of whether the alloy was Invar or non-Invar. The difference of transformation temperature from M_S, $\Delta M_S (=M_S'-M_S)$, increases with increasing critical field, and when plotted against the critical field, it lies on a little curved line for the Invar alloys, but on a single straight line for the non-Invar alloy. This result and a thermodynamical analysis suggest that the influence of magnetic field on the martensitic transformations in the non-Invar alloy comprises the Zeeman and high field susceptibility effects, while in the Invar alloy, it comprises other unknown effects in addition to the above two effects. The amount of the magnetic field for all the three alloys, although a little difference is

observed among the three alloys in the manner of the increase at the critical magnetic field. The morphology of the magnetic field-induced martensite was the same as that of thermally-induced one in each alloy, irrespective of $\Delta T=T-M_S$. However, deformation-induced martensites in the Fe-28.7Ni-1.8C and Fe-24.7Ni-1.8C alloys were lenticular and butterfly, respectively, whereas the magnetic field-induced martensites formed in those two alloys at the same temperature were thin plate-like and lenticular, respectively. This fact indicated that the martensite morphology was not decided by the formation temperature alone.

I. Introduction

By investigating the magnetic field-induced martensitic transformations in poly-and single crystals of Fe-Ni alloys, it was pointed out in Chapter 2 and 3 that martensitic transformations under a magnetic field are influenced not only by the Zeeman and high field susceptibility effects but also by other unknown effects. However, the Fe-Ni alloys previously examined have an Invar effect, and therefore the unknown effects may be related with an Invar effect. In order to directly known such the Invar effect, Fe-Ni and Fe-Pt alloys are apparently convenient, because they become Invar or non-Invar depending on their compositions. However, M_S temperatures of the non-Invar alloys undergoing a martensitic transformation are higher than room temperature, and then it is experimentally difficult to apply a magnetic field in the austenitic state. In that sense, Fe-Ni-C alloys are more convenient, because the alloys with Invar and non-Invar effects can easily be prepared by varying the compositions

of Ni and C, and their M_S temperatures can be lowered below room temperature. However, the studies so far done on magnetic field-induced martensitic transformations in Fe-Ni-C alloys[1] have not been performed from the above view point, and the amount and morphology of the martensites have not been examined systematically by varying ΔT. In the present study, therefore, Fe-Ni-C Invar and non-Invar alloys have been examined to clarify the difference in magnetic effects on their martensitic transformations by means of magnetization measurement and optical microscopy under a pulsed ultra high magnetic field. According to previous reports[2], [3], the morphology of Fe-Ni-C martensites is decided only by the formation temperature. However, the morphology of magnetic field-induced martensites in Fe-Ni alloys has been found in Chapter 2 and 3 to be the same as that of thermally-induced ones irrespective of the formation temperature. A similar result is expected in Fe-Ni-C alloys, and so the morphology of magnetic field-induced martensites has been compared with that of deformation-induced ones formed at the same temperature.

II. Experimental Procedures

Three Fe-Ni-C alloys, Fe-28.7Ni-1.8C, Fe-29.0Ni-1.4C and Fe-24.7Ni-1.8C (at%), were prepared by melting in a high frequency induction furnace under argon atmosphere and by casting into a water-cooled iron mold. According to a previous report[4], the former two alloys are Invar and the last one is non-Invar. The above three alloys will be labelled A, B and C, respectively, hereafter for simplicity. Each ingot of the alloys was hot-forged at 1373K, homogenized at 1473K for 86.4 ks in a silica capsule

filled with argon, and then quenched into iced water. Pieces with 40mm length were cut from the heat-treated ingot, hot-rolled into 0.5mm thick sheets and cold-rolled further into 0.3mm thick sheets. For magnetization and electrical resistivity measurements, specimens with 3mm × 20mm × 0.3mm size were cut from these sheets. Specimens for tensile deformation to induce martensites were also cut from the sheets of Alloys A and C; the specimens have 20mm gauge length and 4mm width. All the specimens were austenitized at 1473K for 10.8 ks in silica capsules filled with argon, followed by quenching into iced water. Austenitized specimens with 20mm length were cut in half by spark cutting; one half (3mm × 10mm × 0.3mm) was used for electrical resistivity measurement to determine M_S temperature and the other half for magnetization measurement. The specimen size was optimized to avoid the Joule heating and the skin effect. Pulsed magnetic field with the maximum strength of about 31.75 MA/m was applied to the austenitic specimens. Details of the pulsed magnetic field instrument have been described in Chapter 2. Chemical analysis of the three alloys was carried out by using the rest part of each alloy sheet, which had been subjected to the same heat-treatments as above in order to avoid a discrepancy in composition between the chemically analysed and experimentally used specimens. The alloy composition thus analysed is indicated in Table 1. Tensile deformation for inducing martensites was made with an Instron Machine TT-CM-L type in the stress control mode at the strain rate of 8.4×10^{-4}/s.

III. Results

3-1. Transformation temperature and austenitic magnetic moment.

Electrical resistivity vs. temperature relations have been measured in the temperature range from 293 to 77K in order to determine transformation temperatures. The determined M_s and M_f of the three alloys are listed in Table 1. The magnetization in the austenitic state has been measured in order to know the spontaneous magnetization of austenite. The obtained austenitic magnetic moments plotted as a function of ΔT are shown in Fig. 1, which reveals that the moment decreases with increasing ΔT. On the other hand, the martensitic magnetic moment can be obtained on the assumption that it originates in magnetic atoms, and therefore it depends only upon the composition of Fe and Ni atoms. In fact, it has been reported that the assumption approximately holds for the Fe-Ni-C alloys [5], provided that the carbon composition is within 2 at%, as is the case of the present alloys. Thus, the martensitic magnetic moment was estimated to be about 2.0μB for the Invar alloys, and about 2.2μB for the non-Invar alloys, in the same way as in Chapter 2. Accordingly, the difference in magnetic moment between the austenitic and martensitic states becomes larger in the order of Alloy A, B and C in this temperature range. The difference at ΔT=10K is shown in Table 1 for the three alloys.

3-2. Critical magnetic field to induce martensite.

Magnetization M(t) has been measured as a function of mag-

netic field H(t) in one pulse whose maximum strength is higher than the critical field to induce martensitic transformation. Typical M(t)-H(t) curves at $\Delta T=50K$ are shown in Fig. 2, (a), (b) and (c) being for Alloys, A, B and C, respectively. In this figure, an abrupt increase in magnetization due to the occurrence of martensitic transformation can be recognized at a certain strength of the magnetic field, as indicated with an arrow on each curve. This abrupt increase in magnetization could not be observed when the maximum strength of a magnetic field below the one indicated with an arrow has been applied to the another specimen at the same temperature. Therefore, this magnetic field corresponds to the critical one to induce martensitic transformation at temperature $T(=M_S')$. The relation between the shift of M_S temperature, ΔM_S, and a critical field is shown for three alloys in Fig. 3. It is seen from the figure that the critical magnetic fields increase with increasing ΔM_S for all the alloys, but they lie on a little curved line for the two Invar alloys (Alloy A and B), while those for the non-Invar alloy (Alloy C) lie on a single straight line. Such a behavior for the Invar alloys is very similar to that for Fe-Ni Invar alloys previously reported in Chapter 2 and 3. The above result shows that the magnetic effect in rising M_S temperature is different between the Invar and non-Invar alloys, and may give a clue to clarify the magnetic effect on martensitic transformation, as will be discussed later.

Another characteristic feature noted in Fig. 3 is that critical magnetic field for Alloy A is lower than that for Alloy B in the whole range of ΔM_S. If the Zeeman effect were on-

ly one as the magnetic effect on martensitic transformation, as proposed by Krivoglaz and Sadovsky[6], the critical magnetic field at a fixed ΔM_S would be smaller for a larger $\Delta M(M_S')$. However, the fact mentioned above is incompatible with such a prediction. This means that the martensitic transformations under magnetic fields are influenced not only by the Zeeman effect but also by other effects, as previously mentioned for Fe-Ni Invar alloys.

3-3. Amount of magnetic field-induced martensite.

The amount of magnetic field-induced martensites has been estimated from the magnetization in the same way as mentioned in Chapter 2. The estimated amounts of martensites for the three alloys are shown in Fig. 4 as a function of the maximum strength of pulsed magnetic field. The amount of martensites increases with maximum strength of magnetic field for all the three alloys. Such a field dependence of the amount of martensites is also seen in the magnetization curves in Fig. 2, all the alloys exhibiting a gradual increase of magnetization above the critical magnetic field. However, some difference is observed between Alloy A and the other two alloys. That is, the amount of martensites in Alloy A increases gradually from the critical magnetic field, but in the other two alloys it increases abruptly to a certain level at the respective critical magnetic field. This difference seems to be due to the difference in morphology of the magnetic field-induced martensites, as will be shown later.

3-4. Morphology of magnetic field-induced martensite.

Fig. 5 shows optical micrographs of thermally-induced martensites formed by cooling a little below M_S temperature ((a), (d) and (g)) and those of magnetic field-induced ones ((b), (c), (e), (f) (h) and (i)). The formation temperature T, its difference from M_S, ΔT, and applied magnetic field H are indicated in each photograph of the figures. It is noted in the figures that the morphology of the magnetic field-induced martensites is the same as that of thermally-induced ones despite of the different formation temperatures; Alloy A exhibiting thin plate morphology and the other two alloys lenticular one in any cases. The difference in martensite morphology between Alloy A and the other two alloys is considered to be the origin of the difference in the increasing manner of martensite amount at the critical magnetic field shown in Fig. 4. That is, the thin plate martensite may grow gradually like a thermoelastic martensite, whereas the lenticular martensite is formed instantaneously to some amount at respective M_S temperature due to the burst nature. It is also noted in Fig. 5 that the martensite morphology is different even if the martensites are formed at nearly the same temperature, as seen from the comparison of (c) with (d). This result is contradictory to a proposition[2],[3] that the martensite morphology in Fe-Ni-C alloys is decided only by the formation temperature. In order to check further on this point, the magnetic field-induced martensites have been compared with deformation-induced martensites at an identical temperature. Fig. 6 (a) and (b) are optical micrographs of the deformation-induced martensites in

Alloys A and C at ΔT=88 and 50K, respectively, which were taken from tensile specimens after fracture. According to previous papers[7],[8], the deformation-induced martensites are supposed to be produced after plastic deformation has occurred in the austenite matrix at those deformation temperatures. Comparison of Fig. 6 (a) and (b) with Fig. 5 (c) and (h), respectively, reveals that the morphology of deformation-induced martensites is different from that of the magnetic field-induced ones even though the formation temperature is the same. This result also indicates that the martensite morphology in Fe-Ni-C alloys is not decided by the formation temperature alone.

IV. Discussion

4-1. Thermodynamical analysis of critical magnetic field.

It has been shown in the above that martensitic transformation in Fe-Ni-C alloys can be induced even at temperatures above M_S by applying a magnetic field higher than the critical one. The shift of M_S temperature plotted as a function of the critical field for the invar alloys forms a little curved line, as for previously examined Fe-Ni Invar alloys, while that for the non-Invar alloys forms a straight line. In this way, the magnetic effect on martensitic transformation is different between the Invar and non-Invar alloys. In order to know the origin of the difference, the critical magnetic field vs. ΔT relation for the Invar and non-Invar alloys has been thermodynamically analysed by taking account of the Zeeman and high field susceptibility effects mentioned in Chapter 2. In the analysis, the high field susceptibility in the austenitic state and the

quantity of $\Delta G(M_S)-\Delta G(T)$ (whose notation was already described in Chapter 2) are needed beside the difference in magnetic moment between the austenite and martensite phases. The former high field susceptibility may be obtained from the M(t)-H(t) curves shown in Fig. 2, and it is plotted as a function of temperature in Fig. 7. The quantity of $\Delta G(M_S)-\Delta G(T)$ is obtained by Kaufman and Cohen[9] and Fisher et al[10],[11]. It is shown in Fig. 8 as a function of temperature, and its numerical values are shown for the present three alloys in Table 2. The calculated critical field dependence of ΔM_S is shown in Fig. 9, together with experimentally obtained ones, (a) and (b) being for the Invar and non-Invar alloys, respectively. (b) shows that the calculated dependence is close to the experimental one over a wide range of ΔM_S, but (a) does that some disagreement is recognized between the calculated and experimental ones, especially for large ΔM_S. It is concluded from the above difference that other unknown effects may be related to the Invar effect.

4-2. Factor to determine the martensite morphology.

It has been pointed out that martensite morphology is not decided by the formation temperature alone. Whereupon another possible factor to determine the martensite morphology may be pointed out in the following. In the case of deformation induced martensitic transformation, a considerable amount of plastic deformation is introduced in the austenite before the transformation occurs. On the other hand, the magnetic field-induced martensites seen in Fig. 5 are produced without any plastic de-

formation. In the former case it may be possible that a particular arrangement of dislocations has been formed in the austenite, which will influence the morphology of martensite. It is well known that a larger number of dislocations are observed in ferrous martensites as the formation temperature becomes higher and as the martensite morphology changes from thin plate to lenticular, butterfly and finally lath. Taking account of these facts, it is not so unreasonable to assume that the martensite morphology is related to the dislocation structure in the austenite before the transformation, and therefore the morphology may be changed by varying the austenite dislocation structure even in an alloy with the same composition and at the same temperature. However, detailed relation between the martensite morphology and the dislocation structure in austenite is not clear yet.

References

(1) YE. A. Fokina, L. V. Smirnov, V. N. Olesov, V. M. Schastlivtsev and V. D. Sadovsky: Fiz. Met. Metalloved., 51 (1981), 160.

(2) T. Maki, M. Shimooka, M. Umemoto and I. Tamura: J. Japan Inst. Metals, 35 (1971), 1073 (in Japanese).

(3) M. Umemoto, Y. Watai and I. Tamura: J. Japan Inst. Metals., 44 (1980), 453 (in Japanese).

(4) S. Kajiwara and T. Kikuchi: Collected Abstracts of the Autumn Meeting of Japan Inst. Metals. (1983), p. 352 (in Japanese).

(5) K. Mitsuoka, H. Miyajima, H. Ino and S. Chikazumi: J. Phys. Soc. Jpn., 53 (1984), 2381.

(6) M. A. Krivoglaz and V. D. Sadovsky: see Shapter 1, (55).

(7) H. Onodera, H. Oka and I. Tamura: J. Japan Inst. Metals, 42 (1978), 898 (in Japanese).

(8) M. Tokizane: Proc. 1st JIM int. Symp. on New Aspects of Martensitic Transformation, Suppl. to Trans. JIM, 17 (1976), p. 345.

(9) L. Kaufman and M. Cohen: see Chapter 1, (28).

(10) J. C. Fisher: Trans. AIME, 185 (1949), 688.

(11) J. C. Fisher, J. H. Hollomon and D. Turnbull: Trans. AIME 185 (1949), 691.

Table 1. Transformation temperatures and the difference in magnetic moment between austenitic and martensitic states at M_S+10K.

Composition (at %)	Fe-28.7Ni-1.8C (A) (Invar)	Fe-29.0Ni-1.4C (B) (Invar)	Fe-24.7Ni-1.8C (C) (non-Invar)
Ms(K)	93	193	223
M_f(K)	<77	87	110
$\Delta M_{(Ms+10K)}$(μ_B)	0.70	1.04	2.01

Table 2. Numerical values of $\Delta G(M_S)-\Delta G(T)$ for various ΔT for the three Fe-Ni-C alloys.

Fe-28.7Ni-1.8C,(A)

ΔT (K)	ΔG(Ms)-ΔG(T) (cal/mol)	ΔG(Ms)-ΔG(T) (J/mol)
-90	-49.9791	-208.913
-85	-49.0005	-204.822
-80	-47.5473	-198.748
-75	-45.7839	-191.377
-70	-43.7776	-182.99
-65	-41.566	-173.746
-60	-39.1728	-163.742
-55	-36.615	-153.051
-50	-33.9055	-141.725
-45	-31.0537	-129.805
-40	-28.0684	-117.326
-35	-24.9558	-104.315
-30	-21.7214	-90.7956
-25	-18.3703	-76.7878
-20	-14.9068	-62.3103
-15	-11.3347	-47.379
-10	-7.6575	-32.0084
-5	-3.87814	-16.2106
0	0	0
5	3.97482	16.6148
10	8.04361	33.6223
15	12.204	51.0126
20	16.454	68.7775
25	20.7912	86.9072
30	25.2139	105.394
35	29.7202	124.23
40	34.308	143.408
45	38.9776	162.926
50	43.7332	182.805
55	48.566	203.006
60	53.4733	223.518
65	58.4053	244.134
70	63.4538	265.237
75	68.575	286.643
80	73.7653	308.339
85	78.9854	330.159
90	84.3082	352.408
95	89.6992	374.943
100	95.154	397.744

Fe-29.0Ni-1.4C,(B)

ΔT (K)	ΔG(Ms)-ΔG(T) (cal/mol)	ΔG(Ms)-ΔG(T) (J/mol)
-100	-95.154	-397.744
-95	-91.1792	-381.129
-90	-87.1104	-364.121
-85	-82.95	-346.731
-80	-78.7001	-328.966
-75	-74.3628	-310.836
-70	-69.9401	-292.35
-65	-65.4338	-273.513
-60	-60.846	-254.336
-55	-56.1764	-234.817
-50	-51.4208	-214.939
-45	-46.588	-194.738
-40	-41.6807	-174.225
-35	-36.7487	-153.61
-30	-31.7002	-132.507
-25	-26.579	-111.1
-20	-21.3887	-89.4047
-15	-16.1686	-67.5847
-10	-10.8458	-45.3352
-5	-5.45477	-22.801
0	0	0
5	5.46526	22.8448
10	11.042	46.1557
15	16.6831	69.7352
20	22.3837	93.5639
25	28.0673	117.321
30	33.8825	141.629
35	39.7597	166.195
40	45.6928	190.996
45	51.5523	215.489
50	57.5775	240.674
55	63.6593	266.096
60	69.792	291.731
65	75.8432	317.025
70	82.0656	343.034
75	88.3415	369.268
80	94.5269	395.122
65	100.845	421.534
90	107.203	448.11
95	113.603	474.861
100	120.039	501.761

Fe-24.7Ni-1.8C,(C)

ΔT (K)	ΔG(Ms)-ΔG(T) (cal/mol)	ΔG(Ms)-ΔG(T) (J/mol)
-100	-103.823	-433.979
-95	-99.3164	-415.142
-90	-94.7285	-395.965
-85	-90.059	-376.446
-80	-85.3033	-356.568
-75	-80.4706	-336.367
-70	-75.5633	-315.854
-65	-70.6312	-295.239
-60	-65.5828	-274.136
-55	-60.4616	-252.729
-50	-55.2712	-231.034
-45	-50.0511	-209.214
-40	-44.7283	-186.964
-35	-39.3373	-164.43
-30	-33.8825	-141.629
-25	-28.4173	-118.784
-20	-22.8405	-95.4733
-15	-17.1995	-71.8938
-10	-11.4988	-48.0652
-5	-5.81522	-24.3076
0	0	0
5	5.87715	24.5665
10	11.8103	49.3671
15	17.6698	73.8598
20	23.6949	99.0448
25	29.7768	124.467
30	35.9095	150.102
35	41.9607	175.396
40	48.1831	201.405
45	54.459	227.639
50	60.6443	253.493
55	66.9629	279.905
60	73.3208	306.481
65	79.7206	333.232
70	86.1561	360.132
75	92.63	387.193
80	99.1418	414.413
85	105.686	441.769
90	112.265	469.269
95	118.879	496.915
100	125.522	524.681

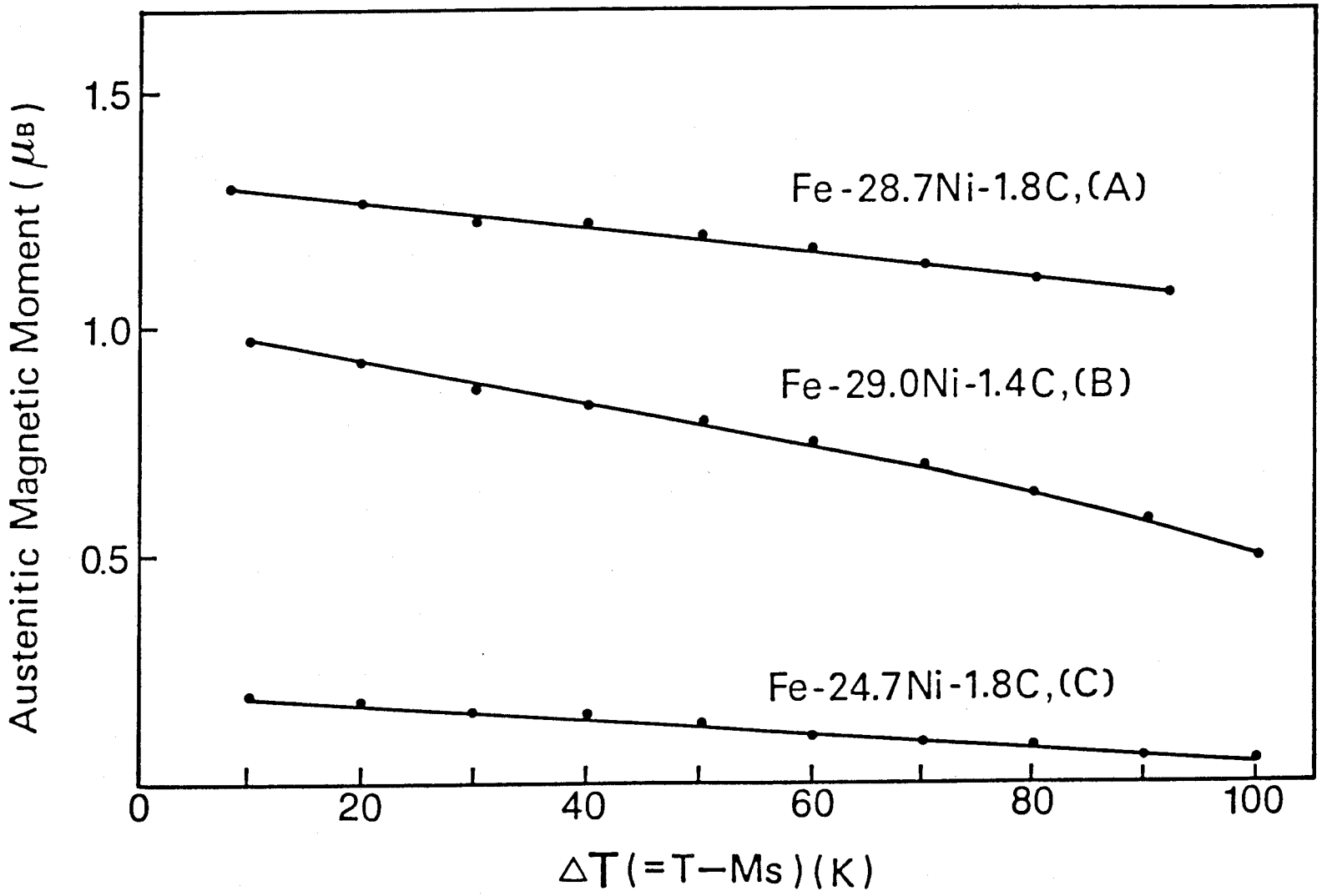

Fig. 1 Austenitic magnetic moments as a function of $\Delta T(=T-M_s)$ for three Fe-Ni-C alloys.

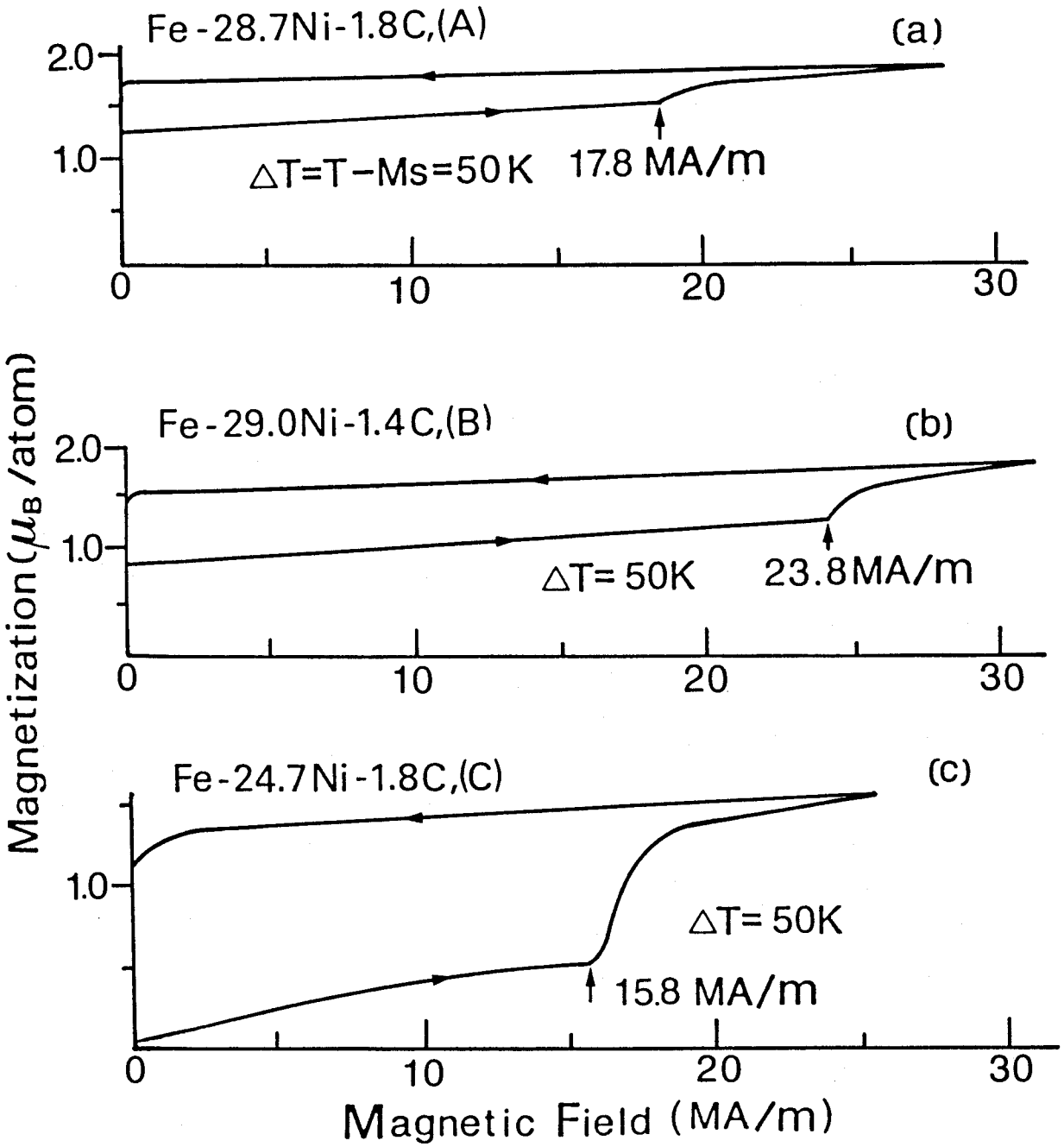

Fig. 2 Magnetization vs magnetic field (M(t)-H(t)) curves for three Fe-Ni-C alloys.

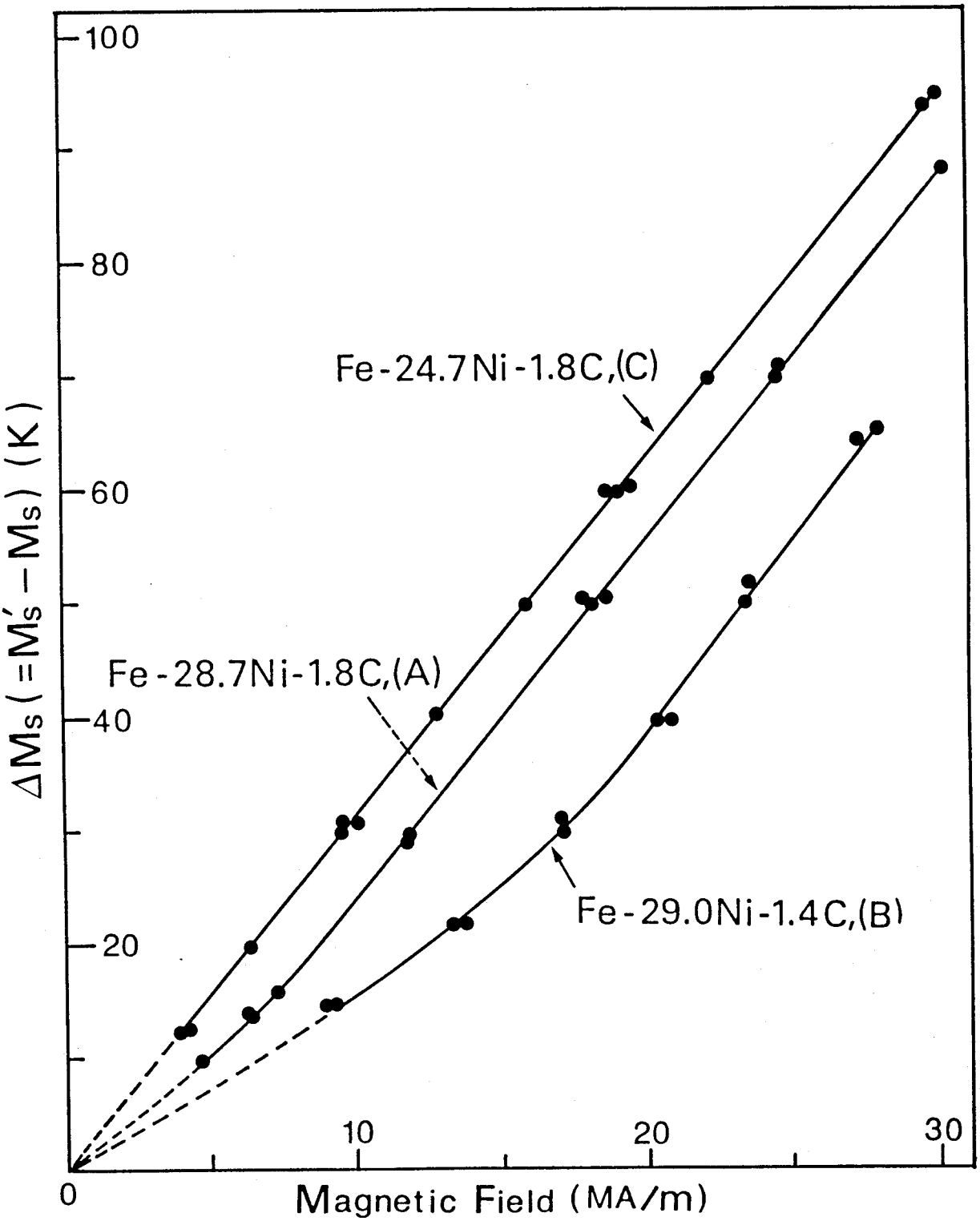

Fig. 3 Critical magnetic field dependence of the shift of M_S temperature, $\Delta M_S (=M_S'-M_S)$.

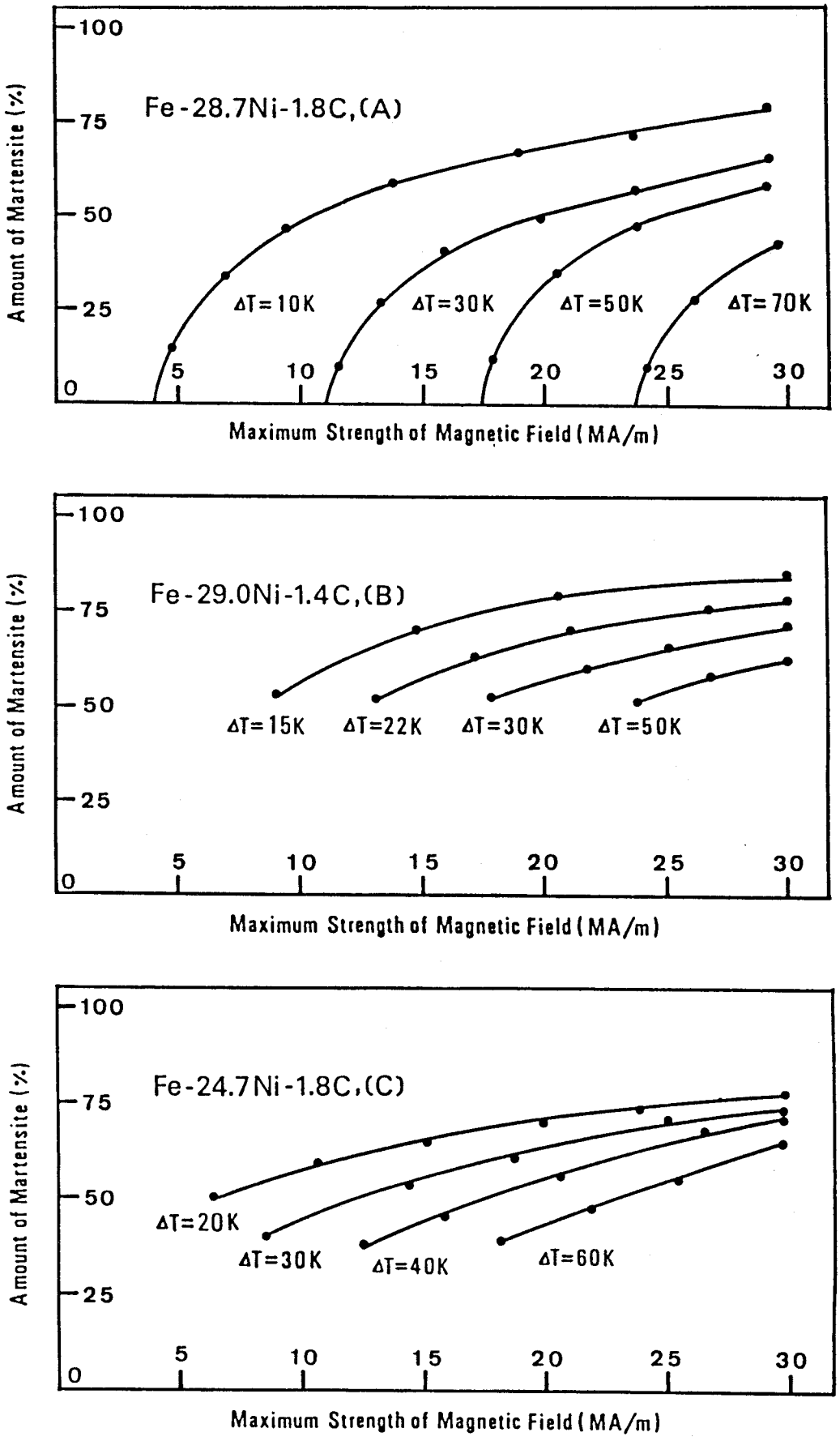

Fig. 4 Amounts of magnetic field-induced martensites, plotted as a function of the maximum strength of pulsed magnetic field.

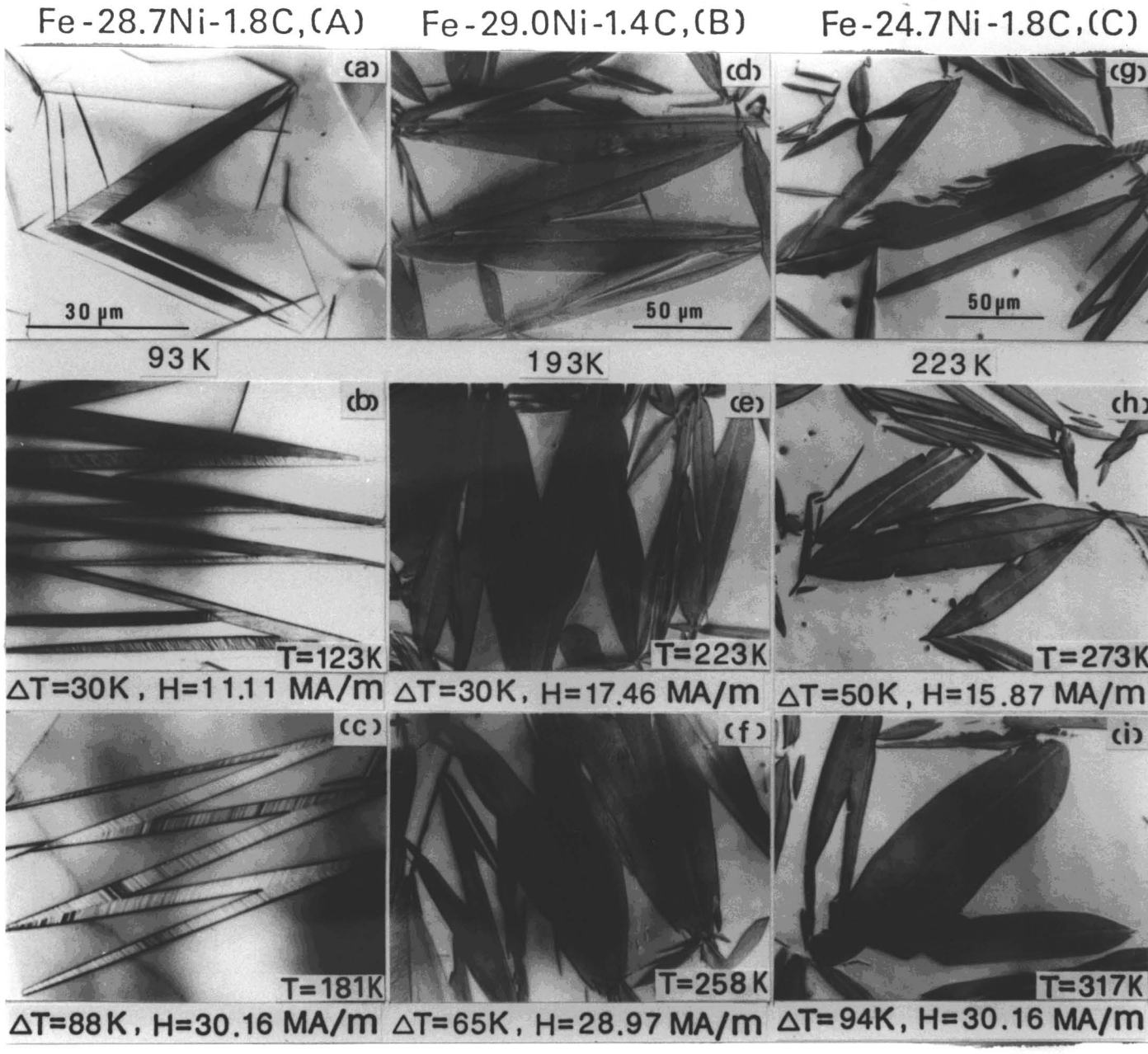

Fig. 5 Optical micrographs of thermally-induced martensites, (a), (d) and (g), and magnetic field-induced ones, (b), (c), (e), (f), (h) and (i). Transformation temperature T, ΔT and H for the magnetic field-induced martensites are shown in each photograph.

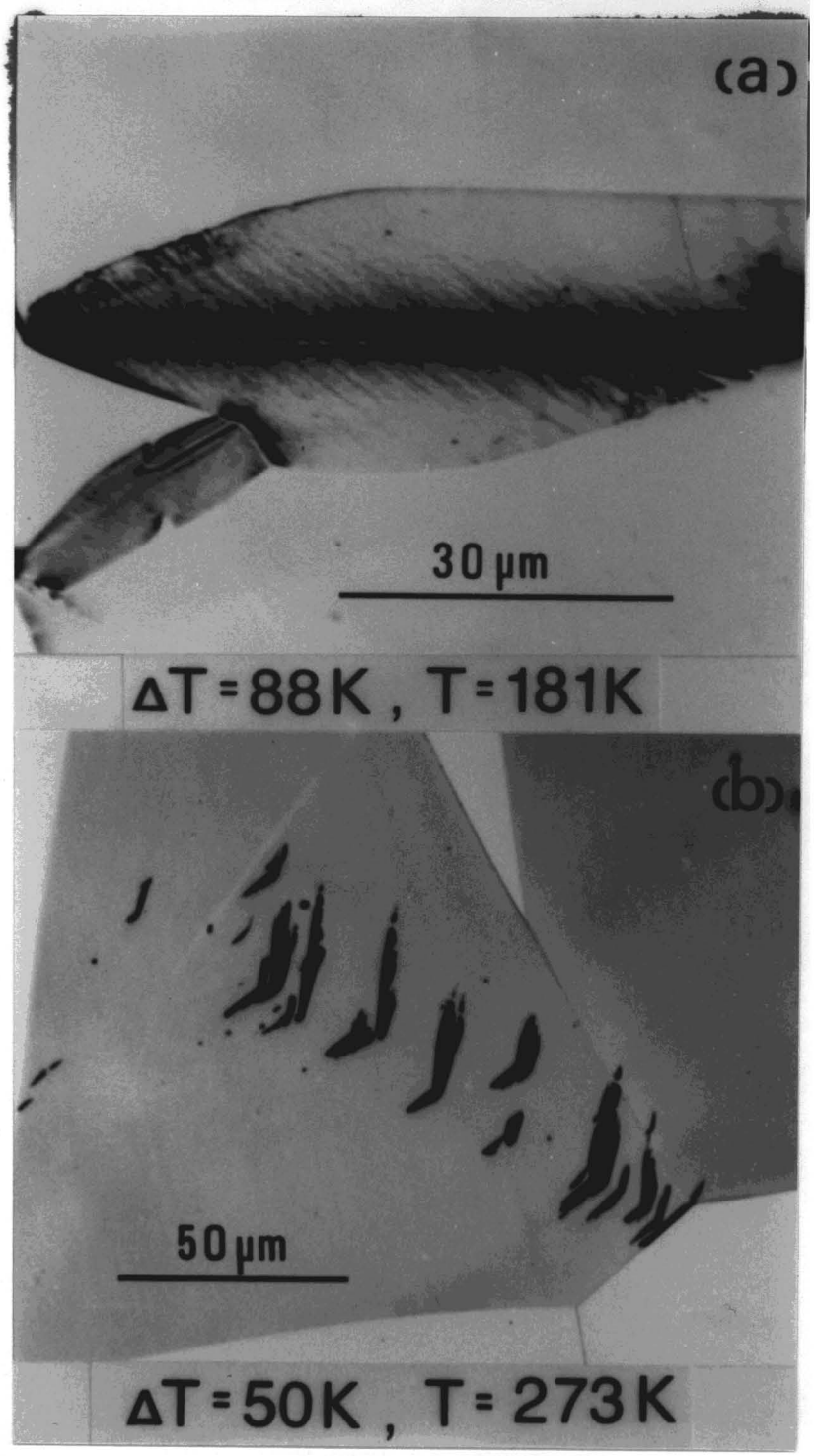

Fig. 6 Optical micrographs of deformation-induced martensites in Fe-28.7Ni-1.8C, (a), and Fe-24.7Ni-1.8C, (b). ΔT and formation temperature T are shown in each photograph.

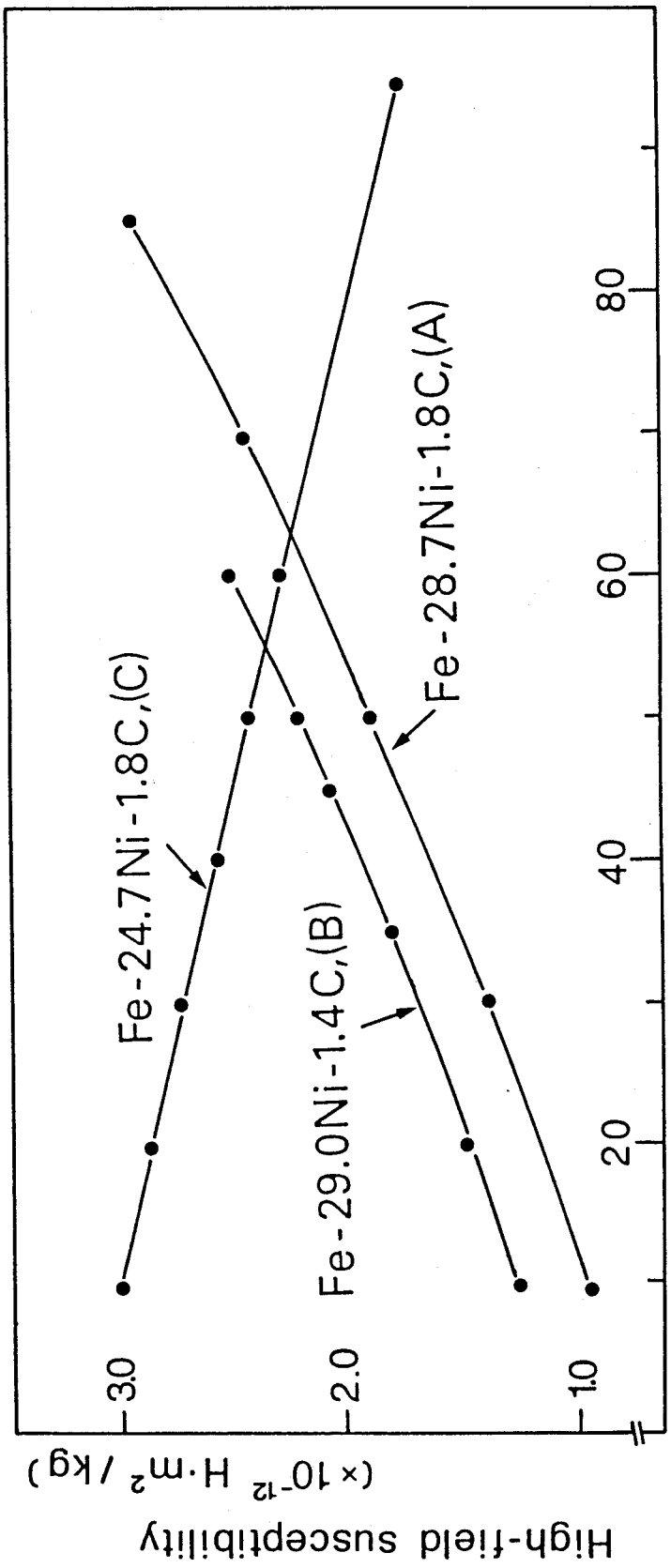

Fig. 7 High field susceptibility as a function of ΔT for three Fe-Ni-C alloys.

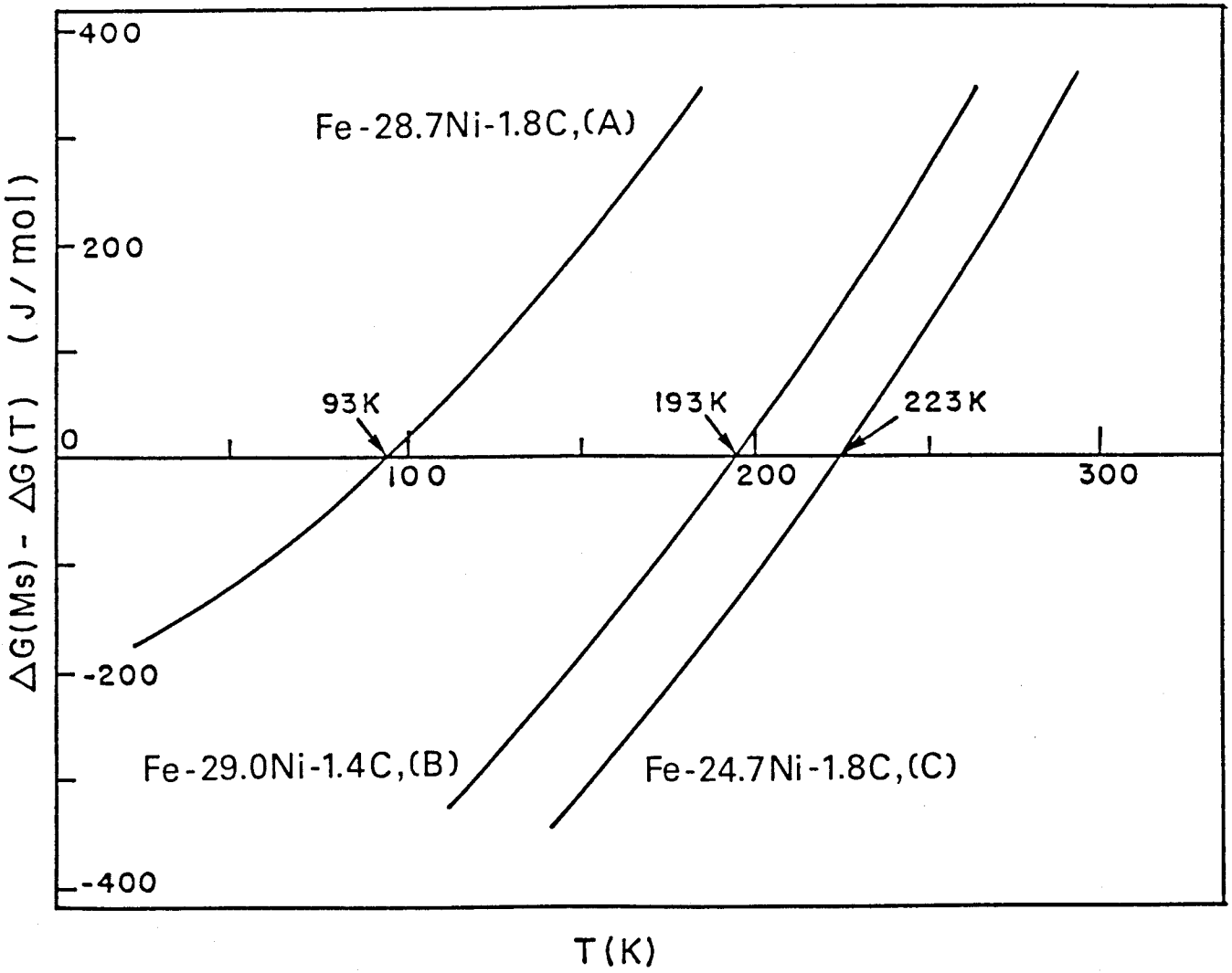

Fig. 8 Calculated $\{\Delta G(M_S)-\Delta G(T)\}$ as a function of temperature for three Fe-Ni-C alloys.

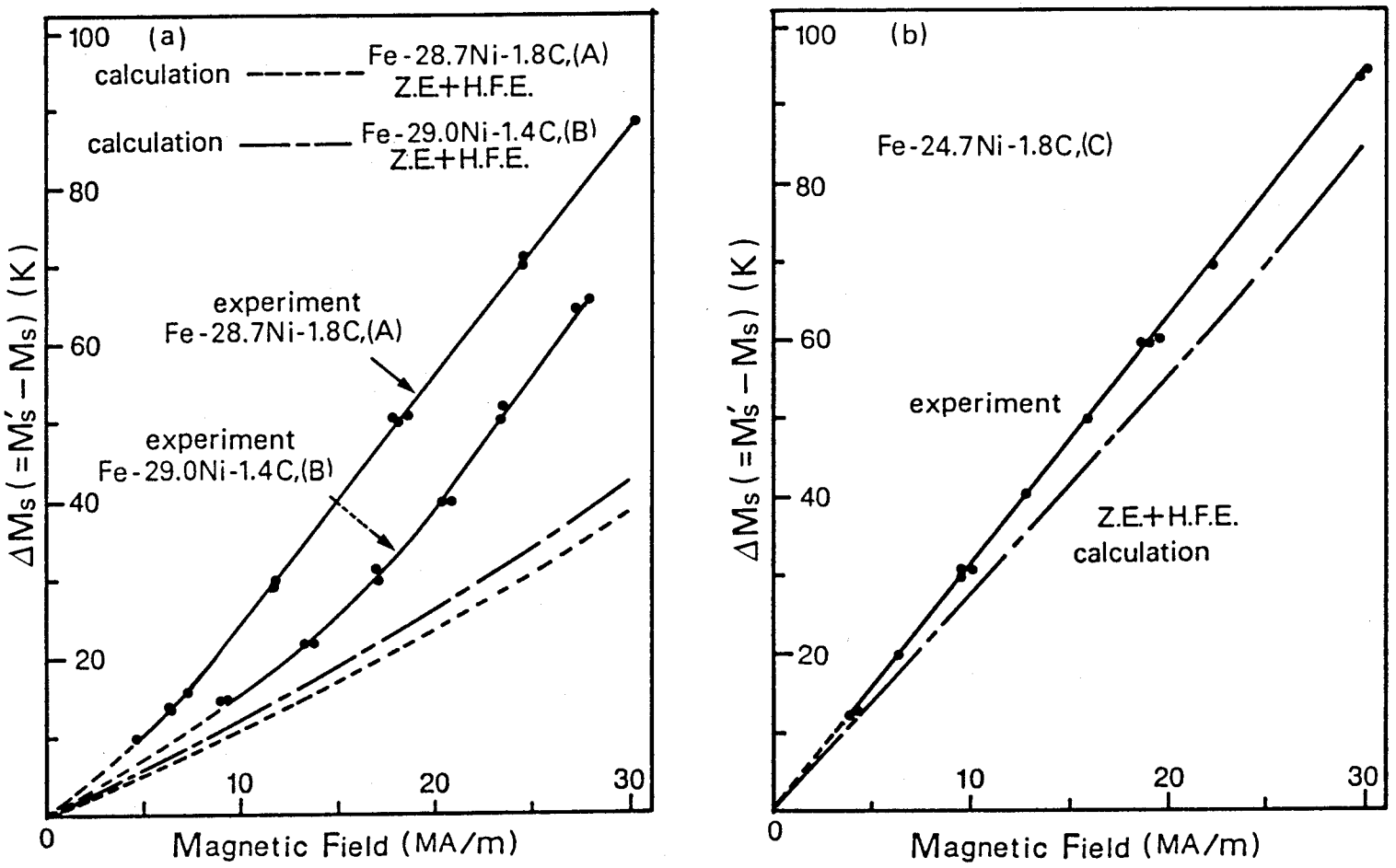

Fig. 9 Calculated and measured critical magnetic field dependence of ΔM_S,(a) for the two Invar alloys and (b) for the other non-Invar alloy. Z.E. and H.F.E. mean the Zeeman and high field susceptibility effects, respectively.

Chapter 5

Magnetic Field-Induced Martensitic Transformations in Fe-Pt Alloys and Their degree of Order Effect.

Synopsis

Magnetic field-induced martensitic transformations in disordered and ordered Fe-24at%Pt alloys have been studied to examine the effect of degree of order (S) on the transformations by measuring the magnetization and electrical resistivity, applying a pulsed ultra high magnetic field. As a result, it is found that a magnetic field higher than a critical field is needed to induce the martensitic transformations at temperatures above M_S without regard to the degree of order. The critical field increases with increasing the shift of M_S temperature, $\Delta M_S (=M_S'-M_S)$, and the shift of M_S as a function of magnetic field lie on a straight line for the non-thermoelastic disordered alloy with $S<0.5$, but on a curved line for the thermoelastic ordered alloys with $S=0.7-0.8$, as if the curve diverges at a certain temperature near the respective T_o temperature. The divergence phenomenon seems to suggest that the certain temperature near To is a maximum one above which martensites can not be induced even though any high magnetic field is applied. The amount of magnetic field-induced martensites increases linearly with increasing the strength of magnetic field for any $\Delta T(T-M_S)$ and any degree of order, and the smaller the ΔT for a given degree of order and the lower the degree of order, the larger the amount of martensites becomes. A thermodynamical calculation for the shift of M_S temperature suggests that the effect of a magnetic field on martensitic transformations may

result in not only the Zeeman and high field susceptibility effects but also other unknown effects.

I. Introduction

All of the studies so far reported on magnetic field-induced martensitic transformations were concerned with disordered alloys. Therefore, there is no information about the effect of the degree of order on magnetic field-induced martensitic transformations. In order to obtain some information about it, Fe-Pt alloys with compositions near Fe_3Pt are convenient[1], because it is easy to adjust the degree of order by varying the annealing period for ordering. It is well known in the Fe-Pt alloy that the temperature hysteresis between M_f and A_f can be reduced arbitrarily by increasing the degree of order, although it was unchangeable and as much as 400K in the case of an Fe-Ni alloy, and that the type of martensitic transformation can be changed from a non-thermoelastic one in the disordered state to a thermoelastic one in the ordered state. Moreover, it is well known in this alloy system that the volume change associated with martensitic transformation becomes negative by increasing the degree of order[2]. On the other hand, the difference in spontaneous magnetization between the austenitic and martensitic states of the Fe-Pt alloy is almost the same as that in the previous Fe-Ni alloys. Therefore, magnetic field-induced martensitic transformations in ordered and disordered Fe-Pt alloys can be examined by applying the same order of strength of magnetic field as in the Fe-Ni alloys mentioned in Chapter 2. In this sense, an Fe-Pt alloy is the only one for which the differ-

ence in the magnetic field effect between non-thermoelastic and thermoelastic martensitic transformations can be investigated by changing the degree of order. However, there has been no report on the magnetic field-induced martensitic transformation in the Fe-Pt alloy. The present study is, therefore, conducted to make the above problem clear by examining the shift of M_S temperature, critical magnetic field to induce martensites, their degree of order dependence and amount of martensites formed in Fe-24at%Pt alloys with different degrees of order. The results are compared with those in the previous Fe-Ni alloy mentioned in Chapter 2.

II. Experimental Procedures

An ingot of the Fe-Pt alloy with a nominal composition of 24at%Pt was supplied by Prof. T. Tadaki at Osaka University, which was melted in a vacuum induction furnace by using 99.99% iron and 99.99% platinum. The ingot was hot-forged at 1273K, homogenized at 1473K for 6.0×10^5 s in an evacuated silica capsule, and then hot- and cold-rolled into 0.3mm thick sheet. Specimens 3mm × 20mm × 0.3mm in size were cut from the sheet. and were austenitized at 1273K for 1.08×10^4 s in evacuated silica capsules, followed by quenching into iced water. Three kinds of specimens with different degrees of order were prepared by annealing at 923K for 1.8×10^3 s, 2.9×10^4 s and 3.8×10^5 s, and are labeled A, B and C respectively for simplicity. All the specimens were cut into half length (3mm × 10mm × 0.3 mm) by a spark-cutting machine; one half was used for electrical resistivity measurements to determine transformation tem-

peratures, and the other half for magnetization measurements. The size of the specimens was optimized to avoid Joule heating and a skin effect. High field magnetization measurements were performed at the High Magnetic Field Laboratory, Osaka University, the magnetic field being a pulsed one with the maximum strength of 31.75 MA/m. Details of the pulsed magnetic field instrument were described in Chapter 2.

III. Results

3-1. Transformation temperature and degree of order.

Prior to magnetization measurements, transformation temperatures (M_s, M_f, A_s and A_f), equilibrium temperature (To), curie temperature of the austenitic state (Tc), and degree of order (S) were determined by measuring electrical resistivity-temperature relations and by referring to the other data published so far[2], as described below. The electrical resistivity of specimens A, B and C was measured as a function of temperature to determine respective M_s, M_f, A_s and A_f temperatures. The obtained electrical resistivity-temperature curves are shown in Fig. 1, (a), (b) and (c) being plotted for the specimens A, B and C, respectively, immediately after their annealing treatments for ordering. Transformation temperatures are indicated with arrows on each of the curves, and their values are listed with parentheses in Table 1. It is noted in Fig. 1 that the M_s temperature decreases and the type of transformation changes from a non-thermoelastic one in (a) to a thermoelastic one in (b) and (c) with increasing degree of order. However, the M_s temperature of specimens B and C exhibiting a thermoelastic type

transformation increase by thermal cycling in the temperature range from 293 to 77K. Such a thermal cycling effect on the M_S temperature can be clearly seen from the electrical resistivity-temperature curves of Fig. 1 (b') and (c') which were plotted after 15 thermal cycles for specimens B and C, respectively. The increased M_S temperatures are indicated with arrows on the curves, and their values are listed without parentheses in Table 1. The increase of M_S temperature is apparently saturated with these values, since it was not recognized after the thermal cycling has been repeated more than 15 times. It is thus noted from Table 1 that the M_S temperatures of thermoelastic specimens subjected to thermal cycling are higher than those not subjected to thermal cycling by 19 and 10K for specimens B and C, respectively. Other transformation temperatures M_f, A_S and A_f, however, are not so much changed by thermal cycling in either specimen, as is seen in Table 1. Thus, specimens B and C used for magnetization measurements have beforehand been subjected to 15 times of thermal cyclings to make their M_S temperatures remain constant. The equilibrium temperature (To) was estimated from the formula $To=(M_S+A_f)/2$ which was defined by Tong and Wayman[1], by using the above transformation temperatures. The To values for specimens B and C are shown in Table 1. The To temperatures thus obtained for those specimens subjected to 15 thermal cycles are higher than the M_S temperatures by about 20 and 12K, respectively. The Curie temperature, Tc, was obtained by measuring the temperature dependence of magnetization in the austenitic state, (Table 1). It is noted that the Curie temperature increases with

increasing the degree of order. The degree of order in each specimen was estimated from the data given in a previous paper by Tadaki et al.[2] for an Fe-24at%Pt alloy. Accordingly, the three kinds of annealing treatments at 923K, which were adopted in the present experiment, will bring the degree of order, less than 0.5, nearly equal to 0.7 and 0.8 for specimens A, B and C, respectively, as shown in Table 1. Spontaneous magnetization in the austenitic state has been measured as a function of temperature, which is shown as a function of ΔT in Fig. 2. On the other hand, spontaneous magnetization in the martensitic state has been also measured by magnetization measurement for ordered Fe-Pt alloys because martensitic state can be realized only in those alloys cooled down M_f. The values thus obtained for B and C are 2.22μB and 2.44μB, respectively. While spontaneous magnetization for the disordered Fe-Pt alloy in the martensitic state can not be obtained, because two phases coexist in this alloy. Then, it is obtained on assumption that the electron atom ratio dependence of spontaneous magnetization lies on the Slater-Pauling curves, as mentioned in Chapter 2, the value being about 2.0μB.

3-2. Critical magnetic field to induce martensite.

A pulsed magnetic field H(t) whose maximum strength is higher than the critical one to induce the martensitic transformation was applied for the specimens, and the magnetization M(t) was recorded as a function of strength in one pulse. Typical M-H curves obtained for the specimens A. B and C are shown as (a), (b) and (c), respectively, in Fig. 3 in which there are inscribed experimental conditions such as degree of order, max-

imum strength of pulsed magnetic field, and temperature difference between M_S and a temperature at which the magnetic field is applied. It is noted in (a), (b) and (c) that an abrupt change in magnetization due to martensitic transformation is not recognized although it has been observed the Fe-Ni and Fe-Ni-C alloy mentioned in Chapter 2, 3 and 4. Therefore, no information exists on the occurrence of martensitic transformation in Fig. 3. Nevertheless, some hysteresis can be observed on the magnetization curves, being representative of the occurrence of martensitic transformation. These results suggest that critical magnetic field can not be determined from magnetization measurements alone even if martensitic transformation occures, and this result is greatly different from that obtained in the previous Fe-Ni and Fe-Ni-C alloys. Thereupon, in order to determine critical magnetic field to induce martensitic transformations, electrical resistivity measurements, have been carried out in combination with magnetization measurements, because the electrical resistivity change is more sensitive to the occurrence of martensitic transformations. The electrical resistivity ratio was measured for every rise of 0.8 MA/m in maximum strength of the pulsed magnetic field, and plotted as a function of the maximum strength of the pulsed magnetic field. Fig. 4 shows such a plot for the specimen B (S=0.7) at ΔT=15K, where R(H) means the electrical resistivity when the maximum strength of the magnetic field is H. This figure indicates that the ratio R(H)/R(0) begins to decrease at a certain maximum strength of magnetic field, corresponding to the occurrence of martensitic transformation. Such a maximum strength of magnetic field is defined as a critical field to induce the marten-

sitic transformation at a given ΔT. In this way, the shift of M_S, $\Delta M_S (=M_S'-M_S)$ was measured as a function of critical magnetic field for each of the specimens A, B and C, as shown in Fig. 5. Fig. 5 clearly indicates that the critical magnetic field to induce martensitic transformations increases with increasing ΔM_S for all specimens. Comparing the shifts of M_S temperatures of the specimens with one another as to the same strength of magnetic fields, they decrease with increasing the degree of order, as easily seen from Fig. 5. For example, when 20 MA/m of magnetic field is applied, the M_S temperatures of specimen A ($S<0.5$) and C ($S\sim0.8$) are 28 and 7K, respectively, which decrease as much as 21K with increasing the degree of order. One of characteristic features in Fig. 5 is that the critical magnetic field for specimens B and C lie on a curved line, and that the curves appear to diverge near their proper temperatures. This characteristic is greatly different from the fact that the critical magnetic field for specimen A lies on a straight line and appears as if it increases unlimitedly. The temperature at which the curved lined diverge seems to correspond to a certain temperature near To temperature of specimen B and C, as indicated in Fig. 5. This means that a maximum temperature may possibly exist, above which no martensitic transofrmation can be induced even if any higher magnetic field is applied. This result seems to be very important in considering the effect of a magnetic field on thermodynamics or kinetics of martensitic transformations, and will be discussed later in more detail.

3-3. Amount of magnetic field-induced martensite

The amount of magnetic field-induced martensites has been determined by calculation, using magnetic moments in the austenitic and martensitic states, in the same way as that described in Chapter 2. The calculated amount for specimens A, B and C is shown in Fig. 6 as a function of the maximum strength of the pulsed magnetic field. This figure shows that the amount linearly increases with the maximum strength of magnetic field independent of the degree of order and ΔT. Such a magnetic field dependence of the amount of martensites can also be recognized from the magnetization curves in Fig. 3 (a), (b) and (c) which exhibit a gradual increase. This result is deffernt from that for the previous Fe-Ni alloy whose amount of martensites is nearly the same without regard to the strength of applied magnetic field, provided that ΔT is kept constant. According to the figure, the amount of martensites also increase with decreasing ΔT when the degree of order is kept constant, as is easily seen if those of specimen A are compared at ΔT=15, 24 and 32K. Furthermore, they also increase with decreasing the degree of order when ΔT is kept constant, as is seen from a comparison between the amounts of martensites of specimens A and B at ΔT=15K. In this way, the amount of magnetic field-induced martensites are dependent on the strength of magnetic field, being greatly different from the case of previous Fe-Ni alloy. The reason for such a difference between the Fe-Pt and Fe-Ni alloys is not known yet, but may be attributed to a difference in mechanical strength of the matrix γ phases and/or in martensite growth mechanism between the two alloys.

IV. Discussion

It has been found in the above that the martensitic transformations in disordered and ordered Fe-24at%Pt alloys can be induced even at temperatures above M_S by applying a magnetic field higher than a critical field, and that the critical magnetic field for the thermoelastic ordered alloys appears to diverge at a certain temperature near To. This result suggests that the martensitic transformations may not be induced at temperatures above To, even if any high magnetic field is applied. This can not be explained by the formula, $\Delta M_S = \frac{\Delta M(M_S') \cdot H \cdot To}{q}$, derived by Krivoglaz and Sadovsky[3]. That is, according to the formula, ΔM_S increases unlimitedly with H, as long as $\Delta M(M_S')$ has a finite value. However, the actual critical field diverges at a certain temperature near To, which contradicted to the formula. This result can not also be explained by another formula consisted of two effects, Zeeman and high field susceptibility effects, which was described in Chapter 2, as shown below. Calculation for the critical field dependence of the shift of M_S temperature has been done for specimen C, because Gibbs chemical free energy difference between the austenitic and martensitic states can be obtained for this alloy[4]. The spontaneous magnetizations of the austenitic and martensitic states are estimated to be 2.06μB and 2.44μB, respectively, and the high field susceptibility of the austenitic state is obtained from the magnetization curve in Fig. 3, being 1.3×10^{-13} H·m²/Kg. On the other hand, the susceptibility for the martensitic state is neglected in the present calculation, because it is considered to be smaller compared with that of the austenitic state, as

is seen in Fig. 3. The calculated relation is shown in Fig. 7. This suggests that the effect of a magnetic field on martensitic transformations may result in not only the Zeeman and high field susceptibility effects but also other unknown effects, and that the unknown effects may be related to the divergence phenomenon of critical magnetic field.

Some discussion will be done about the unknown effects, based on the results of the present Fe-Pt alloys and the previously examined Fe-Ni alloys. According to the previous study on Fe-Ni alloys, the unknown effects are considered to be related to the Invar effect. This may hold for the present Fe-Pt alloys, because they are known to have an invar effect without regard to the degree of order. However, even if the unknown effects are assumed to result in the same invar effect, they must be different between the Fe-Pt and Fe-Ni alloys in the manner of the shift of M_S temperature. That is, for the ordered Fe-Pt alloys, the shift of M_S temperature due to the unknown effects must be decreased by a magnetic field because of the divergence phenomena of critical magnetic fields. On the other hand, for the Fe-Ni alloys, the M_S temperature due to the unknown effects must be rather increased, as mentioned in Chapter 2. In this way, the unknown effects may differently influence on the shift of M_S temperature on martensite transformation depending on alloy system. This decrease or increase of the shift of M_S temperature means that a physical quantity related to the unknown effects changes their sign depending on the alloy system. As for such a quantity, the volume change associated with martensitic transformation may be mostly possible,

because it is negative in the present ordered alloy but positive in the disordered Fe-Pt and Fe-Ni alloys. From this point of view, it may be pointed out that the unknown effects are related to the volume change associated with the martensitic transformations in Invar alloys.

References

(1) H. C. Tong and C. M. Wayman: Acta Met., 22 (1974), 887.

(2) T. Tadaki, K. Katsuki and K. Shimizu: Proc. First Intern. Symp. by Jpn, Inst. Metals (JIMIS-1) on New Aspects on Martensitic Transformations, Kobe (Japan), Suppl. to Trans. JIM, 17 (1976), 187.

(3) M. A. Krivoglaz and V. D. Sadovsky: see Chapter 1, (55).

(4) H. C. Tong and C. M. Wayman: Acta Met., 23 (1975), 209.

Table 1. Data on transformation temperatures, To temperature, Curie temperature of austenite (T_C), and degree of order (S) for specimens used in the present study.

Sample	M_s (K)	M_f (K)	A_s (K)	A_f (K)	To (K)	T_C (K) (austenite)	S
A	(255)	(198)				288	<0.5
B	203 (184)	160 (158)	183 (181)	243 (245)	223 (214.5)	321	~0.7
C	153 (143)	123 (120)	139 (138)	177 (183)	165 (163)	333	~0.8

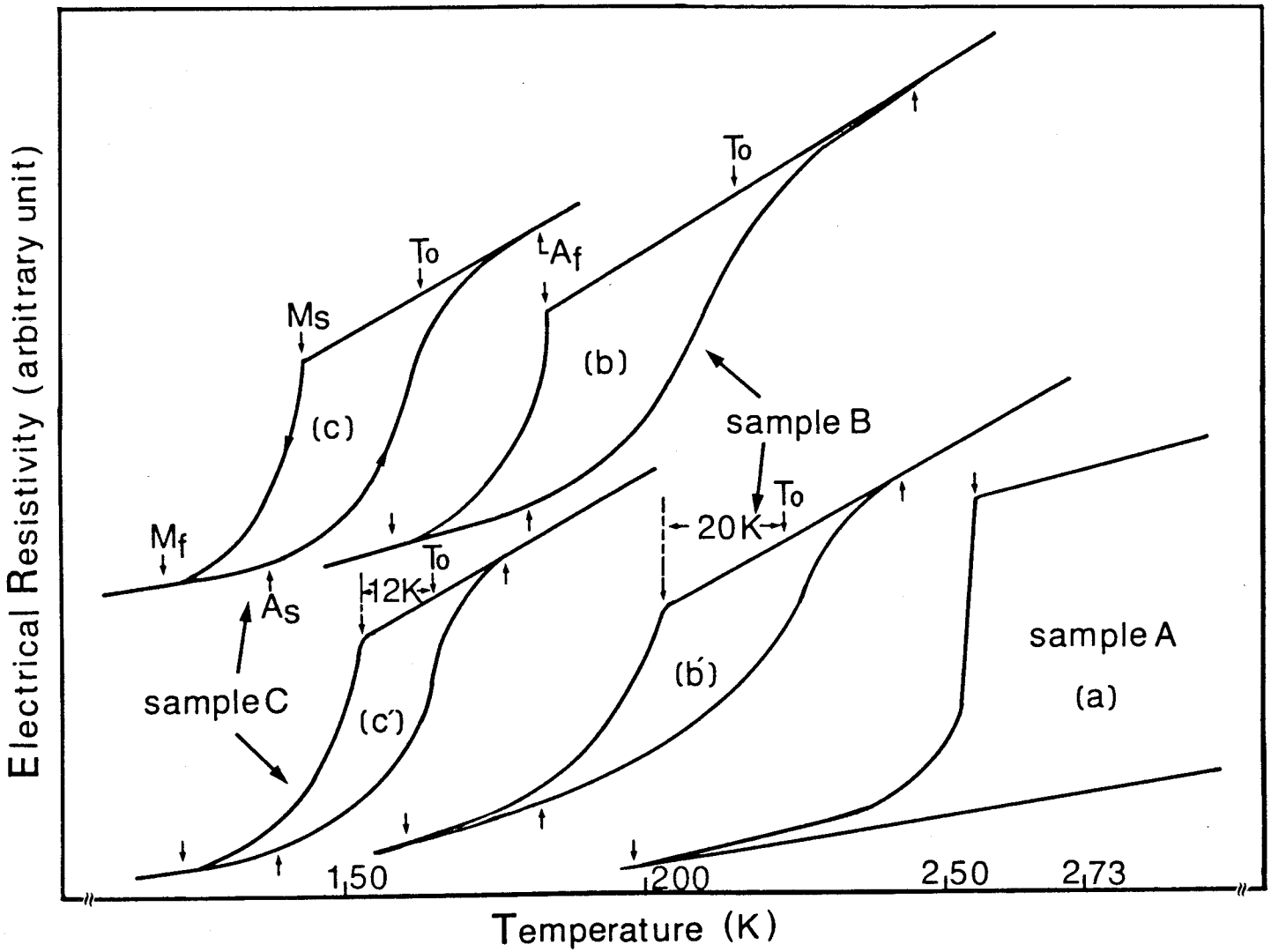

Fig. 1 Electrical resistivity-temperature curves. (a), (b) and (c) are for specimens A, B and C, respectively, immediately after annealing treatments for ordering, and (b') and (c') are for specimens B and C, respectively, after 15 thermal cycles.

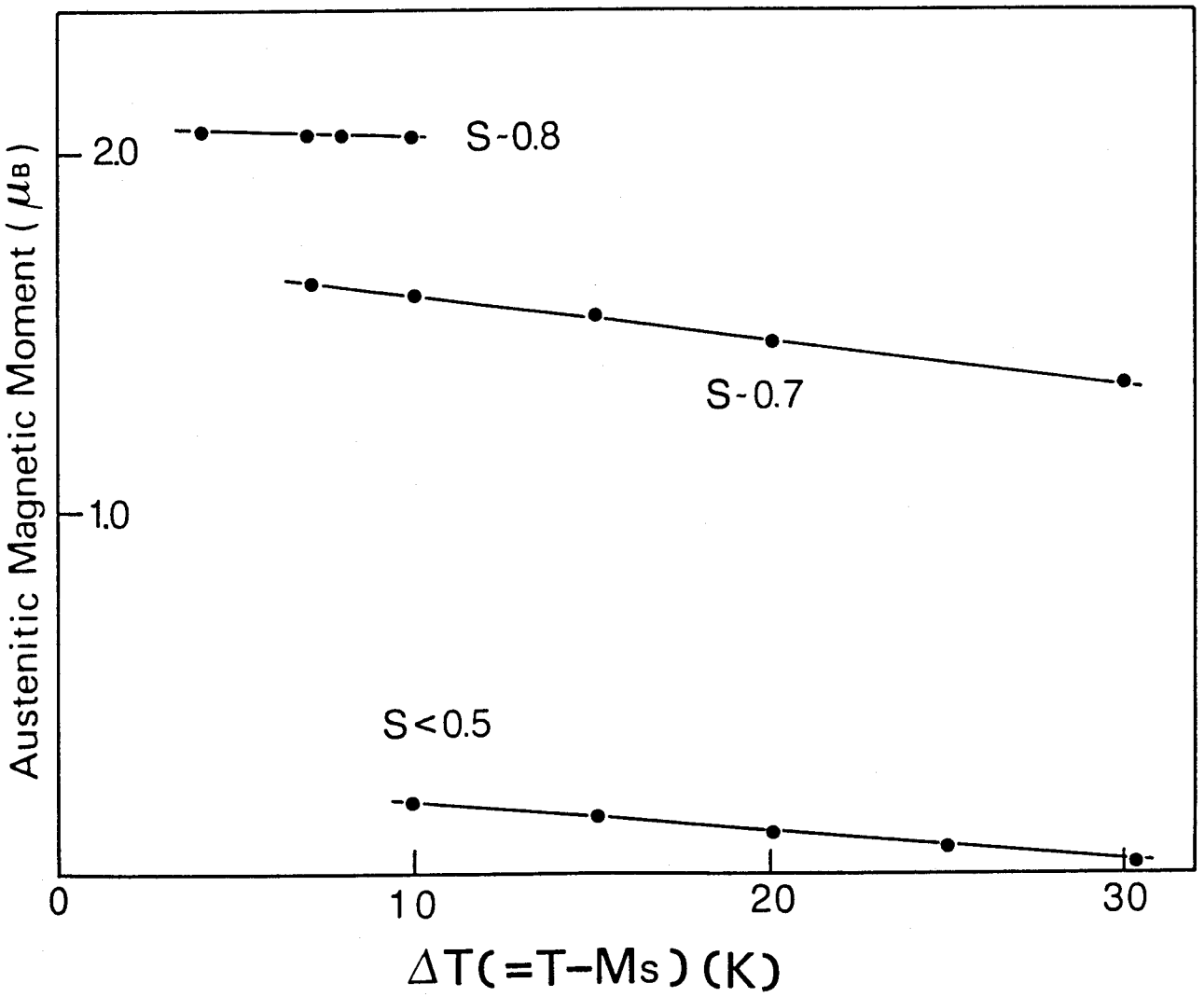

Fig. 2 Austenitic magnetic moments as a function of ΔT for three Fe-Pt alloy specimens with S≳0.8, ≃0.7 and <0.5.

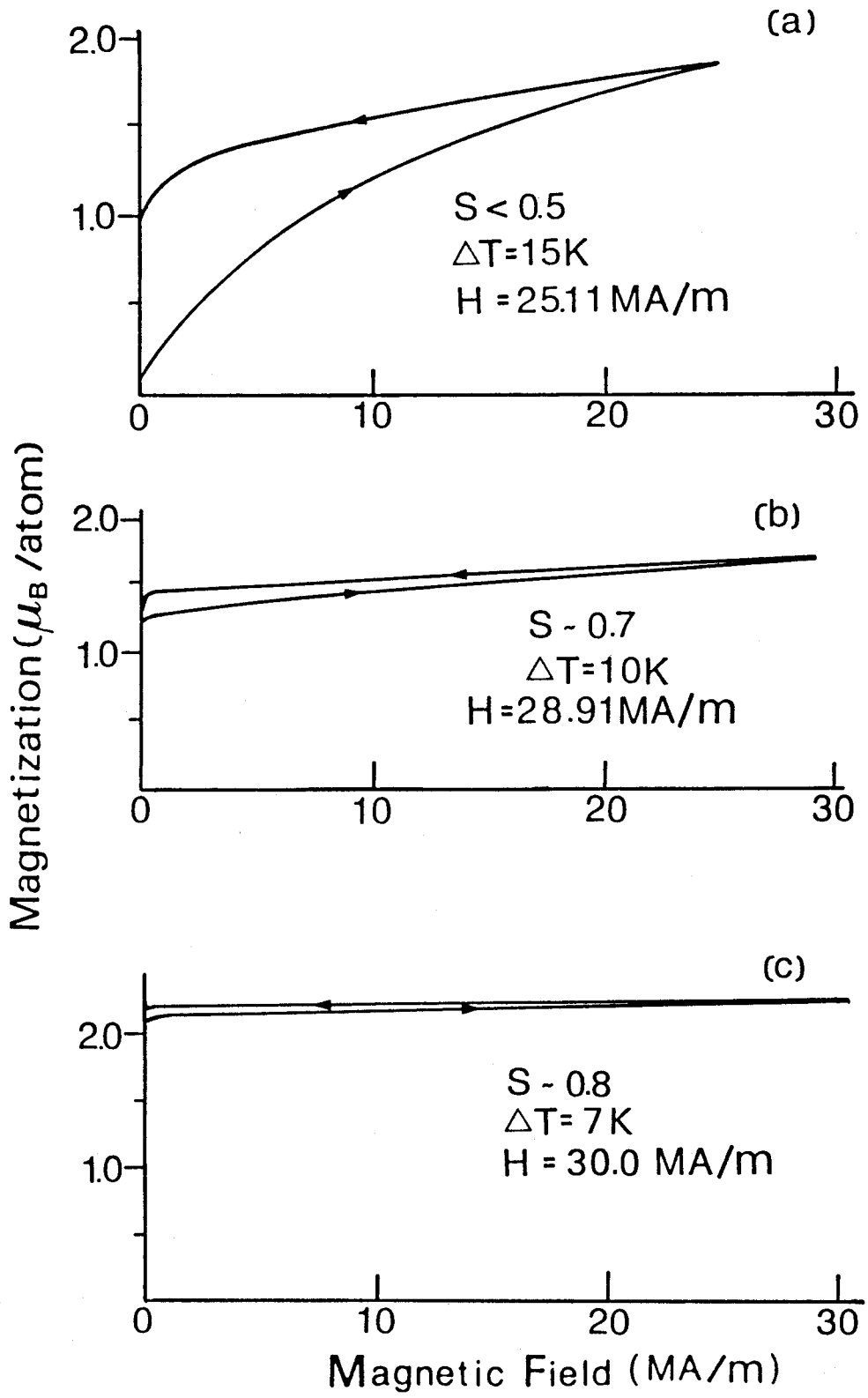

Fig. 3 Magnetization curves as a function of strength of magnetic field in one pulse. (a), (b) and (c) are for specimens A ($S<0.5$) B ($S\simeq0.7$) and C ($S\simeq0.8$), respectively.

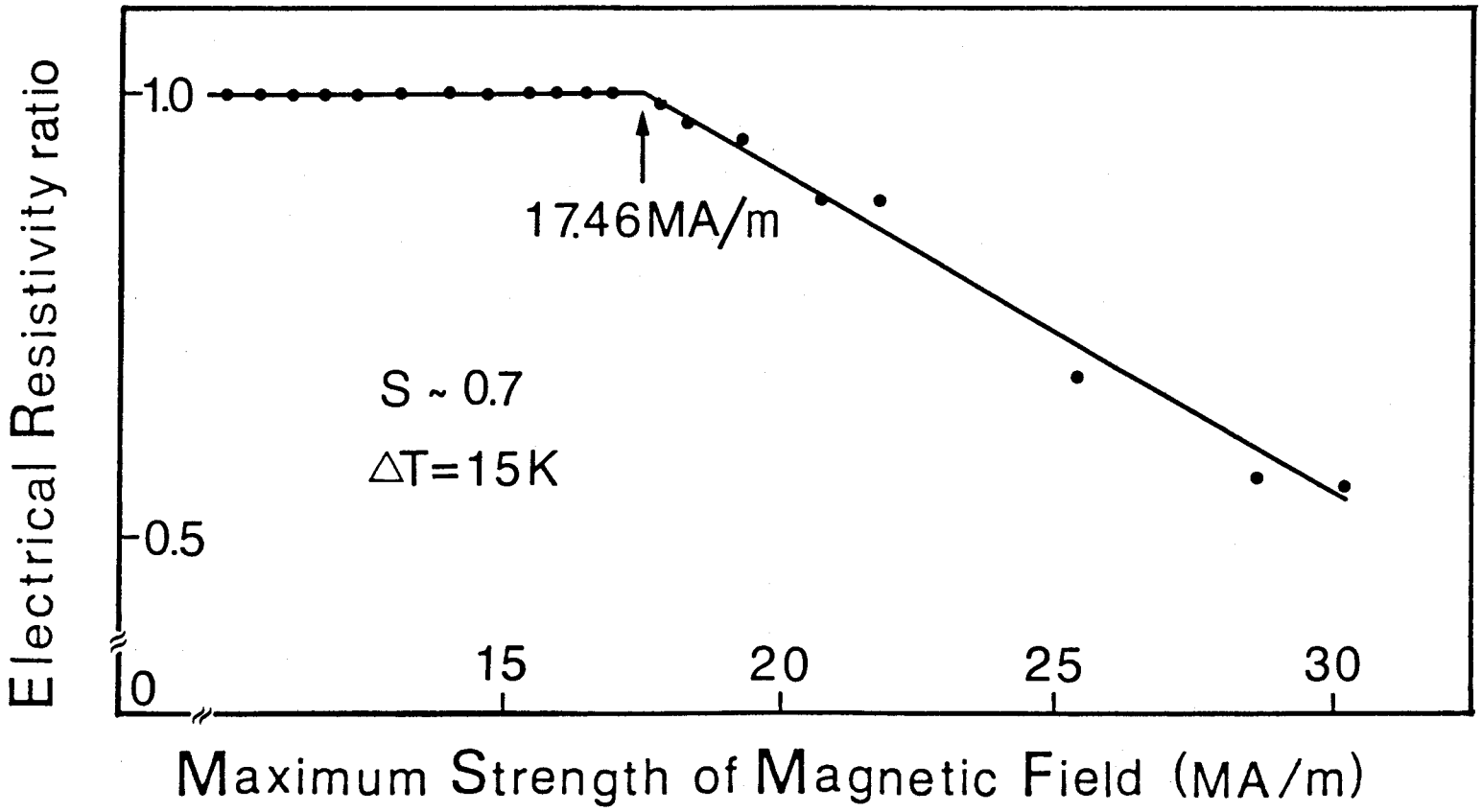

Fig. 4 Electrical resistivity ratio as a function of maximum strength of pulsed magnetic field at $\Delta T=15K$ for specimen B ($S\simeq 0.7$), from which the critical strength of the specimen B was determined.

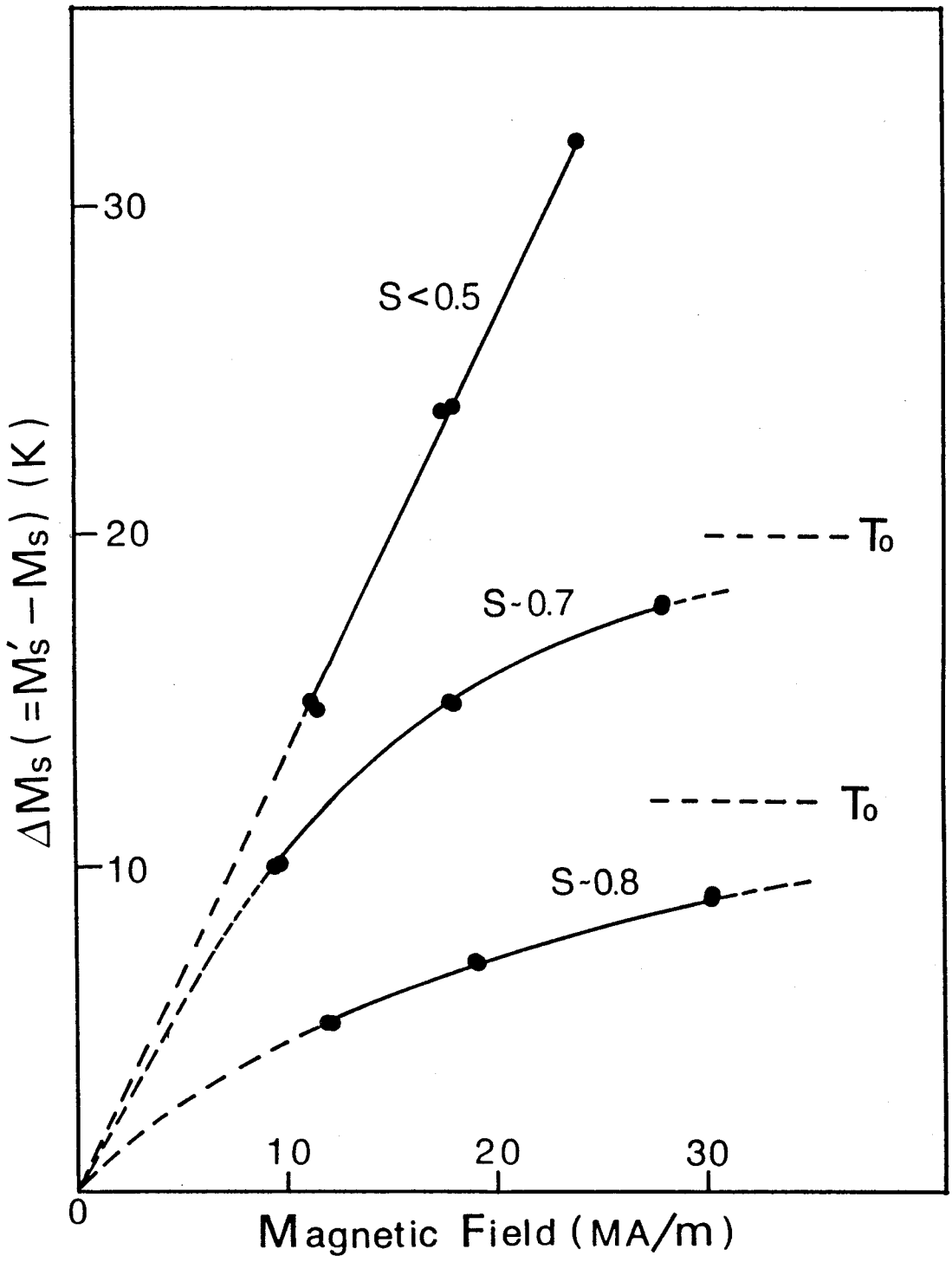

Fig. 5. Critical magnetic field dependence of the shift of M_S temperature, ΔM_S ($=M_S'-M_S$), for three Fe-Pt alloys.

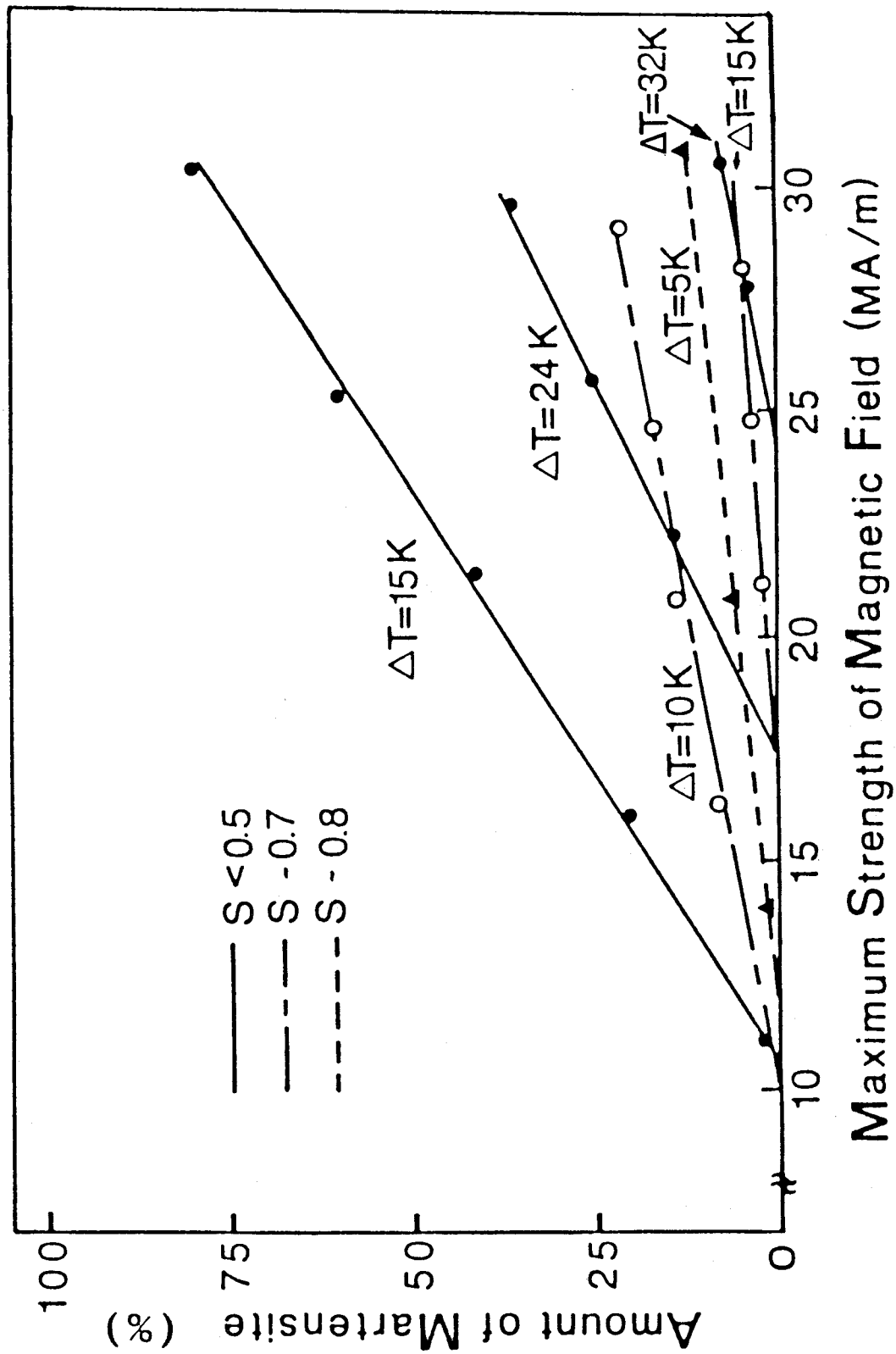

Fig. 6 Amount of magnetic field-induced martensites, plotted as a function of maximum strength of the pulsed magnetic field.

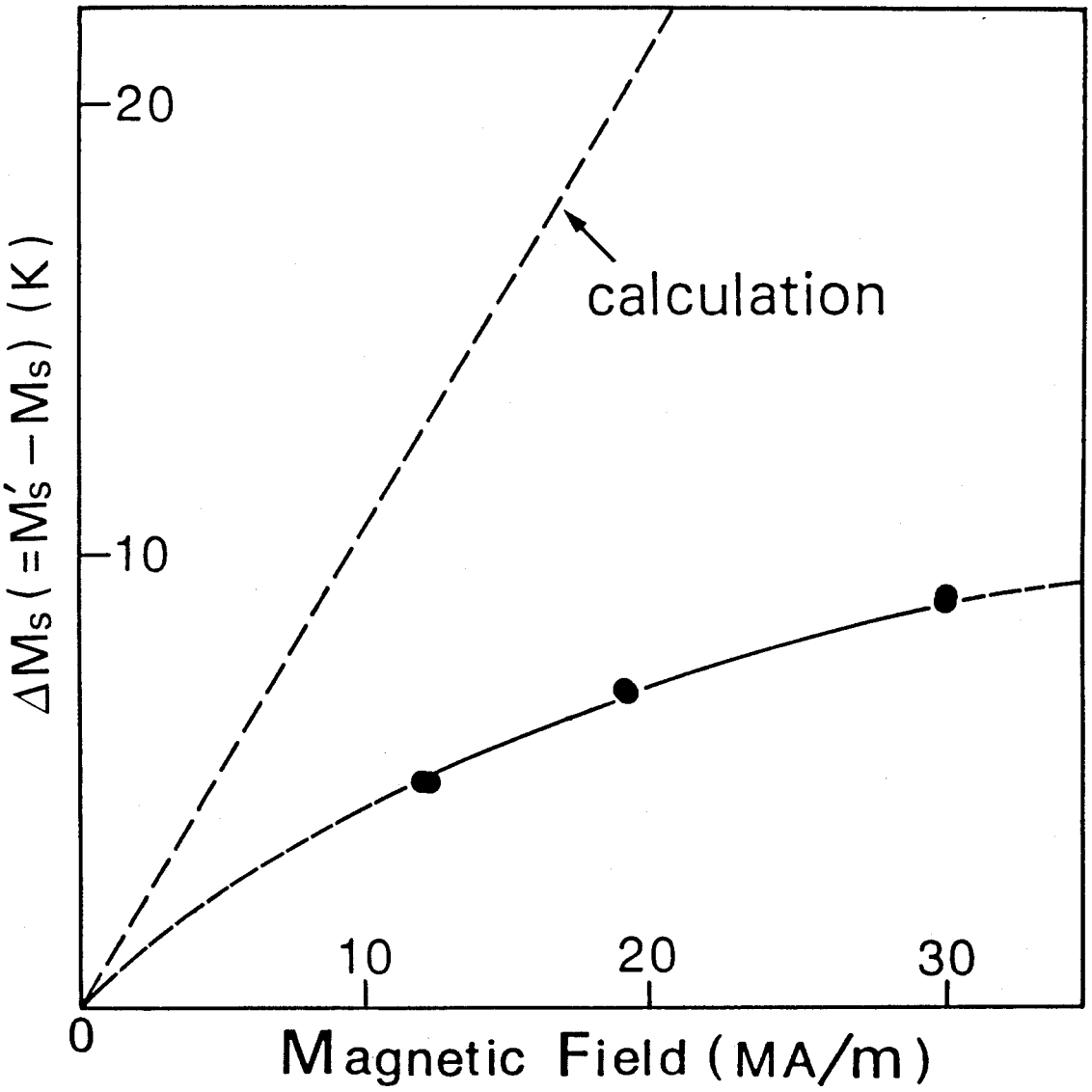

Fig. 7 Calculated and experimental critical field dependence of ΔM_S for the specimen C ($S \simeq 0.8$).

Chapter 6

Magnetic Field-Induced Martensitic Transformation from Paramagnetic Austenite to Ferromagnetic Martensite in an Fe-Mn-C alloy.

Synopsis

The magnetic field-induced martensitic transformation from paramagnetic austenite to ferromagnetic martensite in an Fe-3.9at%Mn-5.0at%C alloy has been studied in detail by means of magnetization measurement, differential scanning calorimetry and optical microscopy, applying a pulsed ultra high magnetic field. As a result, the followings are found: The shift of M_S temperature, $\Delta M_S (=M_S'-M_S)$, increases linearly with increasing the critical magnetic field to induce martensitic transformation. The amount of magnetic field-induced martensites increases with the maximum strength of magnetic field irrespective of $\Delta T (=T-M_S)$. The morphology of the magnetic field-induced martensites is the same as that of thermally-induced ones irrespective of ΔT. A thermodynamical analysis shows that the effect of magnetic field on martensitic transformations is due to the Zeeman effect alone.

I. Introduction

Many studies have been carried out until now[(1)~(3)] on magnetic field-induced martensitic transformations. As a results, a lot of information are obtained about critical field dependence of the shift of M_S temperature, the amount and morphology of magnetic field-induced martensites and so on. However, all of those studies were concerned with ferrous materi-

als undergoing a transformation from ferromagnetic austenite to ferromagnetic martensite. Therefore, the above information may be different from those for materials exhibiting another type of martensitic transformation from paramagnetic austenite to ferromagnetic martensite. An experiment is, therefore, needed to examine the magnetic field-induced martensitic transformation in such materials. An Fe-Mn-C alloy is convenient for such an experiment, because the alloy exhibiting a martensitic transformation from paramagnetic austenite to ferromagnetic martensite can easily be prepared by varying the compositions of Mn and C, and also because its thermodynamics and crystallography of thermally-induced martensitic transformation with fcc→bct have already been well examined[4]. However, the studies so far done on magnetic field-induced martensitic transformations in Fe-Mn-C alloys are not from the point of view. In the present study, therefore, the Fe-Mn-C alloy has been examined to distinguish the magnetic effects from the martensitic transformation from ferromagnetic austenite to ferromagnetic martensite by means of magnetization measurement, differential scanning calorimetry (DSC) and optical microscopy, applying a pulsed ultra high magnetic field.

II. Experimental Procedures

An Fe-3.9Mn-5.0C (at%) alloy was prepared by melting in a high frequency induction furnace under argon atomosphere and by casting into a water-cooled iron mold. Ingot of the alloy was hot-forged at 1273K, homogenized at 1473K for 8.64×10^4 s in a silica capsule filled with argon, and then quenched into

iced water. Pieces with 40mm length were cut from the heat-treated ingot, and they were hot-rolled into 0.5mm thick sheets. For magnetization and DSC measurements, specimens with 3mm × 20 mm × 0.5mm size were taken from the sheets, and were austenitized at 1473K for 7.2×10^3 s in silica capsules filled with argon, followed by quenching into iced water. The austenitized specimens with 20mm length were chemically ploished and cut into 3mm and 10mm in length by spark cutting, the 3mm length one was used for DSC measurement to determine M_S temperature and the 10mm length one for magnetization measurement. Pulsed ultra high magnetic field with the maximum strength of about 31.75 MA/m was applied to the austenitic specimens. Details of the pulsed ultra high magnetic field instrument were described in Chapter 2. After a magnetic field had been applied, each of the specimens was chemically etched by 30% Sodium Pyrosulfite solution and supplied for an optical microscopy observation. Chemical analysis of the alloy was carried out by using the rest part of the alloy sheet, which had been subjected to the same heat-treatments as above in order to avoid a discrepancy in composition between the chemically analysed and experimentally used specimens. The alloy composition thus analysed is the mentioned one above.

III. Results

3-1. Transformation temperature and magnetic property of the austenitic phase.

DSC measurements have been made in the range from 293 to 77K in order to determine transformation temperatures and the latent heat of transformation. The reference material used in

the measurements is the present alloy sub-zero treated down to 77K. A typical DSC profile is shown in Fig. 1. It is noted in this figure that M_s temperature is clearly determined to be 223 K from the change of heat flow, but M_f temperature is not so clearly determined, although it is estimated to be about 170K, judging from no change of heat flow at that temperature. The latent heat of martensitic transformation can be obtained from the integrated value (18.8 J/g) of heat flow with temperature from 170 to 223K and the amount of martensites. The amount of martensites was obtained to be about 40% by magnetization measurement, in the same way as described in Chapter 2. Using these values, the latent heat of the transformation has been obtained to be 2518 J/mol.

The susceptibility in the austenitic state has been obtained by magnetization measurement, a low magnetic field (about 1.6 MA/m) being applied. It is found to be about 3.2×10^{-13} $H \cdot m^2/Kg$ and is independent of temperature in the range from 253 to 293K. This means that the present alloy is surely paramagnetic in the austenitic state. On the other hand, the spontaneous magnetization in martensitic state has been obtained on the assumption that it originates in magnetic atoms and, therefore, depends only upon the compositions of Fe and Mn atoms. Thus, by referring to the Slater-Pauling curve[5], the martensitic magnetic moment at 0K was obtained to be about 2.0μB for the present alloy although it is very rough approximation. This value is considered to be valid in the temperature range where the magnetization measurement has been made in the present study.

3-2. Critical magnetic field to induce martensite

Magnetization M(t) has been measured as a function of magnetic field H(t) in one pulse whose maximum strength of a magnetic field is higher than a critical one to induce martensitic transformation. Typical M(t)-H(t) curves for $\Delta T(T\text{-}M_S)$=60K and 80K are shown in Fig. 2. In this figure, an increase in magnetization is recognized at a certain magnetic field, as indicated with an arrow on each curve. In this way, the martensitic transformation is surely induced even in the paramagnetic austenite by a magnetic field in the same manner as in the ferromagnetic austenite previously examined[(1)~(3)]. Such an increase in magnetization was not able to be observed if the maximum strength of a magnetic field below the one indicated with an arrow is applied to the another specimen at the same temperature. Therefore, the certain magnetic field corresponds to the critical one to induce martensitic transformation. The relation thus obtained between the critical magnetic field and the shift of M_S temperature, ΔM_S ($=M_S'\text{-}M_S$) is shown in Fig. 3. It is seen from this figure that ΔM_S increases linearly with increasing the critical magnetic field. This characteristic is very important to know the magnetic effect on martensitic transformations from paramagnetic phase to ferromagnetic phase. The dotted line in Fig. 3 is the theoretical one described later. Incidentally, another characteristic feature noted in Fig. 2 is that the high field susceptibility in the austenitic state is smaller than that in Fe-Ni alloys in Chapter 2, and is the same value as that obtained at a low magnetic field. It is also noted in Fig. 2 that the high field susceptibility in the martensitic state is also small. These small values will be also discussed later.

3-3. Amount of magnetic field-induced martensite

The amount of magnetic field-induced martensites has been calculated in the same way as in Chapter 2 by using the result of magnetization measurement. The calculated amount of martensites is shown in Fig. 4 as a function of the maximum strength of pulsed magnetic field. In this figure, the amount of martensites increases with increasing the maximum strength of magnetic field, irrespective of $\Delta T(=T-M_S)$, that is, it slightly increases near the critical magnetic field, abruptly at a little higher fields than the critical one, and linearly at more higher fields. Such a magnetic field dependence of the amount of martensites is also seen in the magnetization curve in Fig. 2. Such behavior of the increase of the amount of martensites has been examined by optical microscopic observation. The result is shown in Fig. 5. (a) shows a martensite structure after a magnetic field near the critical one has been applied at $\Delta T=35K$, which was taken at room temperature after polishing and etching. (b) shows an un-etched martensite structure after a magnetic field higher than the critical one has been successively applied to the same alloy at the same temperature as in (a) (which was taken from the same place as in (a) at room temperature). Surface relief newly arises at interfaces of martensites in (b) as indicated with an arrow in (a). This may be due to the growth of existing plates and/or the formation of new martensite plates. In order to make it clear, the sample was observed after polishing and etching, as shown in (c). Comparison of (b) with (c) indicates that the surface relief in (b) is caused by not only a little growth of martensite, as arrowed in (a), but also the

formation of many small martensites. However, crystallographic relationship between the existing martensites and newly formed ones has not been investigated any more in the present study.

3-4. Morphology of the magnetic field-induced martensite

Fig. 6 shows optical micrographs of thermally-induced martensites formed by cooling a little below M_S temperature, (a), and those of magnetic field-induced ones ((b), (c), (d), (e), (f)). The formation temperature T, its difference from M_S, ΔT, applied magnetic field H and field direction are indicated in the figure. It is noted that the morphology of the magnetic field-induced martensites is the same as that of thermally-induced ones irrespective of ΔT. This result is the same as that of Fe-Ni and Fe-Ni-C alloys examined in Chapter 2 and 4. By the way, the micrographs (e) and (f) reveal that several martensite plates grow nearly parallel to the direction of applied magnetic field. This phenomenon is similar to that observed in an Fe-Ni single crystal alloy mentioned in Chapter 3, but it is not so much observed as in the Fe-Ni single crystal alloy. This difference may be attributed to the fact whether grain boundaries exist or not. That is, the directional growth of martensites is disturbed by a back stress originating from the existence of grain boundaries.

IV. Discussion

It has been proposed in Chapter 2 that the magnetic effects on martensitic transformations are due to not only the Zeeman and high field susceptibility effects but also other un-

known effects which are related to the Invar effect. Then, relation between the critical magnetic field and the shift of M_S temperature in the present alloy has been calculated by taking account of the proposed effects. In the present calculation, the high field susceptibility and the other unknown effects may be neglected by the following reason. The high field susceptibility in both the austenite and martensitic phases is very small, as mentioned before, and its effect on the shift of M_S temperature is negligeblly small. The other unknown effects are not effective for the present alloy, because the present alloy has no Invar effect because of the paramagnetic austenite and its temperature dependence of lattice parameter is usual as previously reported[4]. Thus, the proposed equation to determine the shift of M_S temperature of martensitic transformation under a magnetic field can be expressed as follow;

$$\Delta G(M_S) - \Delta G(M_S') = -\Delta M(M_S')\cdot H,$$

where each of the notations is the same as that in Chapter 2. Gibbs chemical free energy in the present Fe-Mn-C alloy has been obtained by following the equation derived by Chang and Hsu[6], and the calculated $\Delta G(M_S)-\Delta G(T)$ is shown in Fig. 7 as a function of ΔT and its numerical value is shown in Table 1. The critical magnetic field vs. ΔM_S relation thus calculated is shown with the dotted line in Fig. 3. It is noted in the figure that the calculated relation is good agreement with the experimental one over the wide range of ΔM_S. It is thus concluded from the good agreement between the calculation and experiment that the magnetic effects previously proposed is valid even in materials undergoing a martensitic transformation from

paramagnetic austenite to ferromagnetic martensite,meaning that the effect of magnetic field is due to the Zeeman effect alone.

References

(1) V. D. Sadovsky, L. V. Smirnov, YE. A. Fokina, P. A. Malinen and I. P. Soroskin: Fiz. Metal. Metalloved., 24 (1967), 918.

(2) M. K. Korenko and M. Cohen: see Chapter 1, (54).

(3) K. R. Satyanaryan, W. Eliasz and A. P. Miodownik: see Chapter 1, (56).

(4) Y. Tanaka and K. Shimizu: Trans Jpn. Inst. Met., 21 (1980), 42.

(5) J. Grangle and G. C. Hallame: see Chapter 2, (5).

(6) Hongbing Chang and T. Y. Hsu: Acta Metall., 34 (1986), 333.

Table 1. Numerical values of ΔG and $\Delta G(M_S)-\Delta G(T)$ for various ΔT.

ΔT (K)	$\Delta G^{\alpha-\gamma}$ (T) (J)	$\Delta G^{\alpha-\gamma}(M_S)-\Delta G^{\alpha-\gamma}$ (T) (J)
0	1425	0
5	1404	21
10	1382	43
15	1360	65
20	1338	86
25	1316	109
30	1294	131
35	1272	153
40	1249	176
45	1226	199
50	1203	222
55	1180	245
60	1157	268
65	1133	291
70	1109	315
75	1086	339
80	1062	363
85	1038	387
90	1014	411
95	990	435
100	966	459

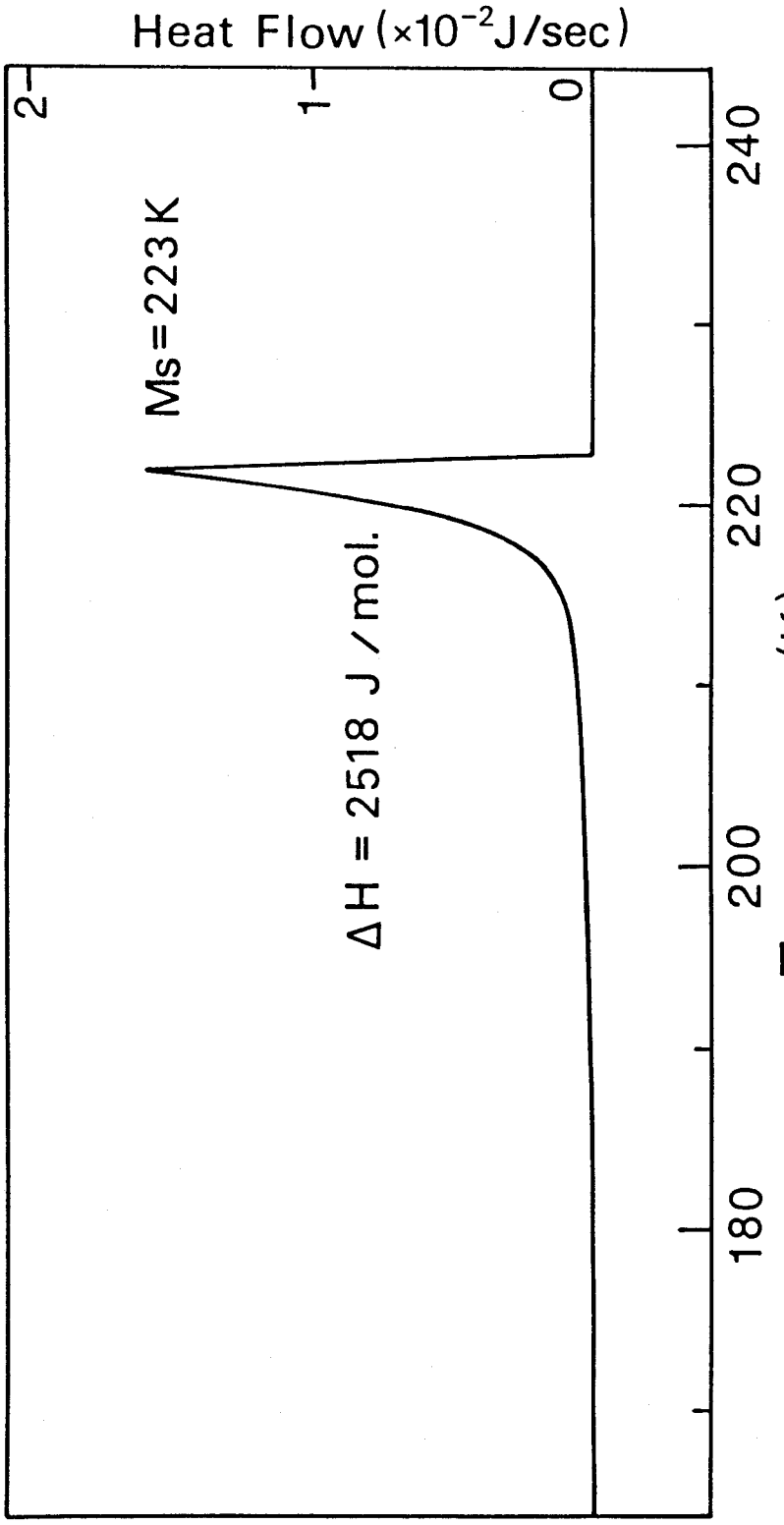

Fig. 1 DSC profile recorded for an Fe-Mn-C alloy in the temperature range from 293 to77K.

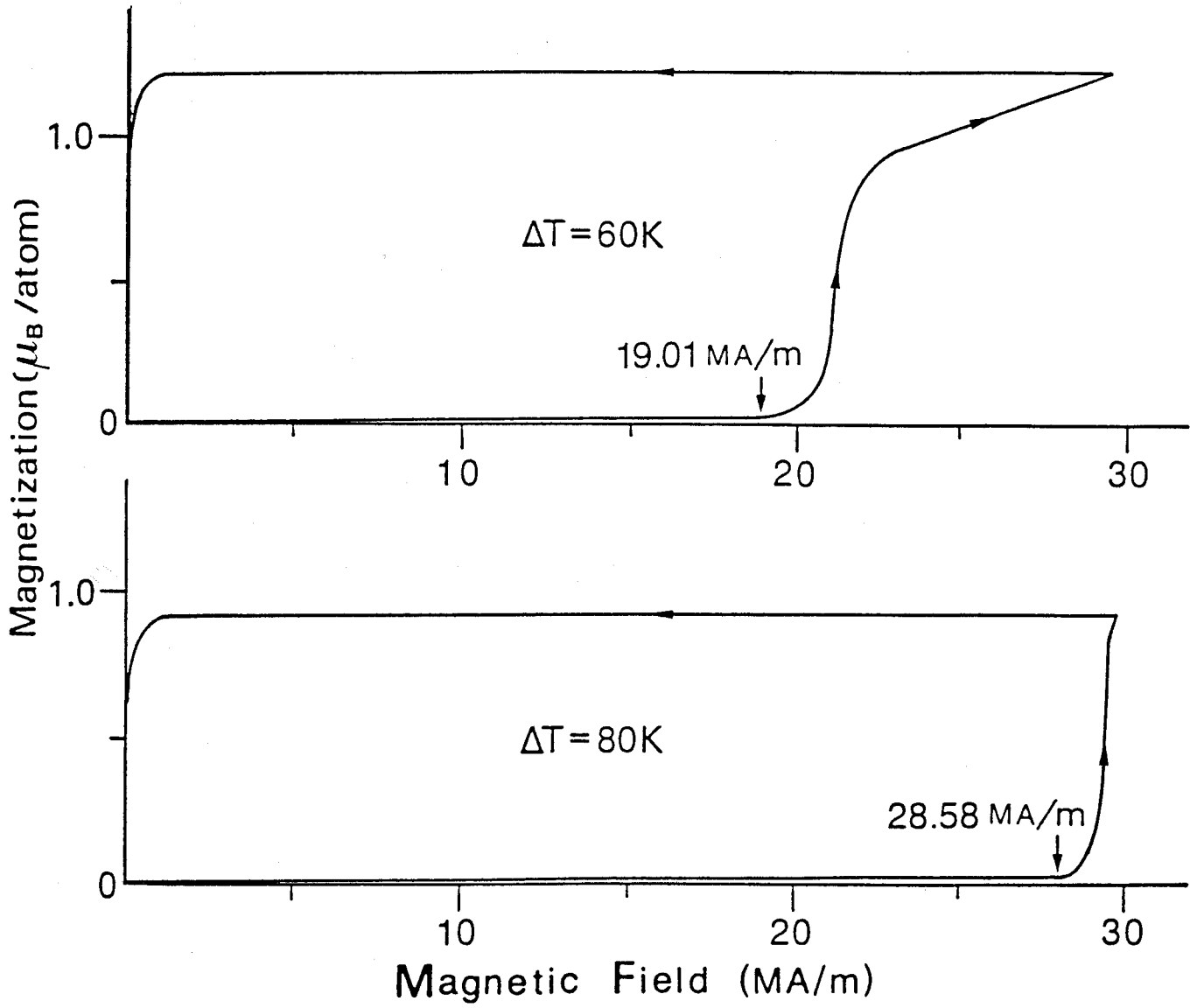

Fig. 2 Magnetization vs. magnetic field (M(t)-H(t)) curves for ΔT=60 and ΔT=80 K.

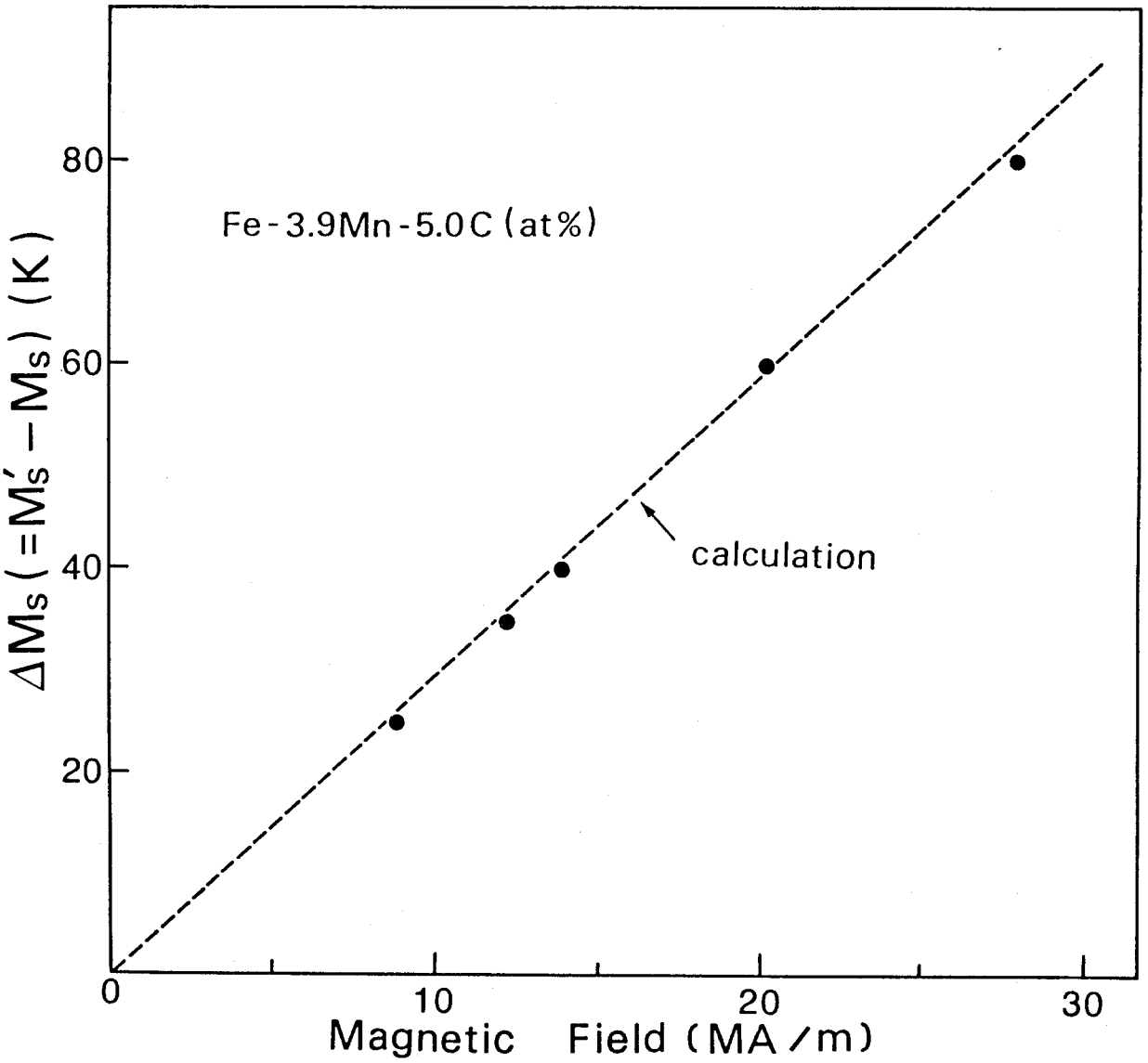

Fig. 3 Critical field dependence of $\Delta M_S (=M_S'-M_S)$, dotted line is the calculated relation.

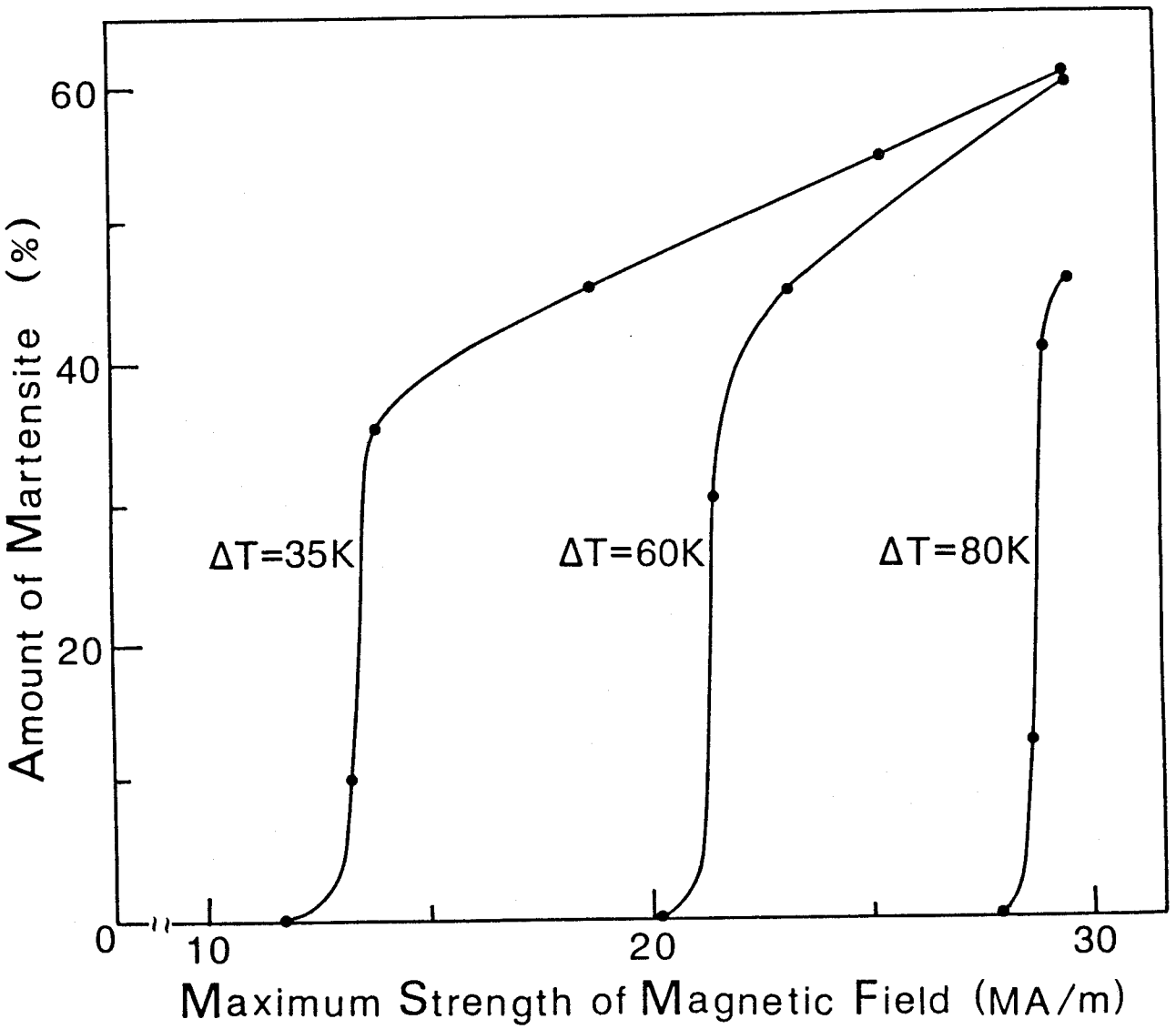

Fig. 4 Calculated amount of magnetic field-induced martensites plotted as a function of maximum strength of pulsed magnetic field.

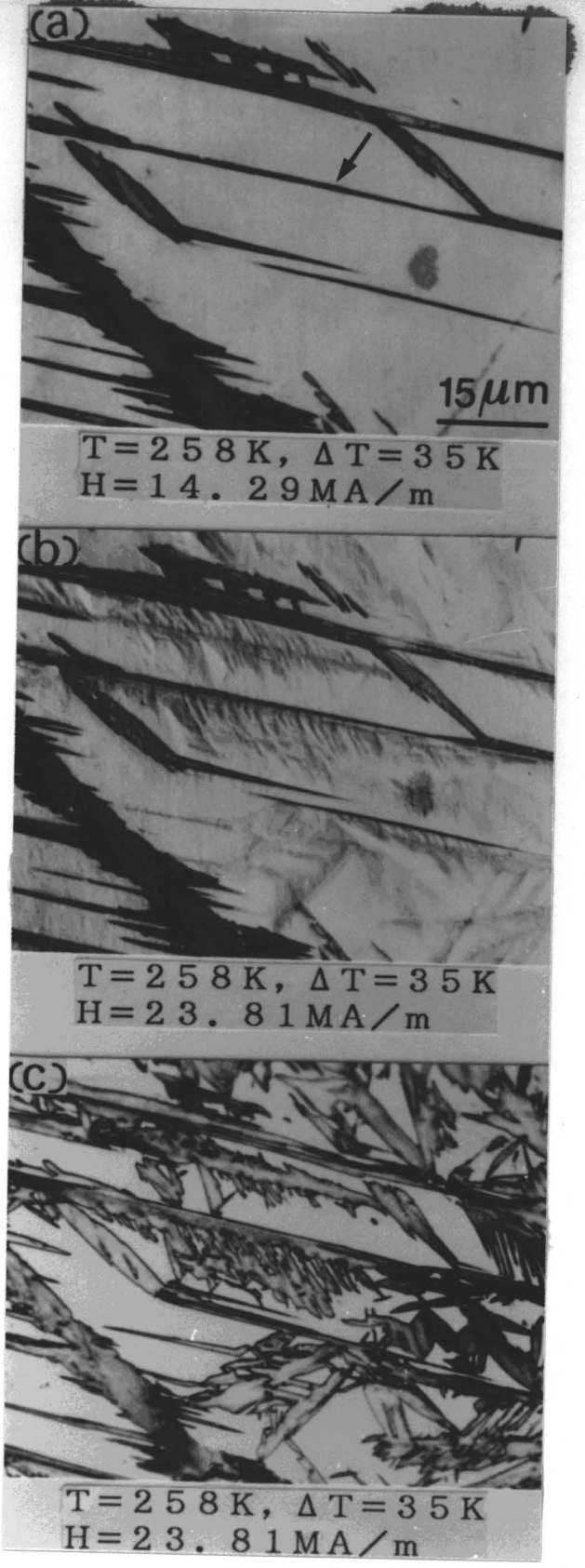

Fig. 5 Optical micrographs showing the growth of existing martensite plates, by applying a higher magnetic field than the critical one. (c) is the etched structure of (b).

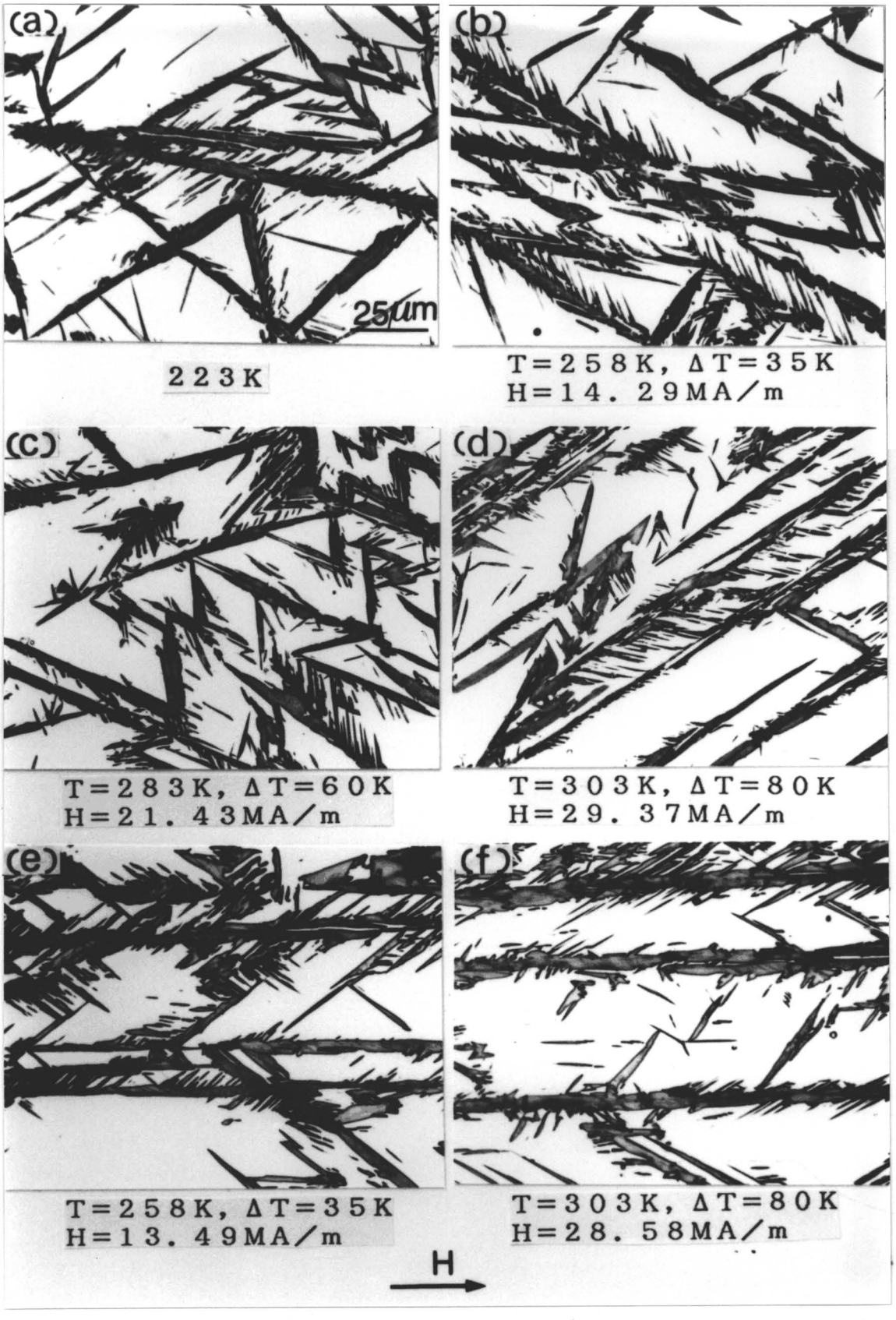

Fig. 6 Optical micrographs of thermally-induced martensites, (a), formed by cooling a little below the M_S temperature, and of magnetic field-induced ones, (b)~(f). ΔT and H for the magnetic field-induced martensites are inscribed in each photograph.

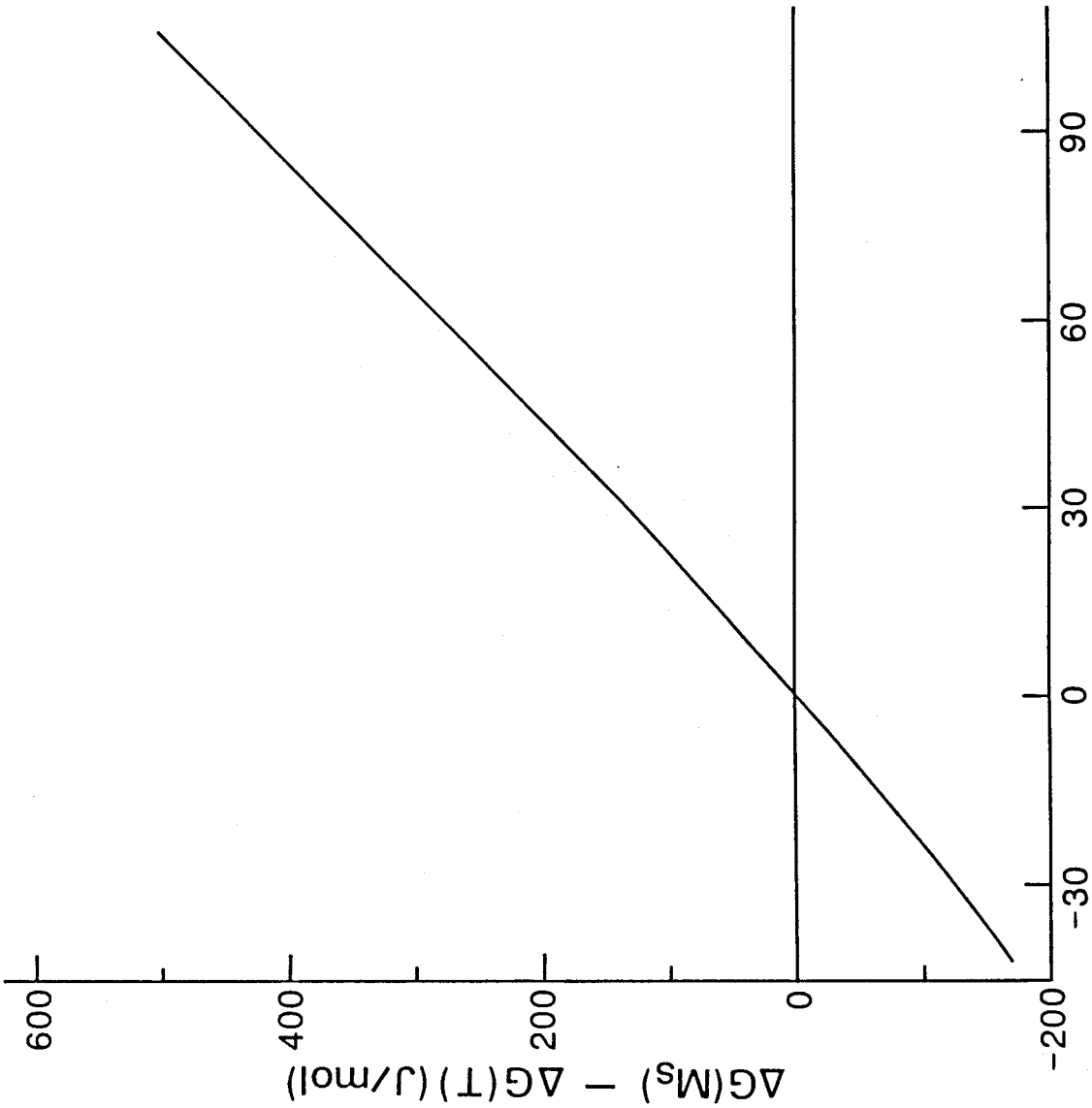

Fig. 7 Calculated {$\Delta G(M_S)$-$\Delta G(T)$}as a function of ΔT for an Fe-Mn-C alloy.

Chapter 7

Magnetoelastic Martensitic Transformation in an ausaged Fe-Ni-Co-Ti alloy.

Synopsis

Magnetic field-induced martensitic transformation in an ausaged Fe-Ni-Co-Ti alloy has been studies to clarify the influence of a magnetic field on thermoelastic martensitic transformations by means of magnetization measurement, applying a pulsed ultra high magnetic field. As a result, the magnetic field-induced martensite at temperatures above A_f disappears after removing the magnetic field. That is, a magnetoelastic martensitic transformation is first found to be realized when a magnetic field higher than the critical one has been applied above A_f. However, when such a magnetic field is applied in the temperature range, $M_S < T < A_f$, some martensites are magnetoelastic but some others are not. The amount of the shift of M_S temperature increases with increasing critical magnetic field. The amount of magnetic field-induced martensites increases with increasing strength of magnetic field irrespective of ΔT, and the martensites disappear when the magnetic field is removed above A_f, but some martensites are retained at $M_S < T < A_f$, because of the magnetoelastic nature.

Introduction

In alloys undergoing a thermoelastic martensitic transformation, a single martensite crystal can gradually grow or shrink

as temperature is lowered or raised, respectively, that is, it elastically responds to temperature, being under a balance between the thermal and elastic energies[1]. If uniaxial stress is applied to such a thermoelastic alloy at a temperature above A_f and then released, the alloy exhibits pseudoelastic behavior due to a stress-induced martensitic and its reverse transformations upon loading and unloading, respectively[2],[3]. The stress-induced martensite above A_f may be called "dynamoelastic", because it elastically responds to an applied dynamical stress.

Magnetic field-induced martensitic transformations in various ferrous alloys and steels above M_s have recently been examined in detail, as described in Chapter 2~6. If a magnetic field is applied to a thermoelastic ferrous alloy above A_f, martensite which elastically responds to the magnetic field may possibly be induced in a similar way to the dynamoelastic martensite. In such a "magnetoelastic martensitic transformation", martensites can be induced only while a magnetic field is applied, and they transform back to the austenite when the magnetic field is removed. In order to verify the existence of such a magnetoelastic martensitic transformation, we have to use a material with the following two conditions.

(i) The material must exhibit a thermoelastic martensitic transformation.

(ii) There must be a difference in magnetization between the austenitic and martensitic phases.

Material satisfying the above two conditions is only the ordered Fe-Pt alloy of many alloys so far used in the present

work. However, the magnetoelastic martensitic transformation was not realized in the alloy, as described in Chapter 5. That is, no martensitic transformation was observed in the alloy under a magnetic field at temperatures above A_f. Fortunately, however, an ausaged Fe-Ni-Co-Ti alloy has recently been found to exhibit a thermoelastic martensitic transformation by T. Maki et al[4]. Moreover, a difference in magnetization is expected to exist between the austenitic and martensitic phases, because the magnetization of fcc structures is generally smaller than that of bcc or bct structures in many ferrous alloys and steels. The purpose of the study in the present chapter, therefore, is to verify the existence of magnetoelastic martensitic transformation by using an ausaged Fe-Ni-Co-Ti alloy and to examine its characteristics, such as the critical magnetic field for inducing the transformation, the amount of martensites and so on, a pulsed ultra high magnetic field being applied.

II. Experimental Procedures

An ingot of the Fe-31.9Ni-9.8Co-4.1Ti alloy (at%) was supplied by Profs. Tamura and Maki at Kyoto University, which was melted in a vacumm induction furnace. After forging and homogenizing at 1473K for 108ks, the alloy was hot- and cold-rolled to 0.28mm thick plates, and specimens for electrical resistivity and magnetization measurements were cut into 3mm × 10mm × 0.28mm size. The specimens were austenitized at 1473K for 3.6 ks in silica capsules filled with argon, followed by quenching into iced water, and the austenitic specimens at room temperature were aged at 973K for 10.8ks to make them partially order-

ed by precipitating the γ' phase (Ni_3Ti). Subsequent treatments for the specimens and experimental methods were similar to those described in Chapter 2.

III. Results and Discussion

3-1. Transformation temperature and magnetic property of the austenite and martensite phases.

Figure 1 shows an example of electrical resistivity vs. temperature curves, from which M_s and A_f are known to be about 127K and 159K, respectively, although A_s and M_f are unknown, being lower than 77K. These transformation temperatures are consistent with those determined from an observation of structural change[4]. The curve of Fig. 1 is very similar to that of the ordered Fe-Pt alloy described in Chapter 5, the temperature difference between M_s and A_f being only 32K. Therefore, the martensitic transformation in the ausaged Fe-Ni-Co-Ti alloy is certainly thermoelastic, as also previously verified by the optical microscopy observation[4]. The magnetization has been measured as a function of temperature in order to determine the spontaneous magnetization in the austenitic and martensitic phases, as shown in Fig. 2. According to the figure, M_s and A_f temperatures shown with arrows are consistent with those determined by the electrical resistivity measurement described above, and A_s temperature is known to be 60K. It is also noted in this figure that the difference in spontaneous magnetization between the two phases is about 0.4μB at M_s temperatures. This value is the same order as in the previously examined Fe-32.5

at%Ni alloy. Therefore, the occurence of magnetoelastic martensitic transformation is expected to be realized by applying the same order of strength of magnetic field as in the case of the Fe-32.5at%Ni alloy.

3-2. Verification of magnetoelastic martensitic transformation and critical field for the transformation.

If a magnetic field is applied to the ausaged Fe-Ni-Co-Ti alloy at temperatures above A_f(159K), magnetoelastic martensitic transformation may be observed as mentioned before. So, the magnetization M(t) has been measured as a function of magnetic field H(t) at temperatures above A_f. The typical M(t)-H(t) curves obtained at T=163K>A_f ($\Delta T=T-M_S=36K$) are shown in Figure 3 (a) and (b). It is noted in (a) that the M(t)-H(t) curve shows no hysterisis when a pulsed magnetic field whose maximum strength is 22.22 MA/m has been applied. This means that the maximum strength is lower than a critical field to induce martensitic transformation, and therefore, no martensitic transformation occures under the magnetic field of 22.22 MA/m. Then, higher maximum strength of magnetic field than 22.22 MA/m has been applied, and the obtained M(t)-H(t) curve is shown in (b). It is noted in (b) that the M(t)-H(t) curve shows a hysterisis, showing a discontinuous increase of magnetization at Hc=23.08 MA/m, as indicated with the arrow. When the magnetic field is removed, the increased magnetization decreases and recovers to the previous one before the increasing at about H_f=5 MA/m indicated with the arrow. This means that a martensitic transformation is induced at Hc (critical field

to induce martensite) and its reverse transformation is completed at H_f. From these observations, the expected magnetoelastic martensitic transformation is certainly recognized in the ausaged Fe-Ni-Co-Ti alloy if a magnetic field higher than a critical one, H_c, is applied. This phenomenon is always realized at temperatures above A_f. On the other hand, when temperature was decreased between M_s and A_f, the reverse transformation is not completed, as described below. The typical M(t)-H(t) curves obtained at T=138K (M_s<T<A_f, ΔT=11K) are shown in Figs. 3 (c) and (d). (c) shows no hysterisis when a pulsed magnetic field of 9.52 MA/m lower than a critical one, H_c, has been applied, this means that no martensitic transformation occures, as in (a). However, if applied magnetic field higher than H_c has been applied, a hysterisis can be observed on the M(t)-H(t) curve, as shown in (d), but the curve is some what different from that in (b). That is, the magnetization after the magnetic field is removed, is larger than that in the initial state, being different from the case of (b). However, this increased magnetization disappears if the specimen is heated up beyond A_f. These results means that a part of magnetic field-induced martensites remains after the magnetic field is removed, that is, the reverse transformation is not completed. This is reasonable because the martensite is still thermodynamically stable in the temperature range of M_s<T<A_f. Figure 4 shows a relation among the critical fields to induce transformation, H_c, and its reversion H_f, and the temperature difference from M_s, ΔT. In this figure, both the critical fields increase with increasing ΔT, but the hysterisis in magnetic field

between those critical fields is nearly the same irrespective ΔT. Unfortunately, thermodynamical analysis of the critical field dependence of ΔT has not been done, because Gibbs chemical free energies of both the phases in the present alloy are very complex and has not been obtained. Incidentally, the magnetoelastic martensitic transformation above A_f has completed within 100μs for the whole process. This means that the pulse width of the magnetic field applied in the present experiment is sufficiently longer than the time necessary to the transformation.

3-3. Amount of magnetic field-induced martensite

Figure 5 shows the amount of magnetic field-induced martensites calculted from the magnetization curves shown in Fig. 3, in the same way as in Chapter 2. In this figure, the dashed and solid lines represent the amounts of magnetoelastically reversed and remained martensites, respectively. It is noted from this figure that all the magnetic field-induced martensites at $T>A_f$ are magnetoelastic and therefore they vanish when the magnetic field has been perfectly removed. On the other hand, some magnetic field-induced martensites at $M_s<T<A_f$ are magnetoelastic and some others are not. For example, the amount of magnetic field-induced martensites is about 55% at ΔT=11K and H=28.0 MA/m, but when a magnetic field is removed it becomes about 23%, because the other martensites magnetoelastically transform back to the austenite. The amount of the residual martensites after removing the magnetic field is found to be saturated depending on temperature, and is found to be the same as that of thermal-

ly -induced martensites at the same temperature, T, (M_s<T<A_f), as shown in Table 1.

Recently, some structural steels used as a supporter for superconducting magnets have come into question in a research field on fusion reactors. Because they exhibit an irreversible magnetic field-induced martensitic transformation, and cause a cracking along the martensite/austenite interface boudaries. Such a question may be solved if such a cracking is avoid or a more stable austenitic steel is adopted. For example, if a Fe-Ni-Co-Ti alloy strengthened by ausaging is used as such a supporter, no crack may be caused because a reversible magnetoelastic martensitic transformation is realized in the alloy, as shown in the above. The ausaged Fe-Ni-Co-Ti alloy is thus now known to exhibit a magnetoelastic martensitic transformation as well as a shape memory effect, and therefore the alloy may be utilized as a magnetically sensitive device in addition to a thermally sensitive one.

References

(1) G. V. Kurdjumov and L. C. Khandros: Dokl. Akad. Nauk S. S. S. R., 66 (1949), 211.

(2) K. Otsuka, C. M. Wayman, K. Nakai, H. Sakamoto and K. Shimizu: Acta Metall., 24 (1976), 207.

(3) K. Otsuka and K. Shimizu: Proc. Intern'l Conf. on Solid-Solid Phase Transformations, Pittsburgh, p. 1267 (1981).

(4) T. Maki, K. Kobayashi, M. Minato and I. Tamura: Scripta Metall., 18 (1984), 1105.

Table 1. Amount of residual martensites at ΔT for thermally-induced and magnetic field-induced martensites

Amount of residual martensite

ΔT	11K	16K	26K
Thermal	21%	15%	3%
Magnetic	23%	15%	2%

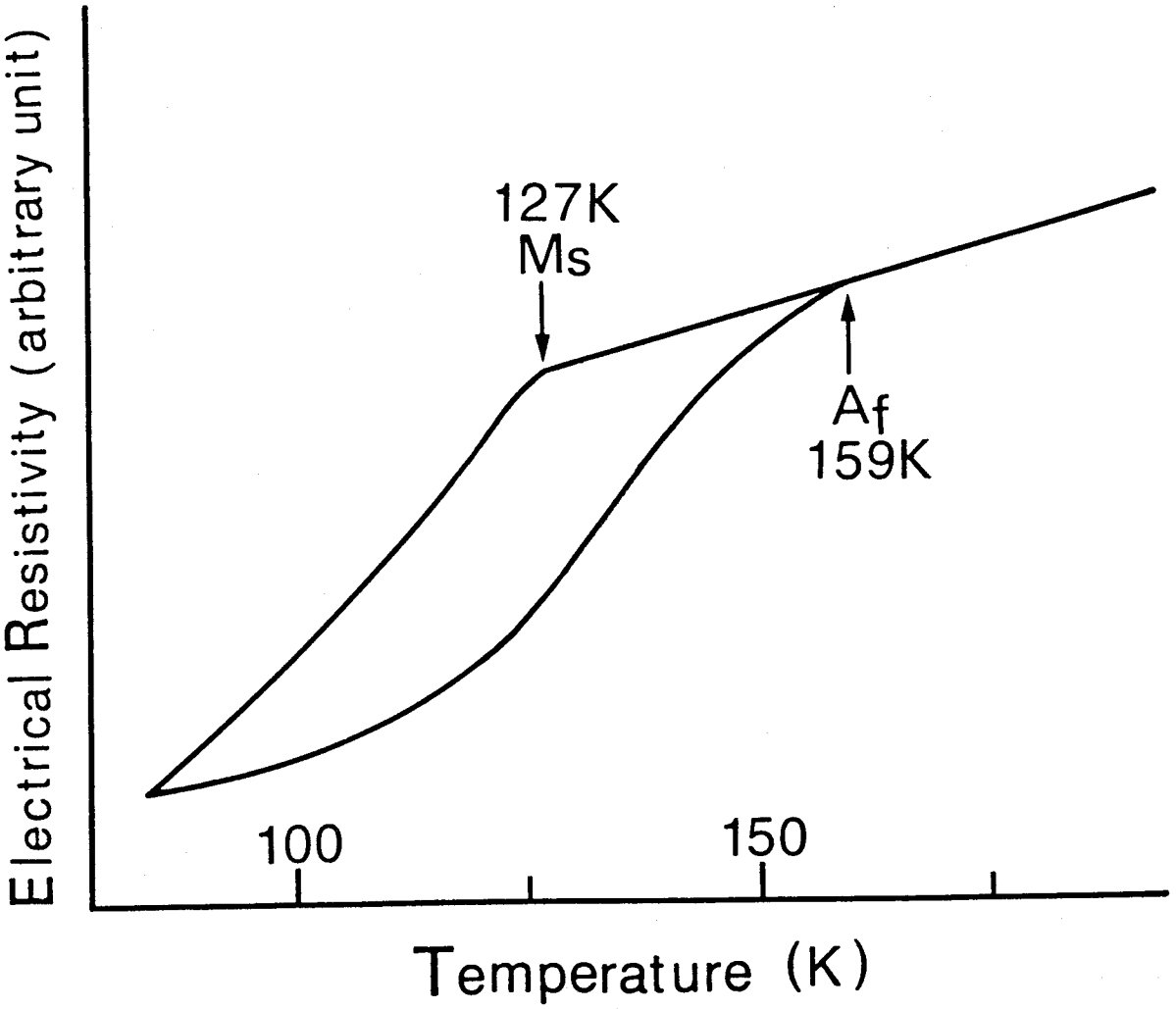

Fig. 1 Electrical resistivity vs. temperature curve of an Fe-Ni-Co-Ti alloy ausaged at 973K for 10.8ks.

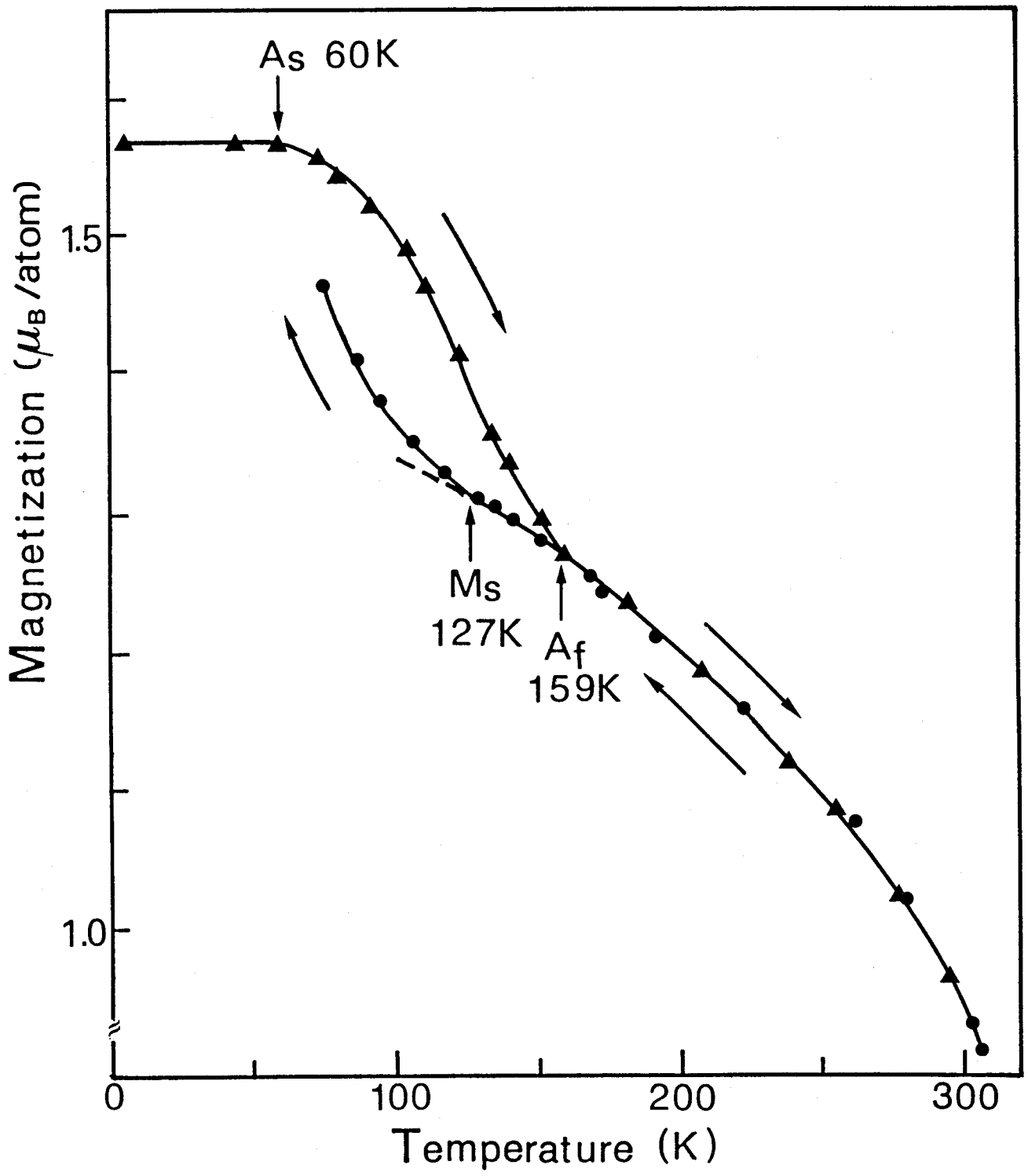

Fig. 2 Magnetic moment as a function of temperature

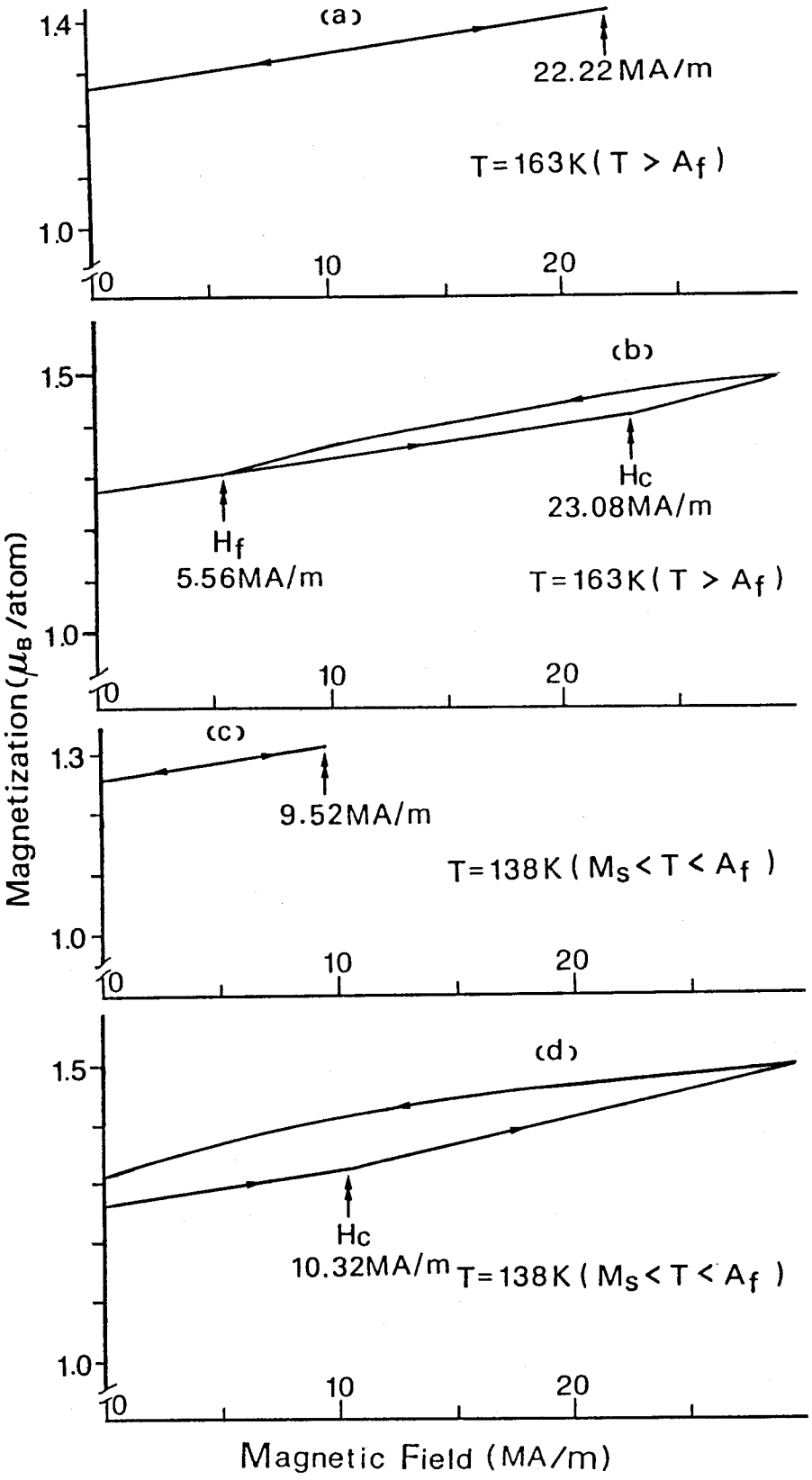

Fig. 3 Magnetization vs. magnetic field (M(t)-H(t)) curves at T=163K($T>A_f$) and T=138K ($M_s<T<A_f$).

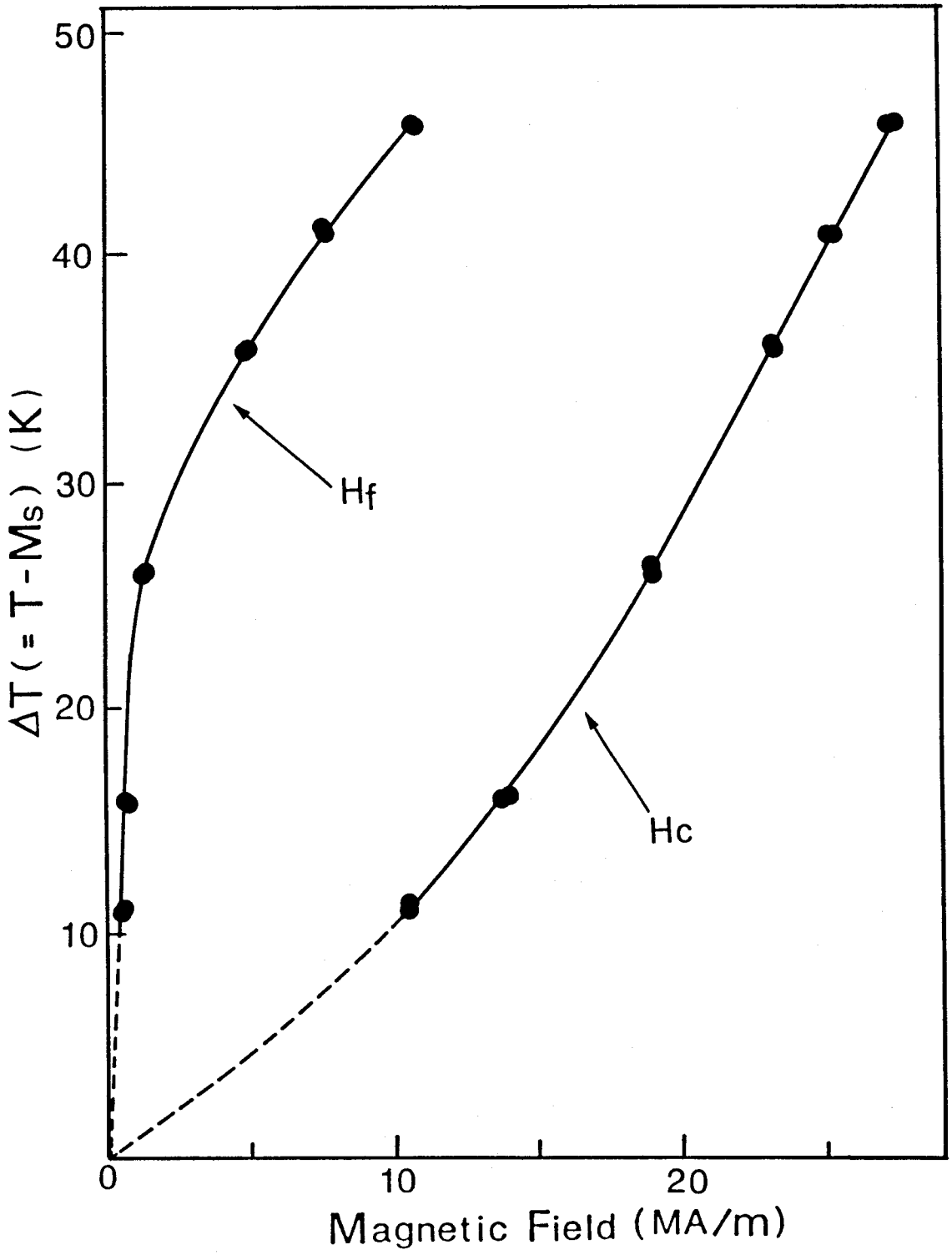

Fig. 4 Critical field vs. $\Delta T(=T-M_s)$ relation in an ausaged Fe-Ni-Co-Ti alloy

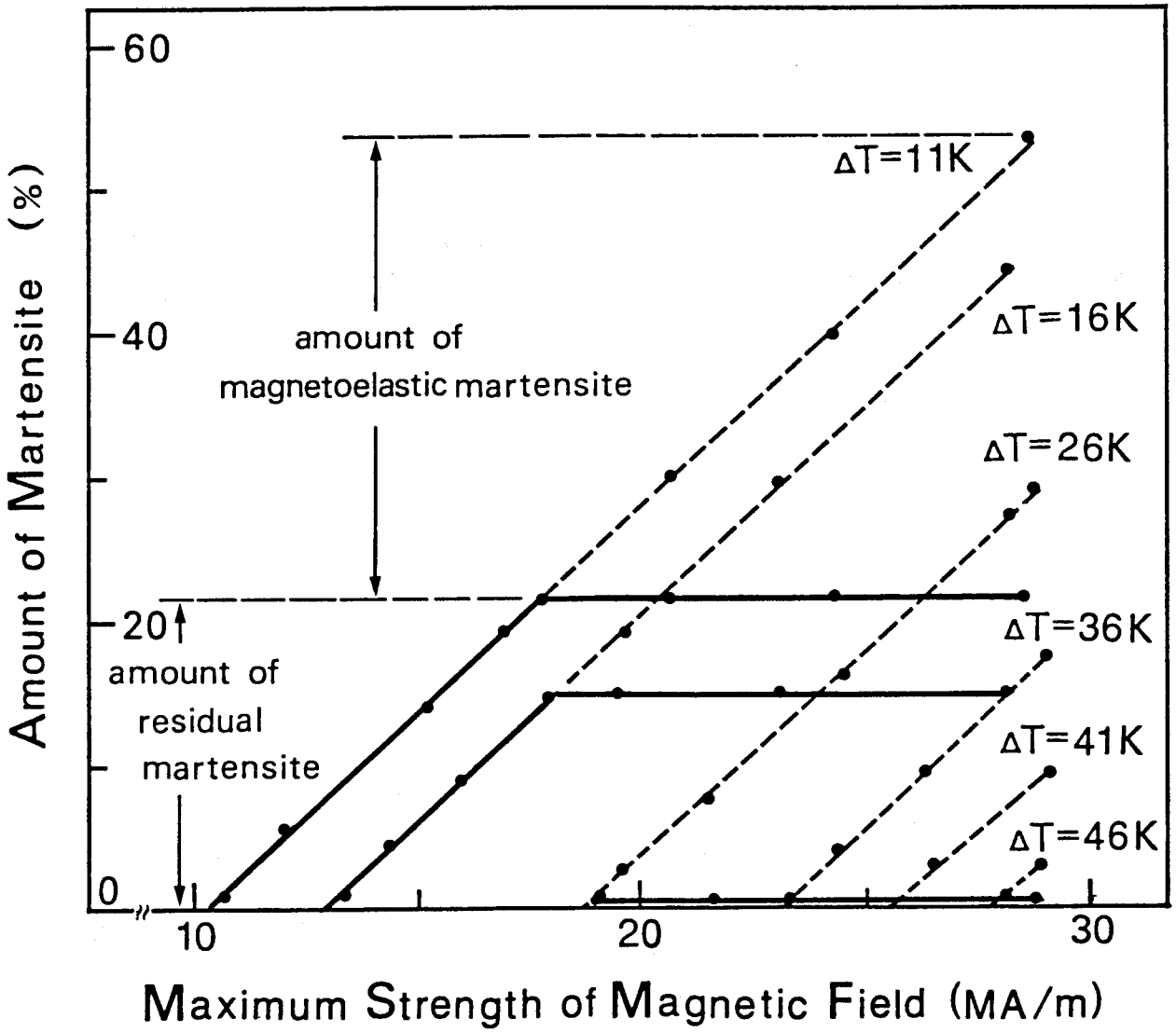

Fig. 5 Amount of magnetic field-induced martensites as a function of maximum strength of pulsed magnetic field.

Chapter 8

Quantitative Evaluation of Magnetic Effects on the Shift of M_S Temperatures of Martensitic Transformations.

Synopsis

An equation for estimating the shift of M_S temperatures of martensitic transformations under a magnetic field is proposed, which consists of three effects of the magnetostatic energy, high field susceptibility and forced volume magnetostriction, the last effect being newly introduced especially for Invar alloys.

The forced volume magnetostriction and transformation strain involved in the last effect have been measured by means of Fabry-Pérot interferometry and X-ray diffraction, respectively, as to three Invar Fe-Ni, one non-Invar Fe-Ni-C and one Invar ordered Fe-Pt alloys. The calculated shift of M_S temperature as a function of magnetic field in those alloys is good agreement with the previously measured one, and thus the propriety of the proposed equation is quantitatively verified.

I. Introduction

As mentioned in Chapter 2~6, measured shift of M_S as a function of magnetic field can be well explained for ferrous alloys except for Invar alloys. The origins considered are the magnetostatic energy and an additional magnetostatic energy due to high field magnetic susceptibility. Therefore, the third origin for the shift of M_S should be taken into account for the Invar alloys. It is well known that the Invar alloys have a large forced volume magnetostriction, and it might have an important role on the shift of M_S.

This Chapter shows how the forced volume magnetostriction explains the residual part of the shift of M_S in the Invar alloys.

II. Effect of forced volume magnetostriction on M_S

The forced volume magnetostriction is defined as a field-induced volume change $\partial\omega/\partial H$, where ω is a volume change per unit volume. $\partial\omega/\partial H$ for some Invar and non-Invar alloys such as Fe-Ni alloys[1]~[3] and for metals such as Ni[4] has been measured. According to the measurements, it is isotropically positive and is about 10^{-10}m/MA for the Invar alloys while it is about 10^{-11}m/MA for non-Invar metals and alloys.

In a microscopic point of view, the volume expansion comes from the Pauli-repulsion in the induced magnetic moment. In a phenomenological point of view, however, it can be regarded as a negative hydrostatic pressure effect for materials. This means that $\partial\omega/\partial H$ corresponds to $-\partial\omega/\partial p$ under hydrostatic pres-

sure. The only difference between $\partial\omega/\partial H$ and $\partial\omega/\partial p$ is their sign, namely $\partial\omega/\partial p < 0$ while $\partial\omega/\partial H > 0$. The effect of a hydrostatic pressure on the shift of M_S temperature of martensitic transformation was quantitatively studied already by Patel and Cohen as mentioned in Chapter 1. When a change of hydrostatic pressure δP is applied on the system, the Gibbs chemical free energies of the austenitic and martensitic states are given by

$$G^{\gamma}(T,\delta P) = G^{\gamma}(T) + V^{\gamma}\cdot\delta P, \tag{1}$$

$$G^{\alpha'}(T,\delta P) = G^{\alpha'}(T) + V^{\alpha'}\cdot\delta P, \tag{2}$$

where $G(T,\delta P)$ and $G(T)$ represent the Gibbs chemical free energies with and without the change of hydrostatic pressure at temperature, T, respectively, V the volume and γ and α' mean the austenitic and martensitic states, respectively.

Subtracting (2) from (1), the difference in Gibbs chemical free energy between two phases is expressed as

$$\Delta G'(T,\delta P) = \Delta G'(T) + \Delta V\cdot\delta P, \tag{3}$$

where

$$\Delta G'(T,\delta P) = G^{\gamma}(T,\delta P) - G^{\alpha'}(T,\delta P), \tag{4}$$

$$\Delta G'(T) = G^{\gamma}(T) - G^{\alpha'}(T), \tag{5}$$

and

$$\Delta V = V^{\gamma} - V^{\alpha'}. \tag{6}$$

Equation (3) is traditionally written for a unit volume of the austenitic phase as

$$\Delta G(T,\delta P) = \Delta G(T) - \varepsilon_0 \cdot \delta P, \qquad (7)$$

where ε_0 (transformation strain) is given by

$$\varepsilon_0 = -\Delta V / V^{\gamma}. \qquad (8)$$

By using the equation (7), Patel and Cohen derived a equation to determine the transformation temperature under hydrostatic pressure. The principle of derivation is schematically shown in Fig. 1, in which $\Delta G(T,\delta P)$ and $\Delta G(T)$ are shown as a function of temperature for a given δP. As mentioned before, martensitic transformation with no change of hydrostatic pressure does not occur at the thermodynamical equilibrium temperature To, but at M_S. $\Delta G(M_S)$ in Fig. 1.is usually called the chemical driving force, which is described in Chapter 1. Patel and Cohen assumed that the chemical driving force is independent of surrounding conditions. Therefore, $\Delta G(M_S',\delta P) = \Delta G(M_S)$ and equation (3) is written as

$$\Delta G(M_S) - \Delta G(M_S') = -\varepsilon_0 \cdot \delta P, \qquad (9)$$

where M_S' represents the transformation temperature under hydrostatic pressure. An extensive use of the equation (9) to the case of magnetic field effect is considered. The central idea of the extension is that a magnetic field effect corresponds to a negative pressure effect because $\partial\omega/\partial p$ corresponds to $-\partial\omega/\partial H$. Therefore, the pressure term in the equation (9) can be replaced by the magnetic field term.

The negative pressure δP which induces an isotropic vol-

ume expansion $-\delta V/V$ is given by

$$\delta P = -B\ (\delta V/V), \tag{10}$$

where the expansion is assumed to be in a Hooke's regime and B the bulk modulus. On the other hand, the magnetic field-induced expansion $\delta V/V$ is given by

$$\delta V/V = \alpha H, \tag{11}$$

where the expansion is again assumed to be linear and α corresponds to $\partial\omega/\partial H$. From equations (10) and (11), the following relation is obtained:

$$\delta P = -B\cdot(\partial\omega/\partial H)\cdot H. \tag{12}$$

Taking into account the other two magnetic effects described in Chapter 2 to the formula given by Patel and Cohen, the following formula is obtained:

$$\Delta G(M_S) - \Delta G(M_S') = -\Delta M(M_S')\cdot H - 1/2\overset{\gamma}{X}_{hf}\cdot H + \varepsilon_0\ (\partial\omega/\partial H)\cdot H\cdot B. \tag{13}$$

In the right hand side of the equation, the first term is due to the effect of magnetostatic energy, the second term is due to the high field susceptibility effect and the last term is due to a newly introduced forced volume magnetostriction effect. The first and second terms have been already measured.

The third term will be estimated in the next section. $\Delta G(M_S)$ and $\Delta G(M_S')$ of the left hand side can be evaluated from published data, as will be shown later. Thus, the relation between M_S' and H is able to be numerically determined.

III. Determination of forced volume magnetostriction and transformation strain.

Three Invar Fe-29.9, -31.7 and -32.5 at%Ni, non-Invar Fe-24.7Ni-1.8C (at%) and ordered Invar Fe-24 at%Pt (S~0.8) alloys were prepared. Details of the alloy preparation were described in Chapter 2, 4 and 5. The M_S temperatures determined by electrical resistivity measurements for the Fe-29.9Ni, -31.7Ni, -32.5Ni, Fe-Ni-C and Fe-Pt alloys were 223, 164, 113, 223 and 153K, respectively.

The forced volume magnetostriction has been measured by means of Fabry-Pérot interferometry, applying a pulsed ultra-high magnetic field (maximum strength is 31.75 MA/m) at the High Magnetic Field Laboratory, Osaka University. The light source used in the interferometry was He-Ne Laser with λ=0.6328 μm, and one of half-mirrors was fixed to each specimen. The transformation strain ε_0 associated with the martensitic transformations in those alloys has been determined by measuring lattice parameters of the austenite and martensite phases by means of X-ray diffraction.

(1) Measurement of the forced volume magnetostriction, $\partial\omega/\partial H$.

Within the Hooke's regime, $\partial\omega/\partial H$ is given by

$$\partial\omega/\partial H = 3\,\partial(\Delta\ell/\ell)/\partial H, \qquad (14)$$

where $\Delta\ell/\ell$ is the elongation ratio of a specimen. $\Delta\ell$ in equation (14) has been measured by means of Fabry-Pérot interferometry, that is, by observing intensity modulation due to interference of Laser beams reflected from one half-mirror and the other one fixed to the specimen which is subjected to a volume expansion under a magnetic field. The instrument used for the Fabry-Pérot interferometry is schematically shown in Fig. 2. Fig. 3 shows an intensity modulation profile thus obtained under a pulsed magnetic field with the maximum strength of 3.97 MA/m to an Fe-31.7 at%Ni alloy at 300K. The intensity modulation profile shows a few peaks and the peak to peak distance corresponds to $\lambda/2$ according to the Airy's formula. Thus, the elongation ratio $(\Delta\ell/\ell)$ can be obtained by counting the number of peaks, and it is measured as a function of the strength of magnetic field for the five alloys at 300K, as shown in Fig. 4. It is seen from the figure that $\Delta\ell/\ell$ increases linearly with increasing magnetic field. Then, $\partial\omega/\partial H$ is determined by the equation (14). Figure 5 shows $\partial\omega/\partial H$ thus obtained as a function of temperature for all the alloys. It is known from the figure that $\partial\omega/\partial H$ linearly increases for the Fe-Ni and Fe-Pt alloys and decreases for the Fe-Ni-C alloy with increasing temperature, and that it decreases with increasing Ni content of the Fe-Ni alloys over the temperature range where the measurement has been done.

Another characteristic feature noted in the figure is that the $\partial\omega/\partial H$ for the Fe-Ni-C alloy is smaller than those for the

Fe-Ni and Fe-Pt alloys. This is because the Fe-Ni-C alloy has not Invar effect, and the forced volume magnetostriction is non-Invar alloys is smaller than that in Invar Fe-Ni and Fe-Pt alloys.

(2) Measurement of the transformation strain, ε_0.

The transformation strain, ε_0, for three Fe-Ni and one Fe-Ni-C alloy is obtained from the lattice parameters measured in the present study, and that for Fe-Pt alloy from those previously measured by Tadaki and Shimizu[5]. The lattice parameters of both the austenite and martensite phases of the Fe-Ni and Fe-Ni-C alloys are measured as a function of temperature by X-ray diffraction. Reflections used in the measurements were the austenite 111 and the martensite 110, and ε_0 has been calculated from those lattice parameters. Fig. 6 shows the ε_0 thus obtained as a function of temperature for the three Fe-Ni and one Fe-Ni-C alloys. It is known from the figure that ε_0 of Fe-29.9, -31.7, -32.5 at%Ni and Fe-Ni-C alloys at room temperature are about 2.1, 1.9, 1.7 and 2.3×10^{-2}, respectively, and these values of the Fe-Ni alloys are almost the same as those previously measured[6].

On the other hand, according to a previous work[5], ε_0 for the ordered Fe-Pt alloy is negative near M_S temperature, and its value is about -5×10^{-3}. An attention should be paid for the fact that ε_0 is negative for the ordered Fe-Pt alloy while it is positive for the Fe-Ni and Fe-Ni-C alloys. Such a difference may bring in some influence on the shift of M_S temperature due to the forced volume magnetostriction effect,

that is, M_S temperature of the ordered Fe-Pt alloy decreases due to the effect, whereas that of the Fe-Ni and Fe-Ni-C alloys increases. Because the evergy due to the effect is negative for the former alloy and positive for the latter alloys, as seen in the equation (13) previously described.

(3) Previously measured spontaneous magnetization difference, $\Delta M(T)$, high field susceptibility, χ^{γ}_{hf}, and bulk modulus, B.

As described in Chapter 2, 4 and 5, the spontaneous magnetization in the austenitic state and high field susceptibility in the present alloys are already measured as a function of temperature, by magnetization measurement under a pulsed magnetic field. On the other hand, the spontaneous magnetization in the martensitic state for those alloys at 0K were obtained from the Slater-Pauling curve. The measured $\Delta M(T)$ and χ^{γ}_{hf} have been used in the present calculation.

The bulk modulus, B, of Fe-30, -32 and -35 at%Ni alloys have already been measured as a function of temperature by Oomi and Mori[7][8]. Those measured values are used in the present calculation of a relation between the shift of M_S temperature and critical magnetic field for inducing martensitic transformation. That is, B for the present Fe-29.9 at%Ni alloy is referred to that for the previous Fe-30 at%Ni alloy[7], and B for the present other two Fe-Ni alloys to that for the previous Fe-32 at%Ni alloy[8], because the compositions are nearly the same. On the other hand, B for the ordered Fe-Pt and non-Invar Fe-Ni-C alloys has not been measured yet in detail.

However, since B of a disordered Fe-Pt alloy has been measured as a function of temperature[7], that value is used for the present ordered Fe-Pt alloy, although it may be a very rough approximation. B of the non-Invar Fe-Ni-C alloy is assumed to be 10^{11} Pa order and to have no temperature dependence over the temperature range concerned, because B of many non-Invar metal and alloys are known to be that order and to have a small temperature dependence over a wide temperature range.

(4) Calculated values of Gibbs chemical free energy difference, $\Delta G(T)$.

The Gibbs chemical free energies of the austenite and martensite phases in the present Fe-Ni, Fe-Ni-C and ordered Fe-Pt alloys have been calculated by using the equations proposed by Kaufman and Cohen[9], Fisher et al.[10][11] and Tong and Wayman [12], as mentioned in detail in Chapter 2, 4 and 5.

(5) Comparison of calculated relation with previously measured relation between the shift of M_S temperature and magnetic field.

Relation between the shift of M_S temperature and magnetic field for inducing martensitic transformation has been calculated for three Invar Fe-Ni, one non-Invar Fe-Ni-C and one ordered Invar Fe-Pt alloys, by substituting the above measured and known physical quantities of those alloys into the previously proposed equation, (13). The calculated shift of M_S temperature($\Delta M_S = M_S' - M_S$) due to each effect of the magnetostatic energy, high field susceptibility and forced volume magnetostriction and their total shift are shown with dotted lined

in Figs. 7, 8, 9, 10, and 11, for Fe-29.9, -31.7, -32.5 at%Ni alloys and ordered Fe-Pt and non-Invar Fe-Ni-C alloys, respectively, together with the shift of M_S temperature as a function of magnetic field, and numerical values of the shift of M_S temperature are shown in Table 1, when a pulsed magnetic field of nearly the maximum strength (about 30 MA/m) has been applied to those five alloys together with the measured ones. It is clearly seen from the figures that the calculated relation between the shift of M_S temperature and magnetic field due to the three effects is almost good agreement with the experimentally measured one in a wide range of ΔM_S. It is also known from the figures and table that the shift of M_S temperature due to the forced volume magetostriction effect for the Invar Fe-Ni and Fe-Pt alloys are larger than that for the non-Invar Fe-Ni-C alloy, and that they are nearly the same order as those due to the effect of magnetostatic energy. This is mainly due to the fact that the forced volume magetostriction in Invar alloys is larger than that in non-Invar alloys (Fig. 5), although other quantities such as $\Delta G(M_S)-\Delta G(T)$ must be also considered. It is also noted in Fig.10 that the shift of M_S temperature due to the forced volume magnetostriction effect is a decrease in the ordered Fe-Pt alloy. This is due to the fact that ε_0 in the alloy is a negative value, as mentioned before.

It is thus concluded from the good agreement between the calculation and experiment that the propriety of the proposed equation for the shift of M_S temperature is quantitatively verified.

References

(1) M. Matusmoto, T. Kaneko and H. Fujimori: J. Phys. Soc. Jpn., 26 (1969), 1083.

(2) W. F. Schlosser, G. M. Graham and P. P. M. Meincke: J. Phys. Chem. Solids, 32 (1971), 927.

(3) D. Gugan: Proc. Phys. Soc. (London), 72 (1958), 1013.

(4) J. H. M. Soelinga, R. Gersdorf and Fe. de Vries: Physica, 31 (1965), 349.

(5) T. Tadaki and K. Shimizu: see Chapter 5, (2).

(6) R. P. Read and R. E. Schramm: J. Appl. Phys., 40 (1969), 3453.

(7) G. Oomi and N. Mōri: J. Phys. Soc. Jpn., 50 (1981), 2917.

(8) G. Oomi and N. Mōri: unpublished work. (1982).

(9) L. Kaufman and M. Cohen: see Chapter 1, (28).

(10) J. C. Fisher: see Chapter 4, (10).

(11) J. C. Fisher, J. H. Hollomon and D. Turnbull: see Chapter 4, (11).

(12) H. C. Tong and C. M. Wayman: see Chapter 5, (4).

Table 1. Numerical values of calculated and measured shifts of M_S temperature, when 30 MA/m of magnetic field has been applied to three Invar Fe-Ni, one non-Invar Fe-Ni-C and one Invar ordered Fe-Pt alloys.

Composition	Fe-29.9at%Ni	Fe-31.7at%Ni	Fe-32.5at%Ni	Fe-24at%Pt	Fe-24.7Ni-1.8C
H (MA/m)	30.16	30.95	30.95	30.16	30.16
$\Delta M \cdot H - \frac{1}{2}\chi_{hf} H^2$ $\Delta M_{s,1}$ (K)	43	41	30	31	83
$\epsilon_0(\frac{\partial \omega}{\partial H}) \cdot H \cdot B$ $\Delta M_{s,2}$ (K)	28	31	28	−25	9
$\Delta M_{s,1} + \Delta M_{s,2}$ (K)	71	72	58	6	92
ΔM_s obs. (K)	72	80	65	9	94

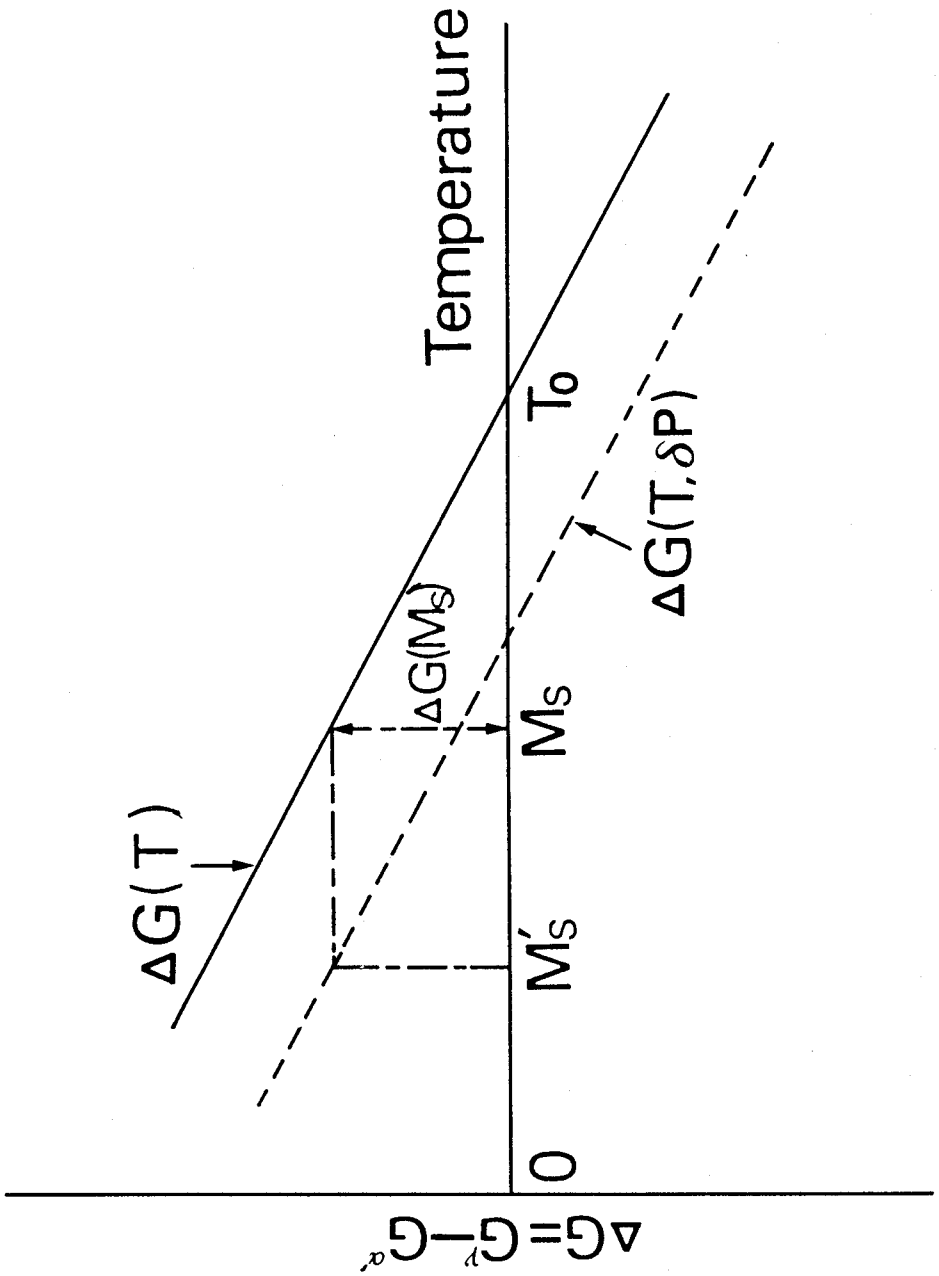

Fig. 1 Schematic illustration of the shift of M_S temperature due to a change of hydrostatic pressure, δp.

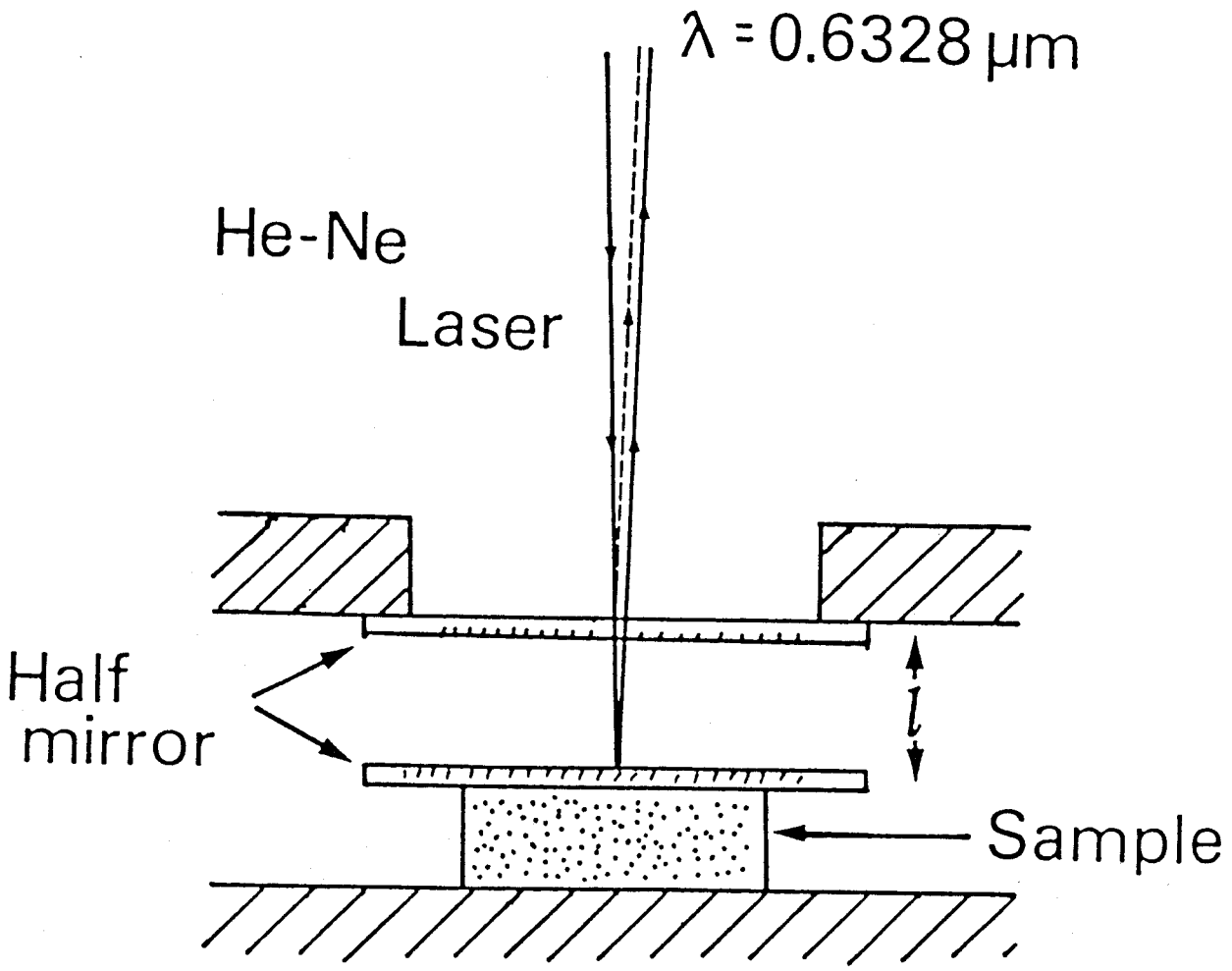

Fig. 2 The schematic illustration of the instrument of Fabry-Pérot interferometry.

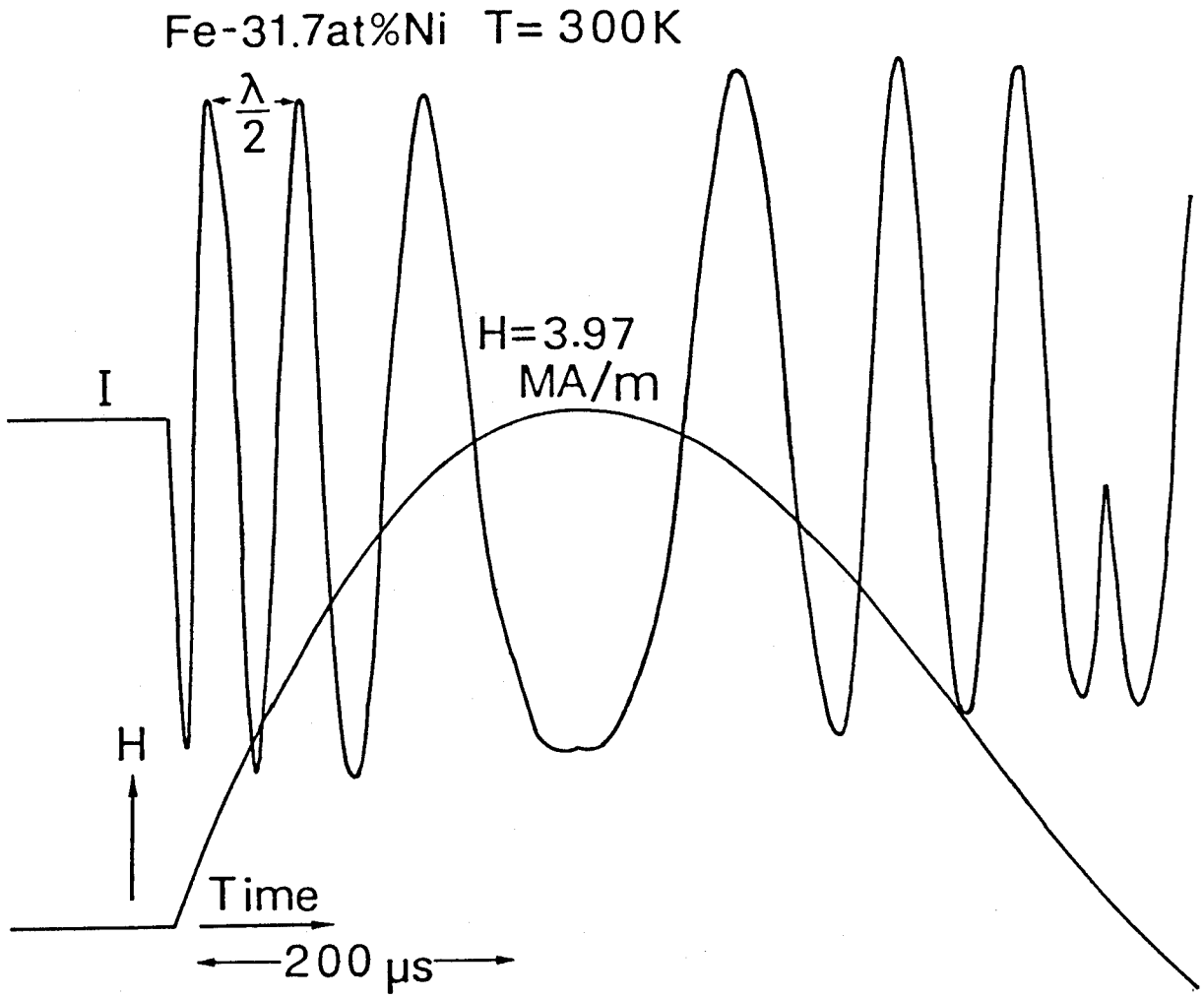

Fig. 3 Intensity moduration curve due to interference of reflected Laser beams together with a strength curve of magnetic field, when a pulsed magnetic field whose maximum strength is 3.97 MA/m has been applied to an Fe-31.7 at%Ni alloy at 300K.

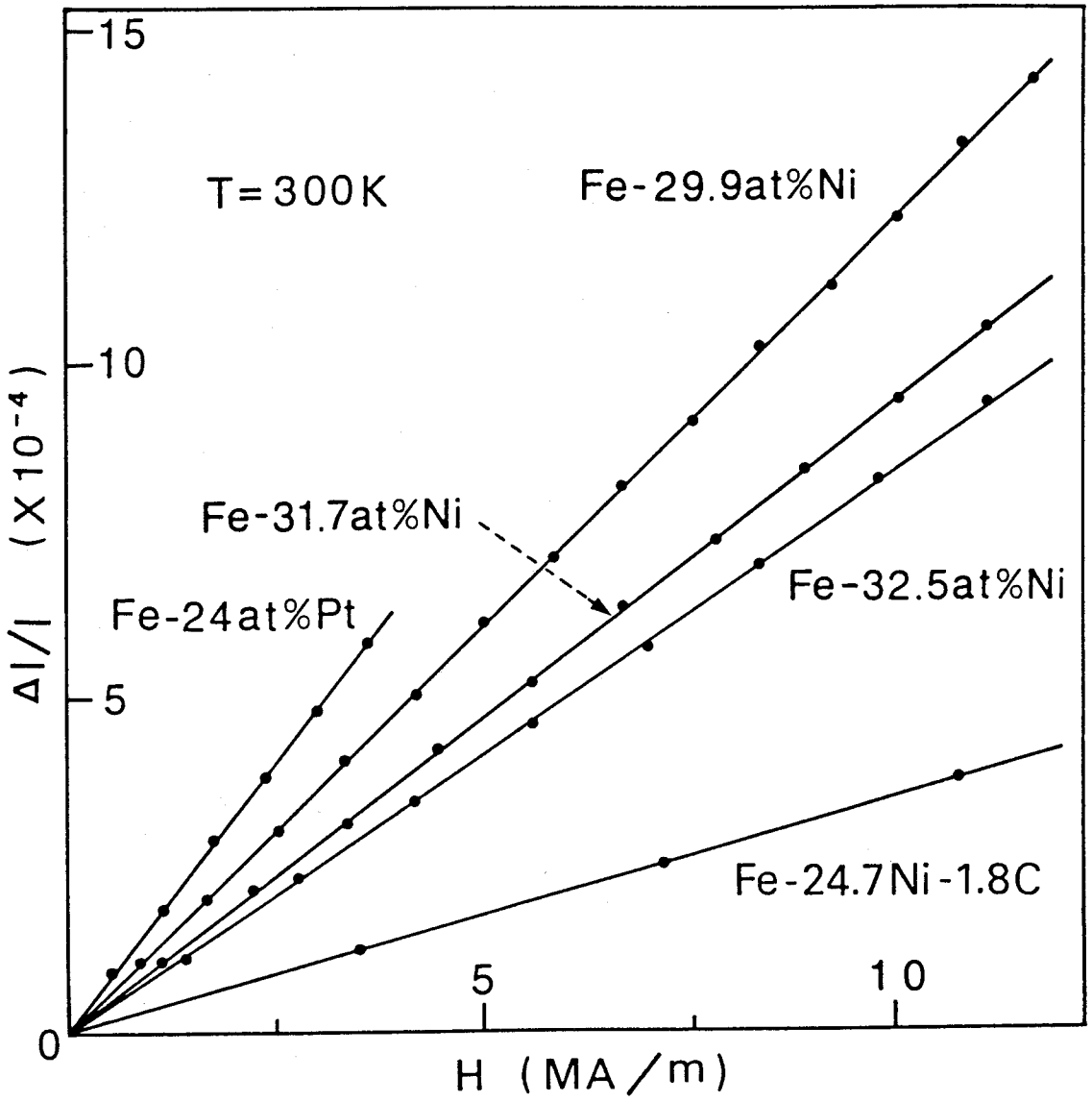

Fig. 4 Elongation ratio plotted as a function of the strength of magnetic field for three Invar Fe-Ni one non-Invar Fe-Ni-C and one Invar ordered Fe-Pt alloys.

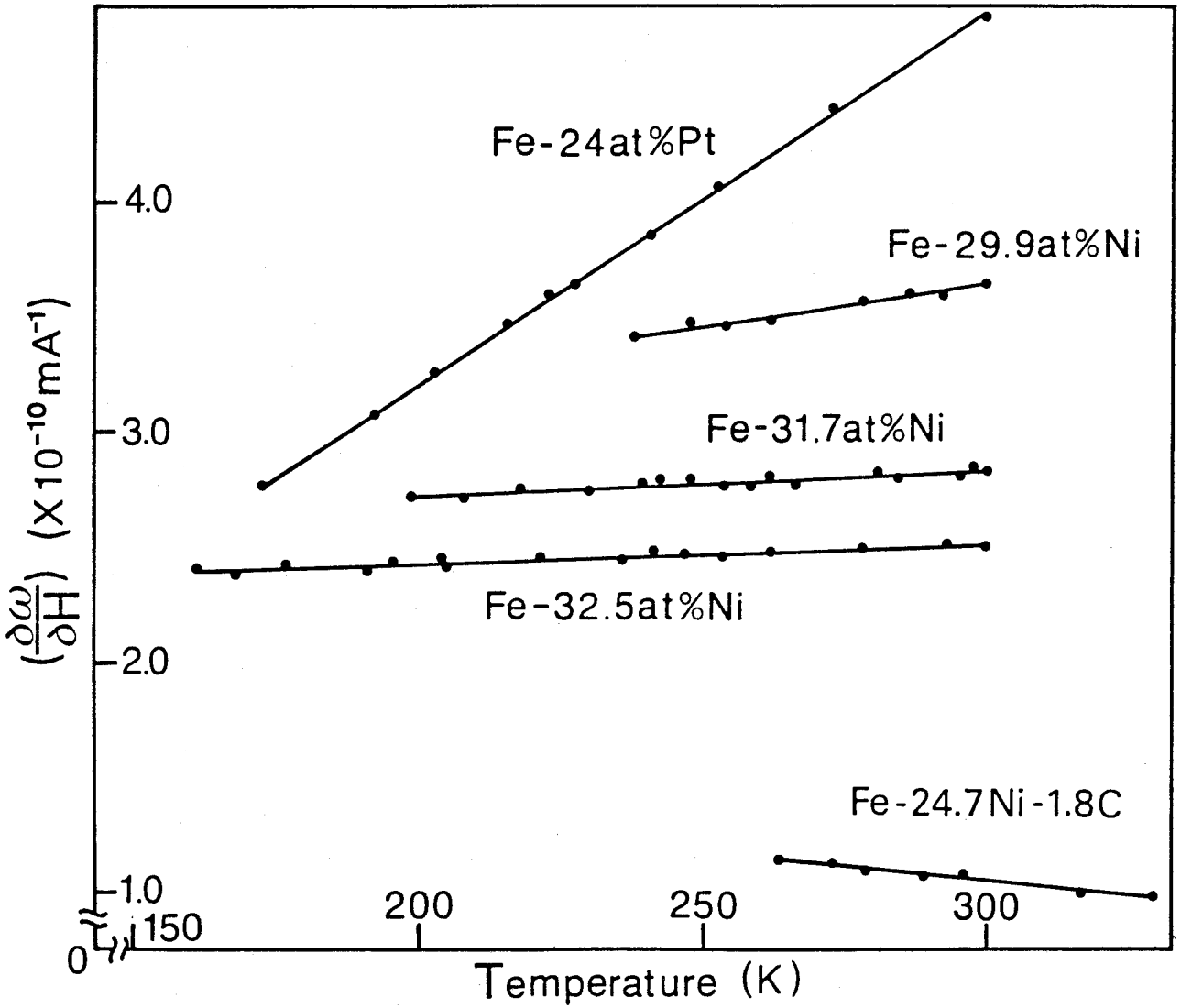

Fig. 5 Forced volume magnetostriction, $(\partial\omega/\partial H)$, plotted as a function of temperature for three Invar Fe-Ni, one non-Invar Fe-Ni-C and one Invar ordered Fe-Pt alloys.

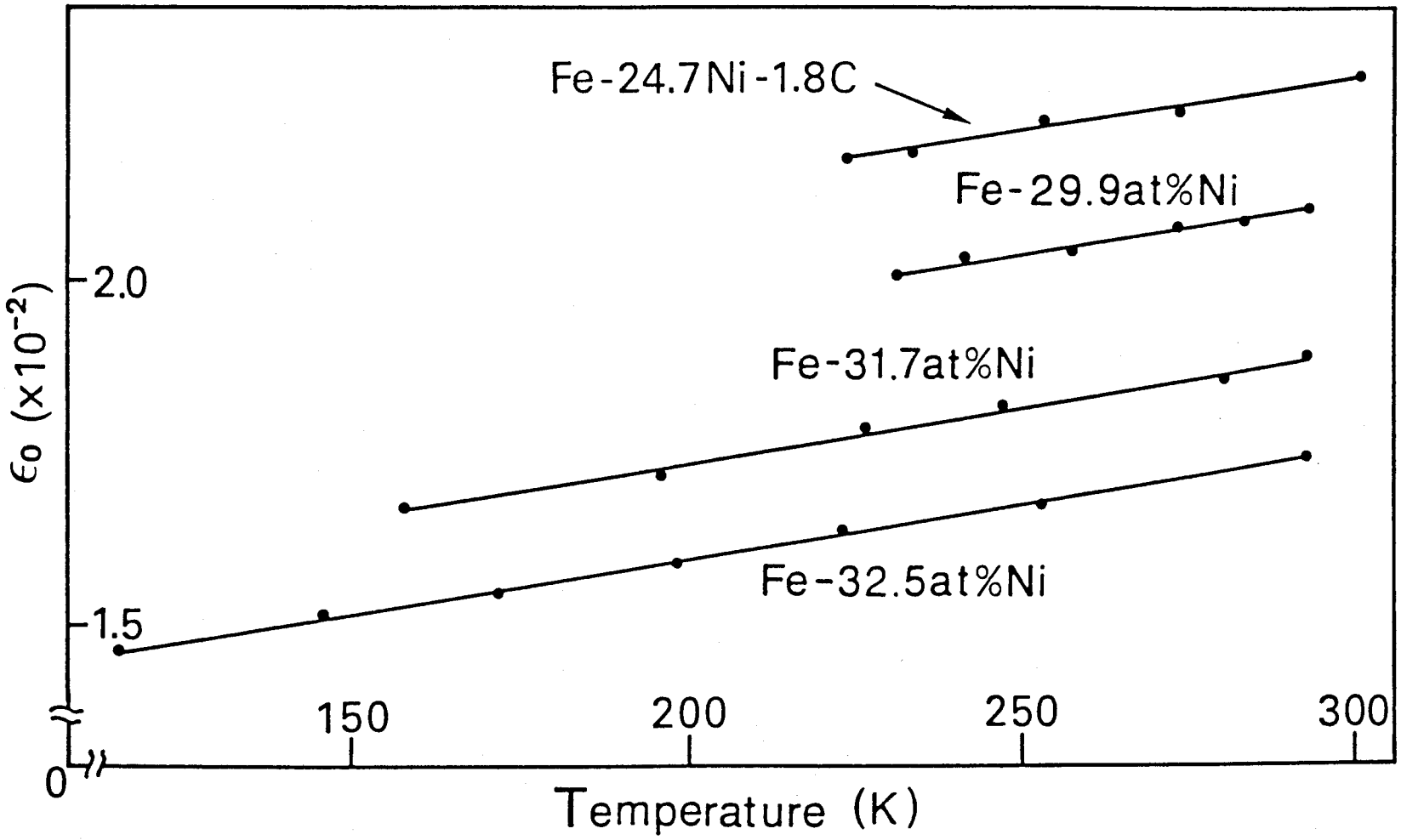

Fig. 6 Transformation strain, ε_0, associated with the martensitic transformation in three Invar Fe-Ni and one non-Invar Fe-Ni-C alloys, which was plotted as a function of temperature.

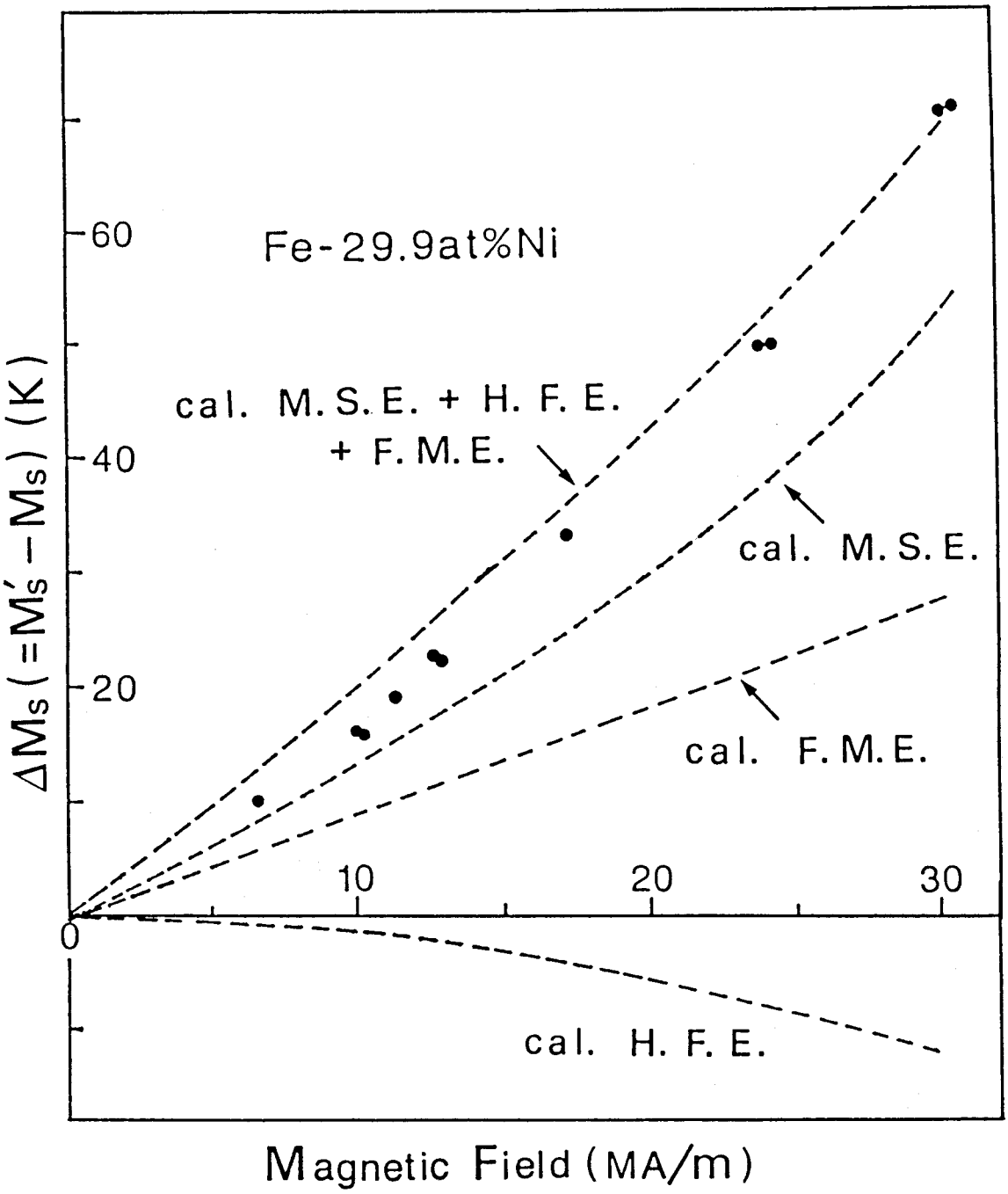

Fig. 7 Calculated and measured shifts of M_S as a function of magnetic field for an Invar Fe-29.9 at%Ni alloy, where M. S. E., H. F. E. and F. M. E. mean the effect of magnetostatic energy, high field susceptibility and forced volume magnetostriction, respectively.

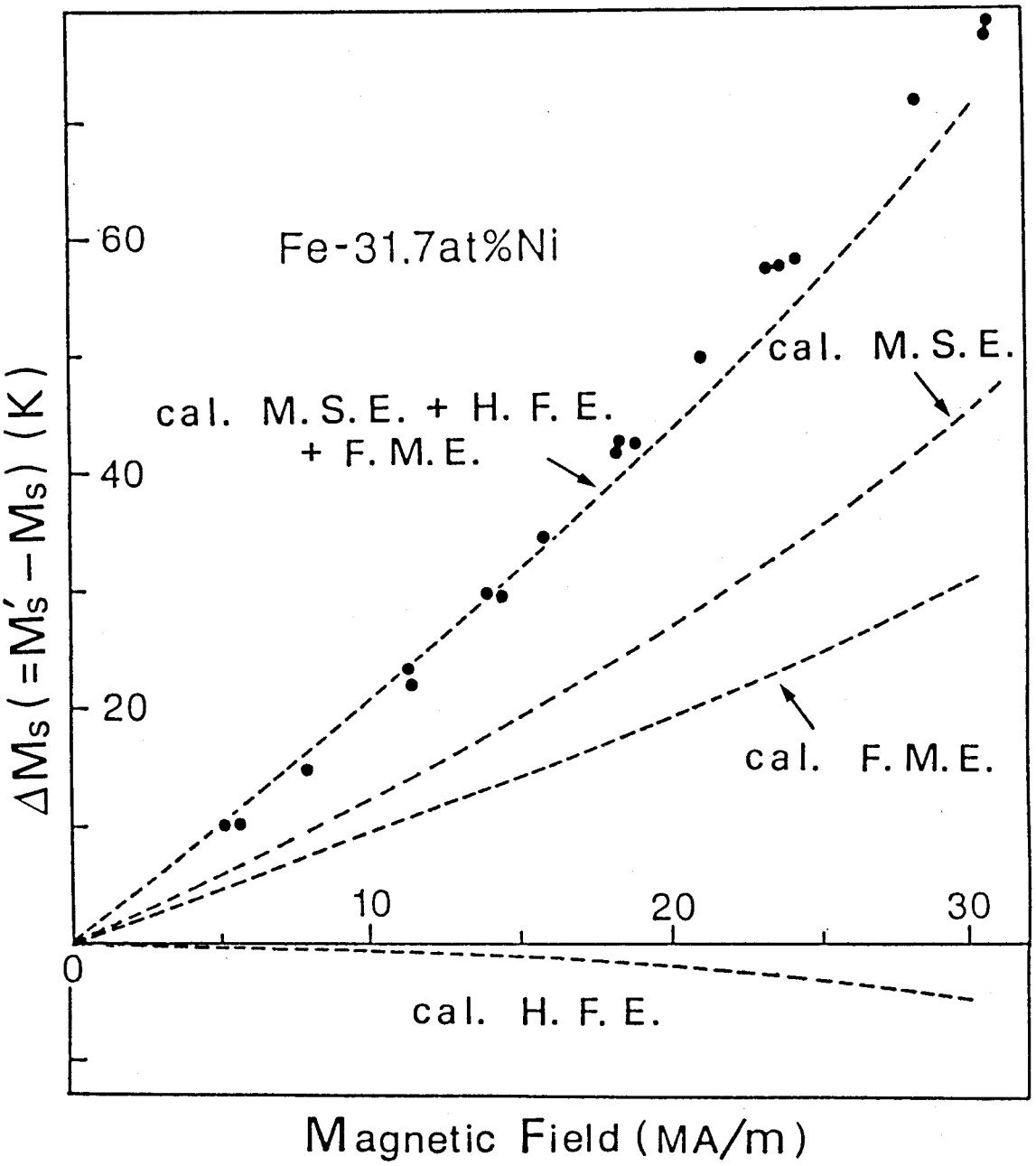

Fig. 8 Calculated and measured shifts of M_S as a function of magnetic field for an Invar Fe-31.7 at%Ni alloy, where M. S. E., H. F. E. and F. M. E. mean the effect of magnetostatic energy, high field susceptibility and forced volume magnetostriction, respectively.

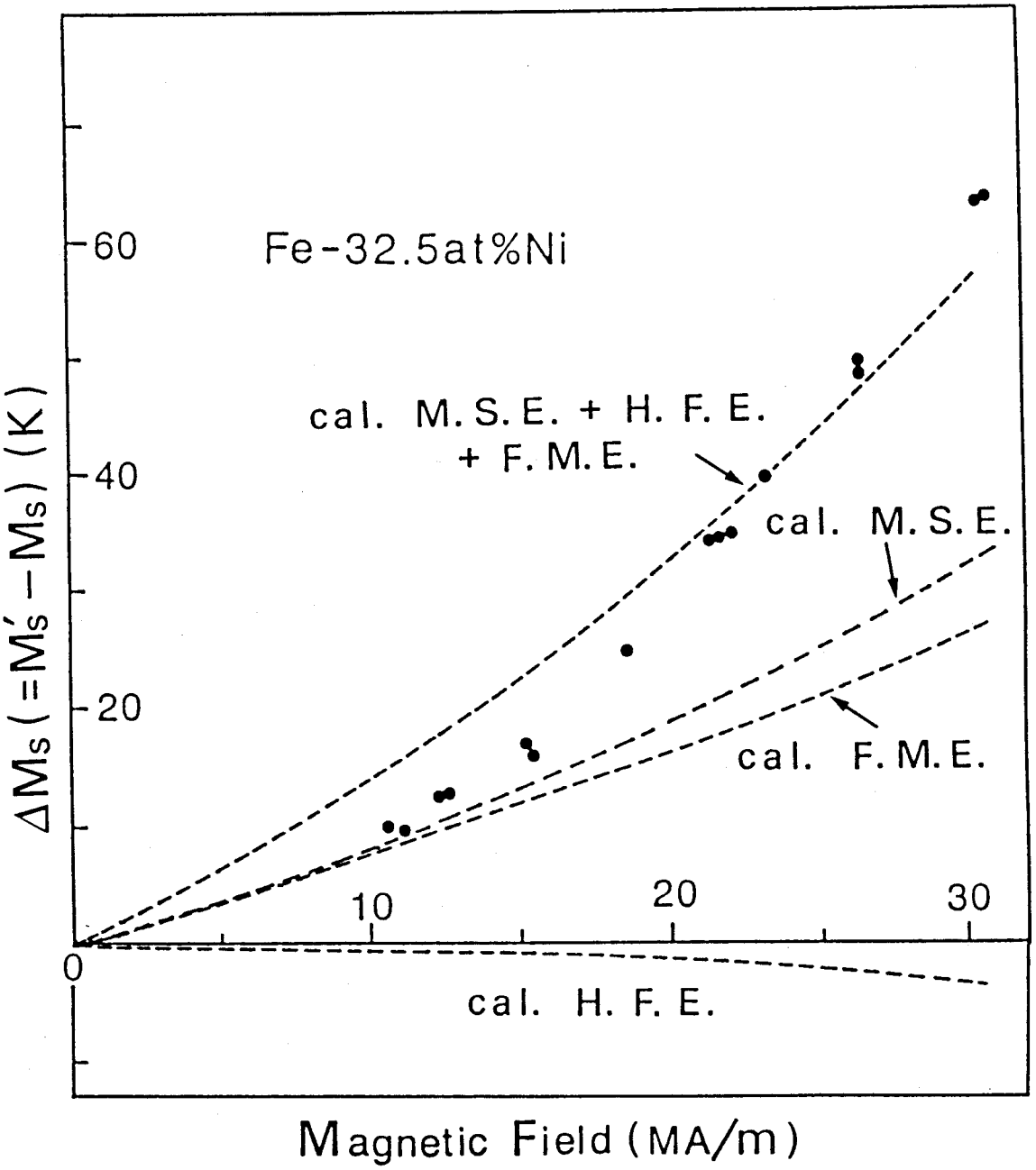

Fig. 9 Calculated and measured shifts of M_S as a function of magnetic field for an Invar Fe-32.5 at%Ni alloy, where M. S. E., H. F. E. and F. M. E. mean the effect of magnetostatic energy, high field susceptibility and forced volume magnetostriction, respectively.

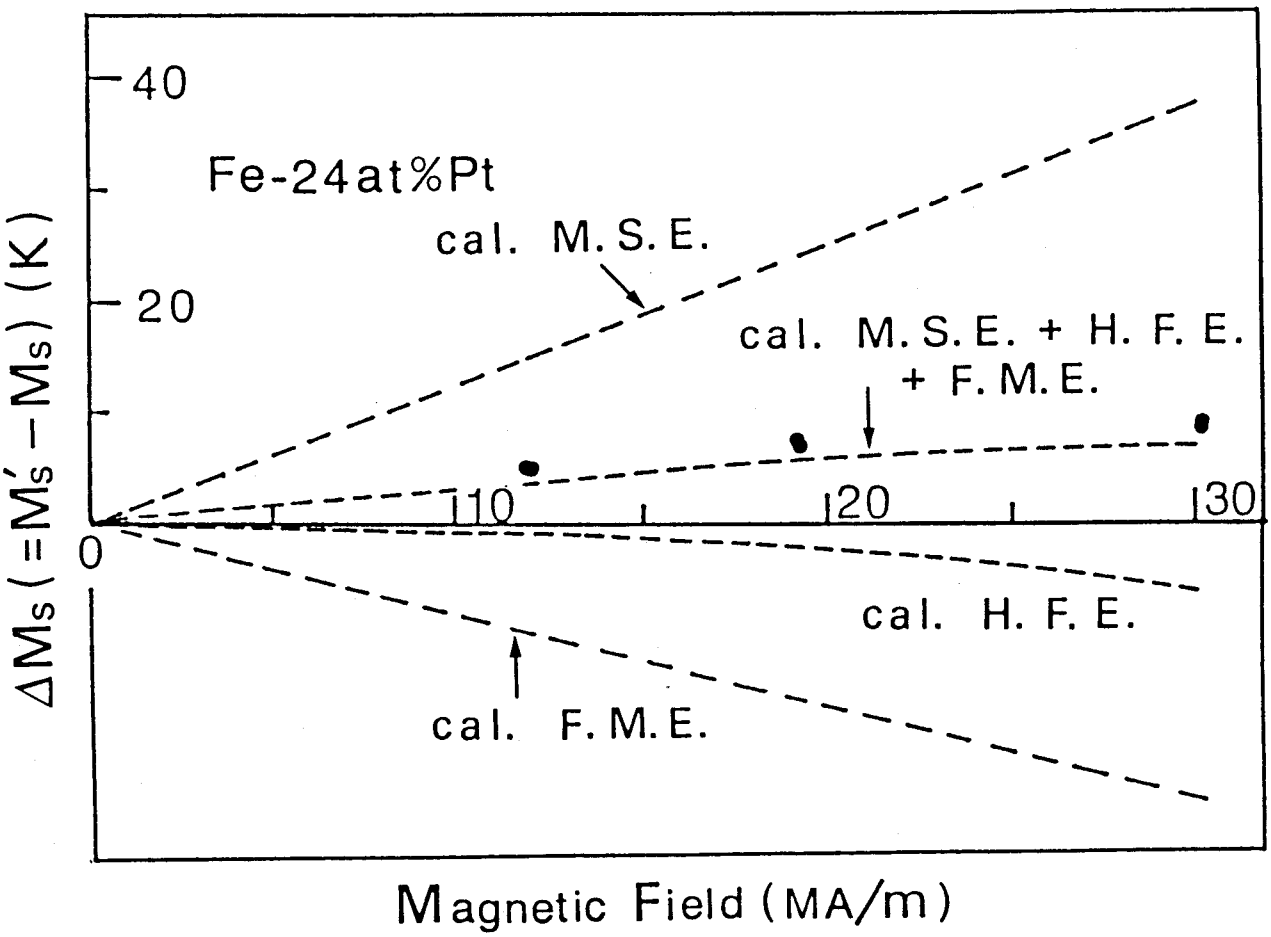

Fig. 10 Calculated and measured shifts of M_S as a function of magnetic field for an Invar ordered Fe-24 at%Pt alloy, where M. S. E., H. F. E. and F. M. E. mean the effect of magnetostatic energy., high field susceptibility and forced volume magnetostriction, respectively.

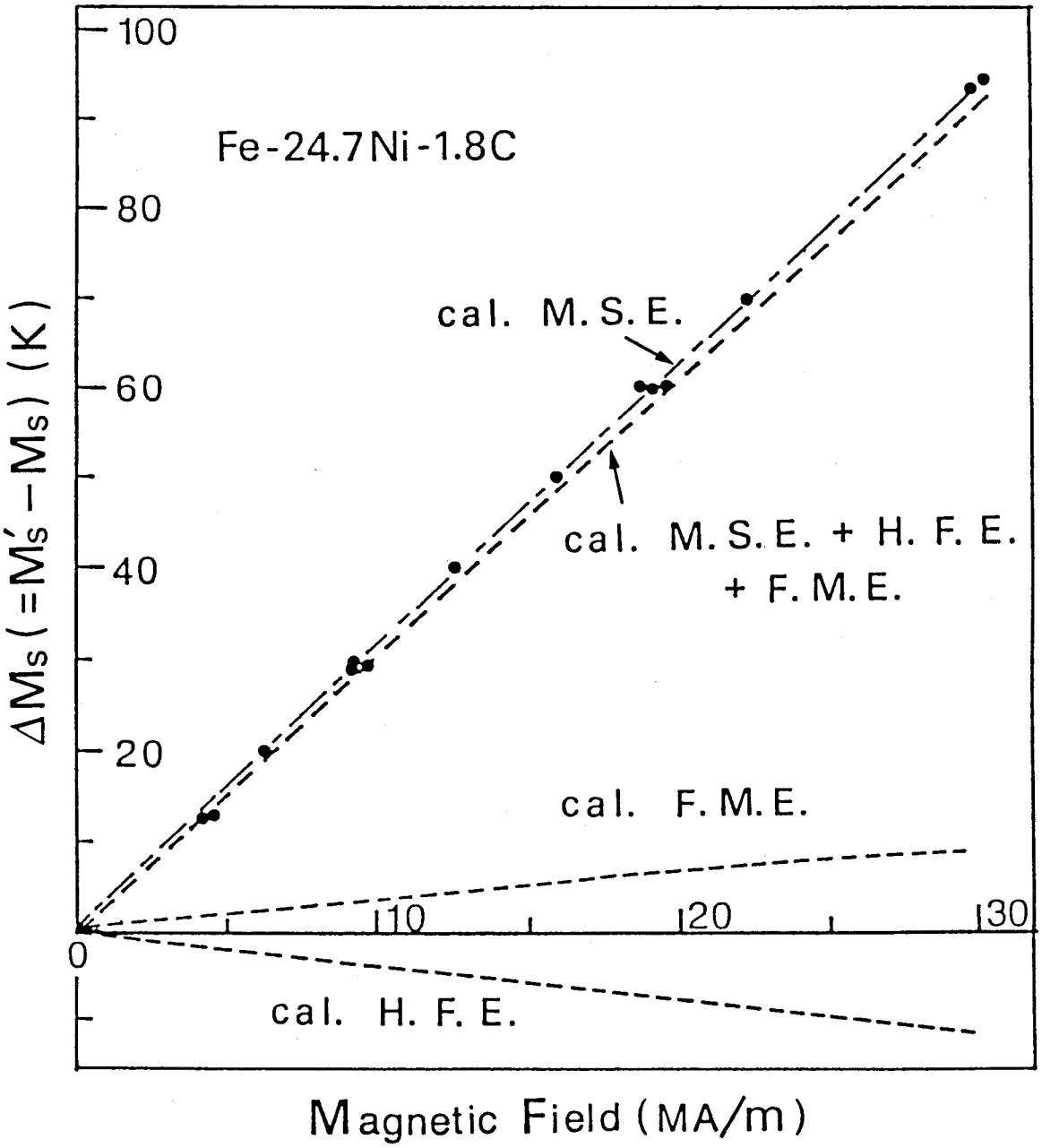

Fig. 11 Calculated and measured shifts of M_S as a function of magnetic field for a non-Invar Fe-24.7 at%Ni-1.8 at%C alloy, where M. S. E., H. F. E. and F. M. E. mean the effect of magnetostatic energy, high field susceptibility and forced volume magnetostriction, respectively.

Acknowlegements

The author wishes to express his sincere gratitude to Professor K. Shimizu for his valuable suggestions and enlightening discussions, and for his continuous encouragement throughout the present work. He would like to express his thanks to Professor M. Date for his cooperation with this study and many helpful discussions throughout the present work, and for permission to use the instrument of a pulsed high magnetic field at the High Magnetic Field Laboratory of Osaka University. He also would like to thank Professor A. Yamagishi and Dr. K. Sugiyama at Osaka University for many helps in using the instrument of a pulsed magnetic field and in measurement of forced volume magnetostriction. He would like to thank Professor K. Otsuka at University of Tsukuba for permission to use the Bridgeman furnace to make the Fe-Ni alloy single crystals, Professor T. Tadaki at Osaka University for his kind supplying an ingot of the Fe-Pt alloy used in the study, and Professors I. Tamura and T. Maki at Kyoto University for their kind supplying an ingot of the Fe-Ni-Co-Ti alloy used in the study, Finally, the author sincerely thanks Messrs. S. Furikado and H. Shirai, graduate students of Osaka University, Messrs. M. Tanimoto and K. Nagata, under graduate students of Kinki University, Messrs. S. Funada and S. Kijima, graduate students of Osaka University, and Mr. K. Hazumi, graduate student of Osaka University, for their assistance to the present study and also thanks all the members of Shimizu Laboratory.